INFORMATION TO USERS

NOTE TO USERS

This reproduction is the best copy available.

UMI

Design, Development and Validation of the
In-Situ Shear Stiffness Test
(InSiSST™)
Facility for Asphalt Concrete Pavements

Researched and Written by:

Stephen Norman Goodman, B.A.Sc., E.I.T.

A thesis submitted to the
Faculty of Graduate Studies and Research
in partial fulfillment of the requirements for the degree of

Master of Engineering

Department of Civil and Environmental Engineering
Carleton University
Ottawa, Canada
September 2000

The author has granted a non-exclusive licence allowing the National Library of Canada to reproduce, loan, distribute or sell copies of this thesis in microform, paper or electronic formats.

L'auteur a accordé une licence non exclusive permettant à la Bibliothèque nationale du Canada de reproduire, prêter, distribuer ou vendre des copies de cette thèse sous la forme de microfiche/film, de reproduction sur papier ou sur format électronique.

The author retains ownership of the copyright in this thesis. Neither the thesis nor substantial extracts from it may be printed or otherwise reproduced without the author's permission.

L'auteur conserve la propriété du droit d'auteur qui protège cette thèse. Ni la thèse ni des extraits substantiels de celle-ci ne doivent être imprimés ou autrement reproduits sans son autorisation.

0-612-57727-9

Canadä

Design, Development and Validation of the
In-Situ Shear Stiffness Test
(InSiSST™)
Facility for Asphalt Concrete Pavements

submitted by:

Stephen Norman Goodman, B.A.Sc., E.I.T.

in partial fulfillment of the requirements for
the degree of Master of Engineering

Thesis Supervisor
Dr. A.O. Abd El Halim
Carleton University

Chair, Department of Civil and Environmental Engineering
Dr. Wayne Parker
Carleton University

Ottawa-Carleton Institute for Civil Engineering
October 2000

ABSTRACT

The past decade has seen many significant improvements in asphalt pavement technology, particularly through large-scale research efforts such as the Strategic Highway Research Programs in the United States and Canada. However, there remains much room for improvement, particularly in the use of shear properties for the design, construction, monitoring and performance prediction of asphalt concrete pavements.

The primary objective of this investigation was the design, fabrication and validation of an advanced field test facility known as the In-Situ Shear Stiffness Test (InSiSST™) for asphalt concrete pavements. The development process took a stepwise approach including the analysis of current testing devices and their related deficiencies. The resulting test facility is portable, stable, and rugged - requiring only a single operator with no heavy lifting or complex set-up. Test results are instantly available and initial validation testing has indicated excellent accuracy and repeatability. Future testing with the InSiSST™ facility will provide invaluable input to pavement performance models and may allow the development of a strength or stiffness-based quality control/assurance (QC/QA) specification.

ACKNOWLEDGEMENTS

TABLE OF CONTENTS - BRIEF

TABLE OF CONTENTS - DETAILED

LIST OF FIGURES

LIST OF TABLES

NOTATIONS AND ABBREVIATIONS

LIST OF APPENDICES

CHAPTER 1: INTRODUCTION

1.1 Asphalt Concrete Pavements in Canada

1.1.1 Asphalt Concrete Pavements Defined

The term "pavement," although seemingly obvious in its usage, may have different meaning to different people or agencies. For example, pavement may simply refer to the surface layer of a road system, or may encompass additional underlying layers. The Transportation Association of Canada (TAC) has defined the term "pavement" as consisting of all structural elements or layers, including the shoulders, *above* the subgrade. While the subgrade is not part of the pavement structure by this definition, its characteristics such as strength or load carrying capacity, drainage, etc. are implied (TAC 1997). This thesis has adopted the TAC pavement definition wherever pertinent.

The term "asphalt concrete" refers to a conglomeration of asphalt cement (binder), aggregate and air (void space). Unless otherwise stated, the term asphalt concrete refers to hot-mix asphalt concrete (HMAC), the most common type of asphalt concrete used in transportation systems, which is mixed and placed at elevated temperatures.

Therefore, for the purposes of this thesis, an "asphalt concrete pavement (ACP)" is a pavement structure whose upper layers are constructed with hot-mix asphalt concrete unless otherwise stated. Figure 1 displays a typical cross section of an ACP, also commonly referred to as a flexible pavement.
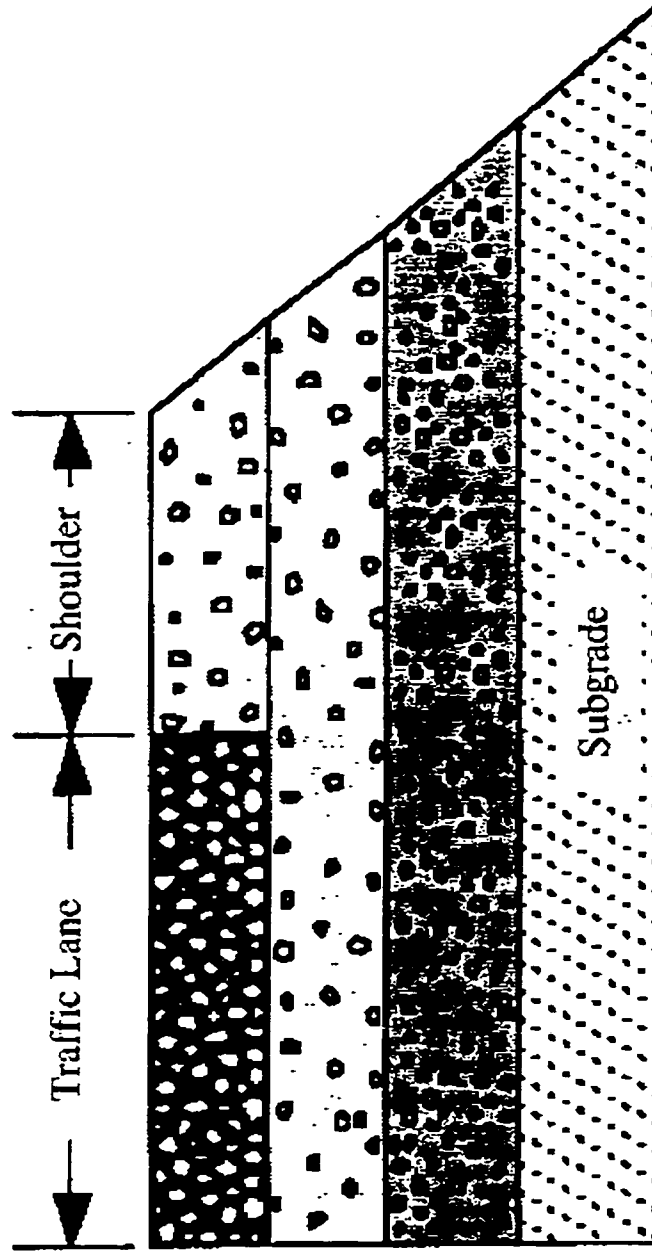
Figure 1: Typical Cross Section for Asphalt Concrete Pavement (from TAC 1997)

1.1.2 Climatic Conditions

Pavements in Canada are subjected to particularly harsh climatic conditions. Furthermore, these harsh conditions are not consistent throughout Canada due to its enormous size. For example, the Canadian Meteorological Centre (2000) reports that northern cities such as Yellowknife in the Northwest Territories consistently experience temperatures of –30 degrees Celsius (°C) for 3 months of the year with extreme temperatures of –51°C not uncommon. Central cities such as Regina, Saskatchewan may experience annual pavement temperature ranges of up to 80°C. Finally, coastal cities such as St. John's, Newfoundland and Vancouver, British Columbia are subjected to 1.6 and 1.2 metres of rain respectively per year.

Figure 2 displays soil temperature zones across Canada. As shown, no less than 7 individual temperature zones are present, ranging from Arctic (extreme cold) in the north to Mild along the Canadian-US border. With the exception of some of the Atlantic Provinces, each province or territory contains at least 2 of these zones with many of the provinces containing 5 zones.

Figure 3 displays the distribution of soil moisture across Canada. As with temperature, the distribution of soil moisture is extreme ranging from aquic-perhumid areas where the soil is fully saturated for long periods of the year to subaquic-arid regions with severe groundwater deficits.

The large variation in climatic conditions across Canada presents pavement designers and contractors with unique regional challenges.
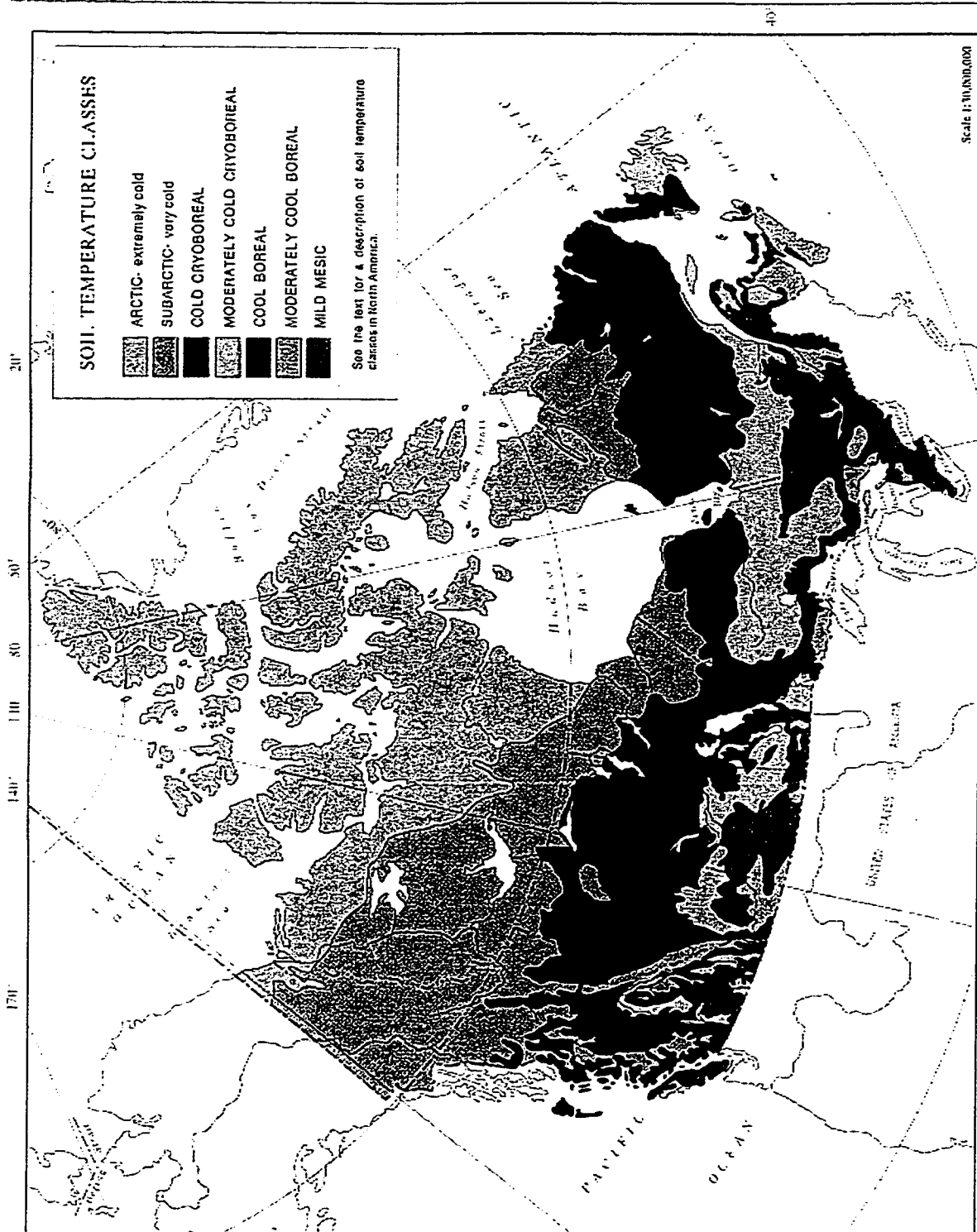
**Figure 2: Canadian Soil Temperature Zones
(from Energy, Mines and Resources Canada 1974)**
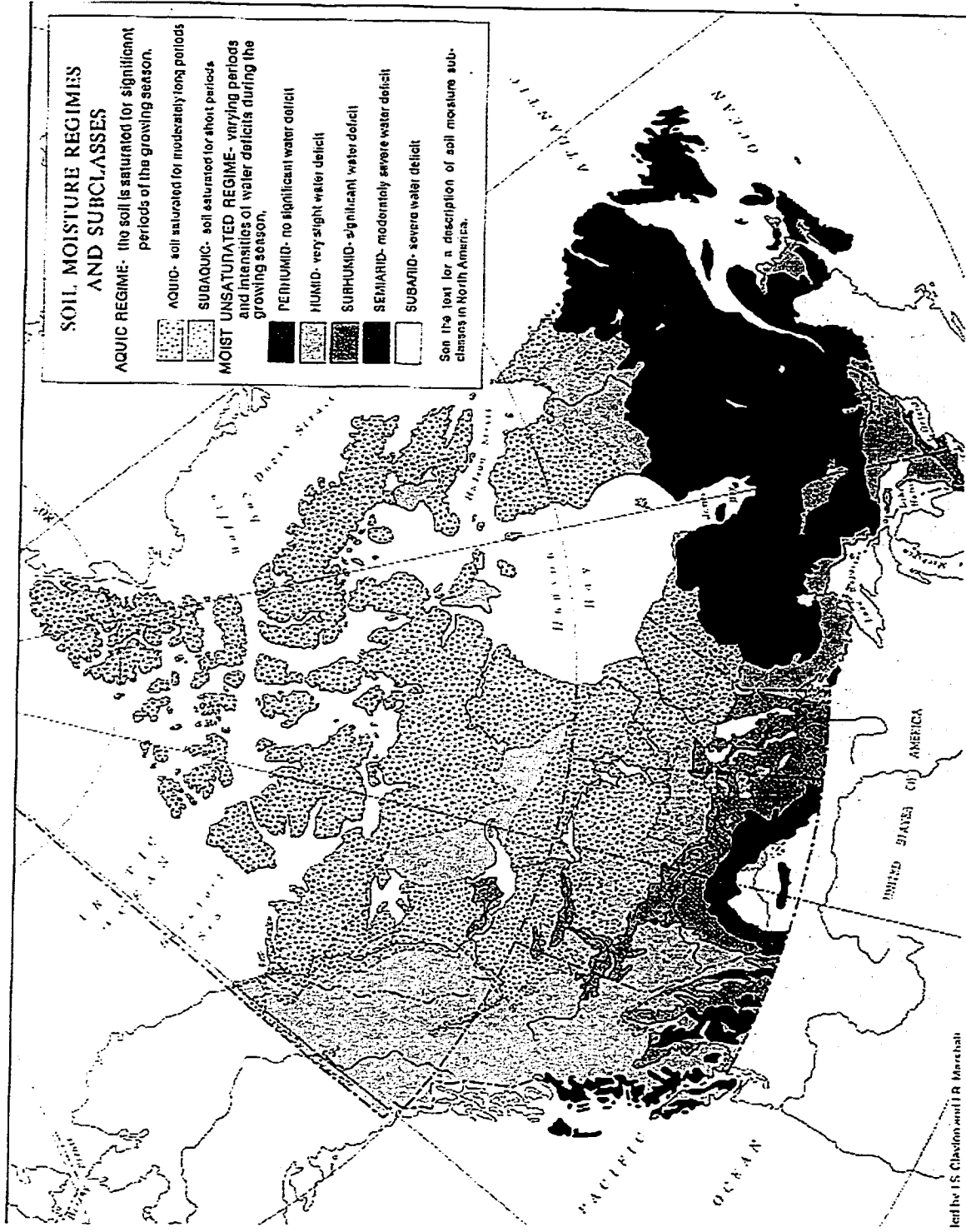
Figure 3: Canadian Soil Moisture Zones
(from Energy, Mines and Resources Canada 1974)

1.1.3 Transportation and the Canadian Economy

In 1999, transportation industries accounted for 30.6 billion Canadian dollars (4.1%) of Canada's Gross Domestic Product (Transport Canada 1999). The trucking sector accounted for the largest proportion of the transportation industries at 1.7% of the GDP ($12.5 billion). The average annual growth of the trucking sector between 1994 and 1999 was 7.7%, more than double of any other transportation sector including rail, marine and air. In 1998/1999 alone, the trucking sector annual growth was 8.2%. These statistics clearly indicate the immense importance of trucking to the Canadian economy and that this importance is growing at a high rate.

The National Highway System (NHS) is a network of roads identified by the Council of Ministers Responsible for Transportation and Highway Safety during a multi-stage policy study initiated in September 1987. The network consists of existing primary routes that provide interprovincial and international trade and travel by connecting a capital city or major provincial population or commercial centre in Canada with another capital city or major population centre, a major point of entry or exit to the United States highway network or another transportation mode served directly by the highway mode (Transport Canada 1999). The NHS is illustrated in Figure 4.

Although the NHS accounts for only 24500 kilometres of the entire Canadian road network of over 900000 kilometres (less than 3%), the NHS experiences nearly one quarter of the total vehicle-kilometres driven (Transport Canada 1999). Ontario and Quebec alone account for 60% of NHS traffic and these traffic levels are increasing every year.
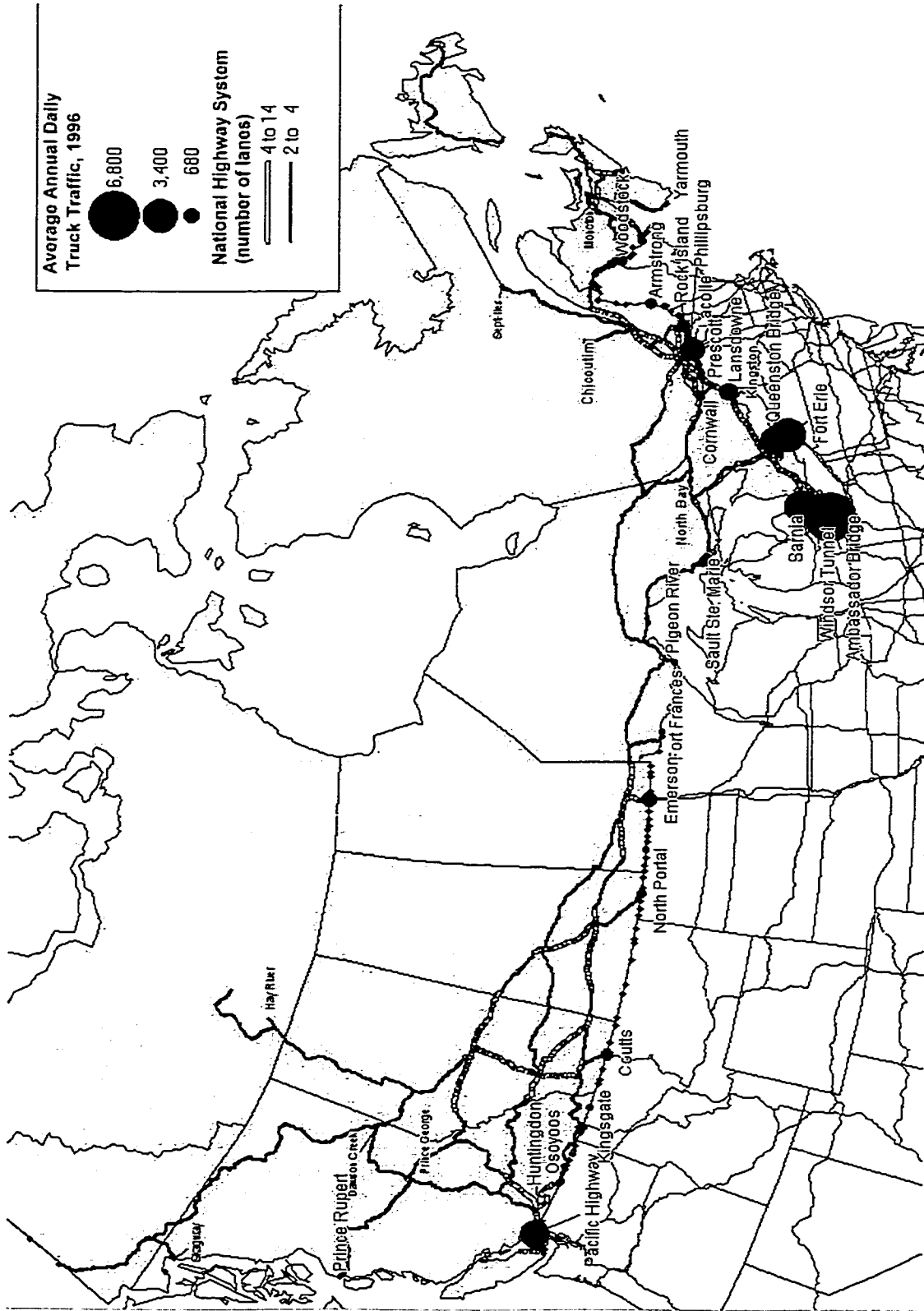
Figure 4: Canada's National Highway System and Major US Border Crossings (from Transport Canada)

The large and continuing increase in truck traffic on Canadian roads may be largely attributed to a new revolution in the way business is done in North America that started in the early 1990's. The main thrust of this new revolution was the implementation of a new manufacturing process referred to as "lean production" - a process that has been shown to improve productivity, efficiency and profits (Farris 1992). While lean production involves numerous new procedures, an essential component is a process called "Just-In-Time Delivery," or JIT. In essence, JIT delivery systems require delivery of inventory only when needed, permitting smaller storage space and faster model change in response to consumer demands. Therefore, the nations highways become linear warehouses for manufacturing companies. This trend is not expected to reverse in the near future.

Unfortunately, although local government spending on transportation has increased over the past five years, spending at the federal and provincial/territorial levels has declined (Transport Canada 1999), leaving an overall decrease in funds available for highway maintenance. Therefore, as truck traffic increases and overall government spending decreases, the pavement industry will face increasingly difficult challenges to provide an adequate highway network for the public.

1.2 Pavement Structural Design and Loading Conditions

1.2.1 Pavement Structural Design

Methods of pavement structural design may be classified into three categories as follows (TAC 1997).

   i)   Experience-based methods using standard sections;

ii) Empirical methods in which relationships between some measured pavement response, usually deflection, or field observations of performance, and structural thickness are utilized;

iii) Theory-based methods, using calculated stresses, strains, or deflections. These are also known as mechanistic-empirical methods.

Currently, most flexible pavement structural design methods are mostly empirical methods that have been improved over the past 40 years to include deflection measurements, subgrade compressive strains and asphalt layer tensile strains. Material properties are typically characterized using elastic or resilient modulus. The most common methods are the Asphalt Institute Thickness Design Method (Asphalt Institute 1991) and the American Association of State Highway and Transportation Officials (AASHTO) Flexible Pavement Design Method (AASHTO 1993). Traffic loading in both methods consists of uniform vertical pressures applied to a multi-layered elastic system.

1.2.2 Pavement Loading Conditions

Although traditional asphalt pavement analysis and design methods focus on uniform vertical stresses applied by traffic loading, there are actually 10 loading conditions commonly applied to pavements in service. These conditions are illustrated in Figure 5 (Gerrard and Harrison 1970).

I(a) UNIFORM VERTICAL PRESSURE P_1

I(b) UNIFORM VERTICAL DISPLACEMENT

2(a) LINEAR VERTICAL PRESSURE P_2

2(b) LINEAR VERTICAL DISPLACEMENT

MAX. STRESS P_2

3(a) LINEAR RADIAL SHEAR STRESS p_1

MAX. STRESS p_1

3(b) LINEAR RADIAL SHEAR DISPLACEMENT

δ_1

4(a) LINEAR TORSIONAL SHEAR STRESS p_2

MAX. STRESS p_2

4(b) LINEAR TORSIONAL SHEAR DISPLACEMENT

δ_2

5(a) UNIFORM UNIDIRECTIONAL SHEAR STRESS p_3

5(b) UNIFORM UNIDIRECTIONAL SHEAR DISPLACEMENT

δ_3

**Figure 5: Common Loading Conditions of Asphalt Pavements
(from Gerrard and Harrison 1970)**

According to Gerrard and Harrison (1970), loading by uniform vertical pressure (sub figure 1a) is typical of pneumatic tires and flexible foundations, while loading by uniform vertical displacement (sub figure 1b) corresponds to relatively rigid foundations. In addition to uniform vertical pressures/displacements, linear vertical pressures and displacements are also applied to pavement structures (sub figures 2a and 2b, respectively). Loading by linear vertical pressure represents moments about the horizontal axis applied to flexible pavements, while linear vertical displacements represent moments about the horizontal axis applied to rigid pavements.

In addition to vertical loading, pavements are also subjected to numerous loading conditions in shear. Linear radial shear stresses (sub figure 3a) are developed at the surface of pavements due to the grip of pneumatic tires. Measurements by Bonse and Kuhn (1959), as well as Marwick and Starks (1941), indicate that the magnitude of the maximum stress is of the order of the tire inflation pressure. Linear radial shear stresses are present both at rest and during constant linear velocity. Linear radial shear displacement (sub figure 3b), when coupled with the uniform vertical pressure loading, gives the exact solution to the problem of a flexible foundation with a rough base (Gerrard and Harrison 1970).

The state of stress defined by linear torsional shear stress (sub figure 4a) is imposed as an automobile turns or enters a curved section of road. Linear torsional shear displacement on the other hand, may be applied to the analysis of vane shear tests at subgrade failure loads (subfigure 4b).

The final set of loading conditions consist of uniform unidirectional shear stress and displacement (subfigures 5a and 5b). Unidirectional shear stress is

applied during braking, acceleration and traction of pneumatic tires, while

unidirectional shear displacement represents lateral loads applied to foundations.

According to Figure 5, six of the ten possible pavement loading conditions

involve shear, however, current practices only consider uniform vertical pressure.

1.3 United States Strategic Highway Research Program (US-SHRP)

1.3.1 Background and Reason for Implementation

The United States Strategic Highway Research Program (US-SHRP) was a 5

year, $150 million dollar research program designed to improve the performance

and durability of highways and make them safer for motorists and highway workers.

US-SHRP was initiated in response to the continuing deterioration of highway

infrastructure in the United States and was intended to make significant advances in

traditional highway engineering and technology through the concentration of new

research funds in four key technical areas – Asphalt, Pavement Performance,

Concrete and Structures, and Highway Operations (C-SHRP 1998). A total of 130

new products emerged from the US-SHRP research in the form of new equipment,

processes, test methods, manuals and specifications for the design, maintenance and

operations of highways (US-SHRP 1992).

1.3.2 The SUPERPAVE™ Mix Design System

Superpave™ (Superior Performing Asphalt Pavements) was one of the major

products of the SHRP asphalt research program. Unveiled in 1992, the Superpave

system represented a fundamentally new system for designing asphalt concrete

mixes. The performance-based nature of the system not only promoted improved

pavement life, but also the potential ability to predict pavement performance based on accelerated testing (C-SHRP 1999).

Briefly, the Superpave system incorporates performance-based asphalt materials characterization with the design environmental conditions to improve performance by controlling rutting, low temperature cracking and fatigue cracking (Asphalt Institute 1997a). The Superpave system consists of three main components – the performance graded (PG) asphalt binder specification, the mixture design and analysis system, and a computer software system (Asphalt Institute 1997b).

Detailed discussion of the Superpave system is beyond the scope of this thesis and has been documented in countless other reports. It should be mentioned however, that by 2001, the AASHTO Task Force on SHRP Implementation predicts that over 80% of the hot mix asphalt produced and constructed in the United States will be designed with the Superpave system (AASHTO 1999). It is therefore clear that Superpave will be the asphalt mix design system in the United States for the foreseeable future. In Canada, Superpave implementation has progressed at a slower rate; however, it appears that Canadian agencies will also adopt Superpave as the new mix design system in the coming years.

1.3.3 Long Term Pavement Performance (US-LTPP) Project

As part of the US-SHRP, a comprehensive 20-year study of in-service pavements was initiated in 1987 to understand why some pavements perform better than others, with the ultimate goal of building and maintaining a cost-effective highway system. This field experiment, known as the Long Term Pavement Performance (US-LTPP) project, is unprecedented in scope, consisting of over 2400

asphalt and Portland cement concrete pavement test sections across the United States and Canada (FHWA 1998a).

The original US-LTPP research plan set forth six objectives for the program (FHWA 1999a):

i) Evaluate existing pavement design methods.

ii) Develop improved design methodologies and strategies for the rehabilitation of existing pavements.

iii) Develop improved design equations for new and reconstructed pavements.

iv) Determine the effects of loading, environment, material properties and variability, construction quality, and maintenance levels on pavement distress and performance.

v) Determine the effects of specific design features on pavement performance.

vi) Establish a national long-term database to support US-SHRP's objectives and to meet the future needs of the highway industry.

To support these objectives, three types of studies were established: General Pavement Studies (GPS), Specific Pavement Studies (SPS) and the Seasonal Monitoring Program (SMP). The GPS experiments focus of the most commonly used structural designs for pavement. Eight types of existing in-service pavements are currently being monitored throughout North America. The performance of these structural designs is tested against an array of climatic, geologic, maintenance, rehabilitation, traffic and other service conditions (FHWA 1999a).

In contrast, the SPS test sections were specially constructed to investigate certain pavement engineering factors. These sections allow critical design factors to be controlled and performance to be monitored for the initial date of construction. It is anticipated that the results from the SPS experiment will provide a better understanding of how selected maintenance, rehabilitation, and design factors affect pavement performance.

The SMP experiment sections were also specially constructed to provide data needed to determine the impacts of temperature and moisture variations on pavement response.

The primary product of the LTPP experiment is the Information Management System (IMS) database that contains the data collected from each of the three LTPP studies. Administered by the Federal Highway Administration (FHWA), the IMS database is available to anyone at no cost. To make the data more accessible and user friendly, portions of the IMS database meeting all quality control levels are released on CD-ROM under the name "DataPave." The latest version of DataPave – version 2.0 released in September of 1999, contains twice as much IMS data as its predecessor (FHWA 1999b).

1.3.4 Introduction to the AASHTO 2002 Pavement Design Guide

As mentioned, most pavement design procedures are based on the AASHTO Guide for the Design of Pavement Structures (TAC 1997). All previous and current versions of this guide have been based on performance equations developed at the AASHO Road Test in the 1950's. While previous versions of the guide have served well for almost four decades, there are a number of serious limitations to their

continued use as the nation's primary pavement design procedures as outlined by

McGee (1999):

- Pavement rehabilitation design procedures were not considered at the AASHO

  Road Test. Full consideration of rehabilitation design is required to meet

  today's needs.

- Since the road test was conducted at one specific geographic location, it is

  difficult to address the effects of differences in climatic conditions on

  pavement performance. For example, at the road test a significant amount of

  distress occurred in the pavements during the spring thaw, a condition that

  does not exist in a significant portion of the country.

- One type of subgrade was used for all of the test sections at the road test.

  Many types exist nationally.

- Only unstabilized, dense granular bases were included in the main pavement

  sections (limited use of treated bases was included for flexible pavements).

  Various stabilized types now are used routinely.

- Vehicle, suspension, axle configurations, and tire types were representative of

  the types used in the late 1950's. Many of these are outmoded in the 1990s.

- Pavement designs, materials, and construction were representative of those

  used at the time of the road test. No subdrainage was included in the road test

  sections.

An additional problem with earlier AASHTO procedures is the order-of-magnitude difference between AASHO Road Test traffic loads and the loads carried by modern new and rehabilitated pavements. Road test pavements sustained at most some 10 million-axle load applications; less than carried by some modern pavements in their first year of use due to the explosive growth of truck traffic over the last 40 years. Equations forming the basis of the earlier procedures were based on regression analyses of the road test data. Thus, application of the procedure to modern traffic streams meant the designer often was projecting the design methodology far beyond the data and experience providing the basis for the procedure. Clearly, the result was that the designer may have been working "in the dark" for highly trafficked projects. Such projects may well have been either "under designed" or "over designed" with the result of significant economic loss (McGee 1999).

Another major extrapolation is design life. Because of the short duration of the road test, the long-term effects of climate and aging of materials were not addressed. The AASHO Road Test was conducted over 2 years, while the design lives for many of today's pavements are 20 to 50 years.

Finally, earlier AASHTO procedures relate the thickness of the pavement surface layers (asphalt layers or concrete slab) to performance. However, the observed performance of pavements reveals that many pavements need rehabilitation for reasons that are not directly related to pavement thickness (i.e. rutting, thermal cracking, faulting etc.). Further, the primary measure of pavement performance in the earlier procedures is present serviceability (PSI or PSR) and the dominant factor effecting serviceability is pavement ride. Yet, in many cases

pavement managers find that distress factors other than ride, such as cracking and rutting, control when pavement rehabilitation is required. To improve the reliability of design and to meet the needs of asset management, the management criteria and the pavement design procedure must relate to the same performance factors. To help alleviate these problems, the 2002 Guide will use the international roughness index (IRI) as a major pavement performance measure (McGee 1999).

The AASHTO Joint Task Force on Pavements (JTFP) has responsibility for the development and implementation of pavement design technologies. In recognition of the limitations of earlier Guides, the JTFP initiated an effort to develop an improved Guide by the year 2002. At the time of this writing, the National Cooperative Highway Research Program (NCHRP) is developing a major revision and update to the current AASHTO pavement design guide, under NCHRP project 1-37A, due for release in 2002. A draft version of the new guide was completed in April 1999 although it has not been formally published (McGee 1999). Unlike previous design guides, the 2002 guide will incorporate mechanistic-empirical concepts to better characterize the pavement structure and its constituent materials.

Although this move represents a major step forward toward a more accurate pavement design and analysis system, the 2002 guide will only focus on vertical loading conditions on a multi-layered elastic system. Researchers concede that shear loading is important to pavement performance, however, Witczak (2000) explained that the 2002 guide will not include shear properties or loading conditions as the guide is being developed from already existing databases and test procedures.

1.4 Canadian Strategic Highway Research Program (C-SHRP)

1.4.1 Background and Reason for Implementation

In 1987, The Canadian Strategic Highway Research Program (C-SHRP) was created in response to the commencement of SHRP in the United States. The objective of C-SHRP is to improve the performance and durability of highways and to make them safer to motorists and highway workers by extracting the benefits of the United States Strategic Highway Research Program (US-SHRP) and by solving highway problems having a high priority in Canada that were related to, but not duplicates of, US-SHRP projects (RTAC 1986).

C-SHRP is a dedicated program of the Council of Deputy Ministers Responsible for Transportation and Highway Safety and is managed by the C-SHRP Executive Committee. Unlike US-SHRP, C-SHRP was always envisioned as a 15 year program with three 5-year program phases (C-SHRP 1998). Due to delays with the US-SHRP, the C-SHRP Executive Committee extended the first program phase by two years. C-SHRP Phase 1 ran from April 1987 until March 1994 and involved coordinating Canadian involvement with the US-SHRP research as well as conducting independent Canadian research related to US-SHRP. The complimentary C-SHRP research produced an additional 8 research products. Phase 1 also saw the initiation of the Canadian Long Term Pavement Performance (C-LTPP) project, an independent experiment designed with Canadian pavement design and climatic conditions in mind.

The second phase of C-SHRP was completed between April 1994 and March of 1999. The focus of Phase 2 was technology transfer in the form of evaluating

SHRP/C-SHRP research results and applying the findings to mainstream practice. The C-LTPP project continued with a focus on data collection and management, with initial analysis of performance through Bayesian modelling procedures (Kaweski and Nickeson 1997).

The third and final phase of C-SHRP is currently underway and will conclude in April of 2004. As with Phase 2, technology transfer of SHRP products will continue as a primary focus, however, the range of products evaluated and promoted will be expanded to include products of the FHWA and AASHTO. The C-LTPP experiment will conclude in 2004 and the resulting database will be completed for use by pavement designers and researchers to provide more cost effective pavement designs.

1.4.2 Canadian Long Term Pavement Performance (C-LTPP) Project

The Canadian Long Term Pavement Performance (C-LTPP) project was initiated in 1987 as an independent Canadian experiment to investigate pavement performance. However, whereas the US-LTPP project covered all pavement types, the overall goal of the C-LTPP project is to increase pavement life through the development of cost-effective pavement rehabilitation procedures, based upon systematic observation of in-service pavement performance. As the majority of Canadian roads are asphalt concrete pavements, only new asphalt concrete overlays were selected for investigation under C-LTPP. Therefore, if comparing to the US-LTPP project, the C-LTPP test sites could be considered SPS-5 sections, although the C-LTPP sites are independent of US-LTPP.

In formulating the overall goal of C-LTPP, four distinct objectives were identified (C-SHRP 1997):

i) to evaluate Canadian practice in the rehabilitation of flexible pavements, and to subsequently develop improved methodologies and strategies;

ii) to develop pavement performance prediction models and validate other models or calibrate then to suit Canadian conditions;

iii) to establish common methodologies for long-term pavement evaluation, and to provide a national framework for continued pavement research initiatives;

iv) to establish a national pavement database to support the preceding C-LTPP objectives as well as future needs.

A total of 24 test sites were selected for C-LTPP each with 2 to 4 adjacent test sections for a total of 65 test sections within the experiment. Each test section received an asphalt concrete overlay for the experiment. The use of adjacent sites allows for the comparison of different rehabilitation methods under identical traffic loading, climate and soil conditions. The alternative rehabilitation strategies employed on the C-LTPP test sections included variable overlay thickness, hot and cold-mix recycling, milling, inclusion of performance enhancing additives, or a combination thereof.

As with the US-LTPP, the primary product of C-LTPP is the C-LTPP pavement performance database.

1.5 Specific Problem Definitions and Need for New Test Facility

The preceding sections were included to provide some context of current research activities in the area of pavement performance, materials and design. While the past decade has seen many significant improvements in asphalt pavement technology, there

remains much room for improvement, particularly in the use of shear properties to design, construct, monitor and predict the performance of ACP's. The following sections provide rationale for the current investigation; that being to design, develop and verify an advanced in-situ shear strength/stiffness test for asphalt concrete pavements.

1.5.1 Improved Characterization of Pavement Structure and Design Inputs

As outlined in Section 1.2, pavement design procedures in use today only consider loading in the vertical direction, despite the fact that six of the ten common pavement loading conditions described involve shear stresses or displacements. As indicated, the NCHRP is developing a major revision and update to the current AASHTO Guide for the Design of Pavement Structures (AASHTO 1993) under NCHRP project 1-37A due for release in 2002. Unlike previous design guides, the 2002 guide will incorporate mechanistic-empirical concepts to better characterize the pavement structure and its constituent materials. Although this move represents a major step forward toward a more accurate pavement design and analysis system, the 2002 guide will only focus on vertical loading conditions on a multi-layered elastic system. Although the vertical loading condition represents a large portion of the applied stress, the measurement of shear parameters of asphalt pavements and incorporation into analysis and design should significantly improve the reliability of pavement design, providing more cost effective pavements. Clearly, the inclusion of shear loading into the design process will be a complex undertaking that will require extensive research prior to implementation. Development of an in-situ test device will provide an important step toward this goal.

1.5.2 Simple Performance Test for Superpave Verification and QC/QA Testing

One major issue not addressed in the original Superpave system was the adoption of a strength or durability test. Unlike the Marshall or Hveem methods that utilize stability or flow tests, Superpave was originally based solely on volumetric properties with no strength test for performance verification. To address this deficiency, the NCHRP initiated project 9-19 "Superpave Support and Performance Models Management" to recommend a laboratory "simple performance test" suitable for evaluating the rutting and fatigue performance of asphalt mixes and to ultimately provide input to performance models. In addition to performance testing, the simple performance test should also be capable for use in quality control and quality assurance (QC/QA) testing.

However, there is currently no in-situ performance test for Superpave or any other asphalt mix design system. The development of an in-situ shear strength/stiffness test would provide an excellent complimentary field test device allowing both faster and more cost effective performance testing and QC/QA testing due to its portable nature.

1.5.3 The Need to Measure Field Properties

Peck and Lowe (1960) perhaps gave the best reasoning for the introduction of field shear testing (of soils) as opposed to laboratory testing during the 1960 ASCE Research Conference on Shear Strength of Cohesive Soils in Colorado:

"It seems apparent that there are numerous unanswered questions with regard to the shear strength of undisturbed soils. Many of these arise because of doubts regarding the applicability of laboratory findings to field conditions. It is recognized that the mere act of obtaining a sample from a natural deposit

radically alters the state of stress and induces strains, and that natural deposits are rarely homogeneous. Yet there seems to be an inclination to feel that the really fundamental research on shear strength of undisturbed soils must be done in the laboratory, and that the results of the laboratory studies may be applied to field conditions with a minimum of evidence to support the extrapolation. The panel discussions have indicated that there may be dangerous pitfalls in this path."

1.6 The Innovations Deserving Exploratory Analysis (IDEA) Program

The Innovations Deserving Exploratory Analysis (IDEA) programs, managed by the Transportation Research Board (TRB), provide start-up funding for promising but unproven concepts in surface transportation systems (TRB 2000).

The goal of the IDEA programs is to seek out and support new transportation solutions unlikely to be funded through traditional programs. IDEA programs differ from the more traditional research programs in the following ways:

1. They offer an arena for innovation. Topics are not restricted; good ideas that support the general goals of safe and efficient surface transportation are eligible.

2. Their impact is timely. Fledgling ideas take flight only when their development is nurtured. The IDEA programs foster good ideas at a critical early stage in the hope that they soon will take off on their own.

3. The proposal process is simple and accessible. Proposals are accepted at any time and awards are made twice each year. There are no prerequisites for submitting proposals; good ideas are welcome from anyone.

There are IDEA programs covering four major transportation areas – Highways, High Speed Rail, Intelligent Transportation Systems and Transit. As part of the NCHRP, the Highway-IDEA program is managed by the TRB and jointly supported by the FHWA and the member states of AASHTO. The program seeks advances in the construction, safety, maintenance, and management of highway systems (TRB 2000).

In September of 1997, a proposal entitled "Design, Development and Verification of an Advanced In-Situ Shear Strength Test for Asphalt Concrete Pavements" was submitted to the TRB for a NCHRP Highway IDEA Concept Exploration project (Goodman and Abd El Halim 1997). In February of 1999, Carleton University was awarded NCHRP IDEA Project #55 to develop the in-situ shear strength/stiffness test facility. The work completed for that project constituted a substantial portion of this thesis.

1.7 Organization and Scope of Thesis

1.7.1 Chapter 1: Introduction

Chapter 1 commences with a definition of asphalt concrete pavements and their importance to the Canadian economy, followed by a description of the various pavement loading conditions. A brief introduction of the United States and Canadian Strategic Highway Research Programs (US-SHRP and C-SHRP) is then provided to introduce recent and ongoing research efforts, as well as give context to the specific problems associated with current practice and the need for a new field test device for asphalt concrete pavements. Chapter 1 finishes with an introduction to the Innovations Deserving Exploratory Analysis (IDEA) Program, which

provided substantial funding toward the development of the test facility, as well as the organization and scope of this thesis.

1.7.2 Chapter 2: Literature Review

Chapter 2 consists of an extensive literature review completed to examine all aspects of the asphalt pavement rutting phenomenon including its manifestations, mechanisms, procedures for quantification, and a detailed review of the contribution of numerous variables toward rutting resistance. Furthermore, a state-of-the-practice review of current laboratory and field rutting test methods is provided with a discussion of the various limitations associated with these devices.

1.7.3 Chapter 3: Review of Previous Work and Analytical Modelling

The foundation for the current investigation was laid by two previous investigations completed at Carleton University. The first was a comprehensive laboratory investigation of asphalt shear properties and pavement rutting completed by Zahw (1995). Chapter 3 begins with a review of that investigation, followed by the results of a new study to investigate the relationships between asphalt mix characteristics, shear properties and pavement rutting, using data collected during his research. The second underlying research effort involved the construction of a first generation in-situ shear strength test device by Abdel Naby (1995). A review of the device, known as the Carleton In-Situ Shear Strength Test (CiSSST), is provided including its main benefits and the results of his research concerning in-situ shear strength and its relation to pavement performance. The chapter concludes by introducing an improved analytical approach to derive asphalt pavement shear properties from the surface plate loading condition using closed form equations and the finite element method.

1.7.4 Chapter 4: Development of the In-Situ Shear Stiffness Test (InSiSST™)

The primary basis for this thesis was the design and development of an advanced in-situ shear stiffness test for asphalt pavements. The design of the new device, entitled the In-Situ Shear Stiffness Test (InSiSST™) was conceived through an analysis of the deficiencies observed with the CiSSST prototype built in 1995. The advantages and benefits of the InSiSST™ are described, as well as some of the challenges experienced during its fabrication. Chapter 4 concludes with an initial set of instructions and procedures to carry out field testing with the InSiSST™.

1.7.5 Chapter 5: Preliminary Testing and Validation

Once fabrication of the InSiSST™ was complete, preliminary field tests were completed for validation purposes. Chapter 5 first presents the results of an exercise to validate the linear elastic assumption made by the analytical models presented in Chapter 3. Next, the results of comparison testing with the CiSSST and InSiSST™ devices are presented, as well as an interesting observation concerning the test plate diameter. Chapter 5 concludes with a comparison of field shear properties to those observed in the laboratory by Zahw (1995).

1.7.6 Chapter 6: Conclusions and Recommendations

The final chapter summarizes the project objectives and the rutting phenomenon, as well as the conclusions observed during the investigation. Recommendations for additional modifications to the InSiSST™ and future testing are also presented.

CHAPTER 2: LITERATURE REVIEW

2.1 Permanent Deformation of Asphalt Concrete Pavements

Although the term "rutting" is often used interchangeably with permanent deformation, it is only one of four observed manifestations as described below:

• *Rutting* is characterized by channelized depressions (troughs) that run longitudinally in the wheelpaths. Rutting may or may not be accompanied by shoving of the pavement adjacent to the wheelpaths.

• *Corrugations and Shoving* is characterized by ripples along the pavement surface formed by alternating areas of settlement and/or heave.

• *Grade Depressions and Settlement* are manifested as irregular or localized areas of settlement (not specifically in the wheelpaths).

• *Upheaval or Swell* consists of localized upward expansion of pavement due to swelling of underlying soils (base or subgrade) through moisture infiltration or frost heave.

However, rutting is the most common form of permanent deformation analysed. Therefore, the terms rutting and permanent deformation will be considered the same for the purposes of this thesis.

2.2 Manifestations of Rutting

Rutting itself is manifested in a number of forms depending on which of the pavement layers was responsible for the deformation. A novel and accurate method of determining the layer at which rutting occurred was investigated by Simpson et. al. (1995). During their investigation, it was observed that the shape of the pavement

transverse profile was theoretically indicative of where the rutting originated within the pavement structure. Using data from the US-LTPP Program, it was shown that the transverse profiles generally fit into one of four categories representing (a) subgrade rutting, (b) base rutting, (c) surface rutting, or (d) heave. Illustrations of these categories are shown in Figure 6.

Classification of transverse profiles into the four above categories was completed using the algebraic area between the transverse profile and the straight line connecting its end points as illustrated in Figure 6. Profile areas that were entirely negative proved to be the result of subgrade settlement while areas that were entirely positive were the result of heave. Furthermore, marginally positive profile areas were the result of surface rutting, whereas marginally negative areas were the result of base layer rutting. The criteria used to classify transverse profiles from the US-LTPP database are shown in Table 1. Of the 134 US-LTPP sections analyzed, only six transverse profiles did not agree with the classification system. Therefore, over 95% of transverse profiles were correctly classified using Table 1.

Table 1: Classification Criteria for Transverse Profiles (from Simpson et. al. 1995)

Layer Responsible for Rutting	Transverse Profile	
	Area of Distortion (mm^2)	Ratio of Positive to Negative Area of Distortion
Subgrade	< -4500	< 0.4
Granular Base	-4500 to 700	0.4 to 1.25
Surface (Asphalt)	700 to 5000	1.25 to 3.0
Heave	> 5000	> 3.0

a. SUBGRADE

b. BASE
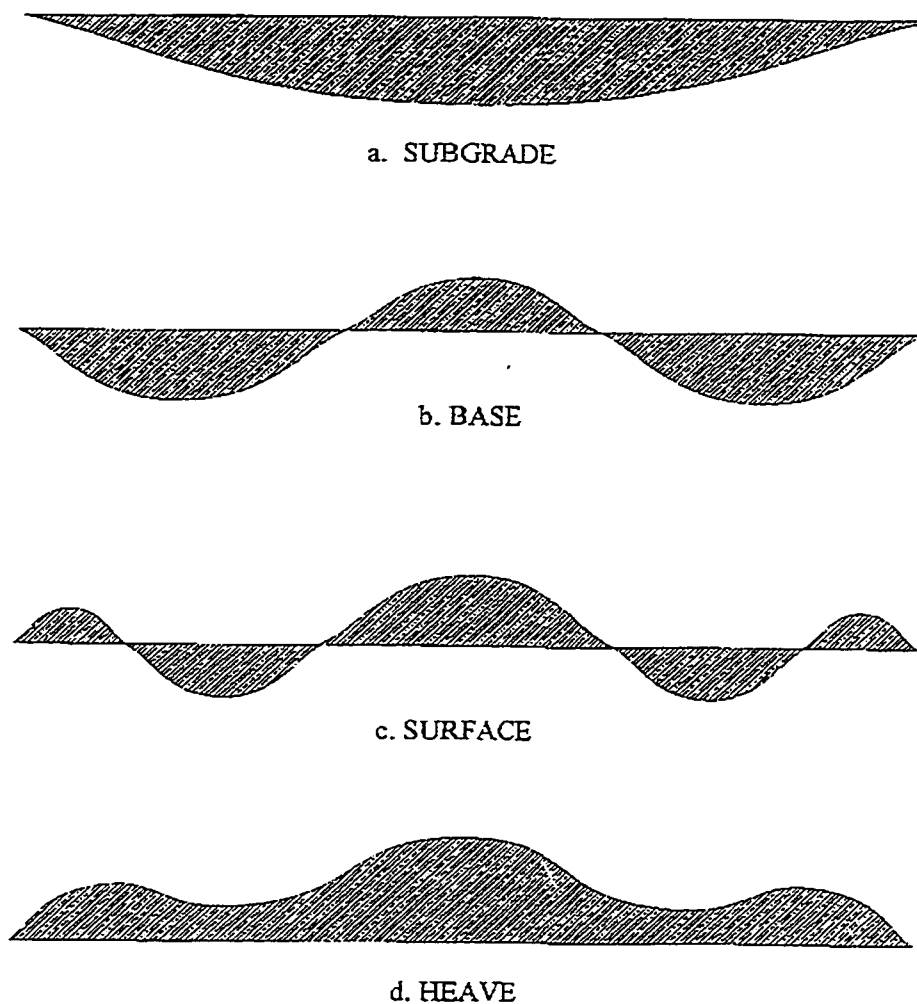
c. SURFACE

d. HEAVE

Figure 6: Transverse Profiles of Various Rutting Manifestations (from Simpson et. al. 1995)

2.3 Asphalt Surface and Overlay Rutting

2.3.1 Location of Pavement Rutting

Although rutting due to heave, subgrade or granular base failure can and does

occur, rutting in properly constructed pavements is usually observed due to

deformation of the asphalt layers. This statement was confirmed through a

comprehensive National Rutting Study that was completed in United States by the

National Center for Asphalt Technology (NCAT) in 1987. As part of the

investigation, trench cuts were made in selected roads to observe where in the

pavement structure that rutting was occurring. Reports by Cross and Brown (1992,

1991) revealed that most of the rutting occurred in the top 75 to 100 mm (3 to 4 in.)

of the pavement, therefore, almost exclusively in the asphalt concrete layer. The

amount of rutting in the base coarse was insufficient to measure. The results of the

NCAT study have been confirmed in other studies including Gervais and Abd El

Halim (1990). Figure 7 illustrates a cross section of an asphalt pavement section

displaying surface rutting. Note that the bottom edge of the asphalt layer is almost

completely flat while the surface is severely rutted.
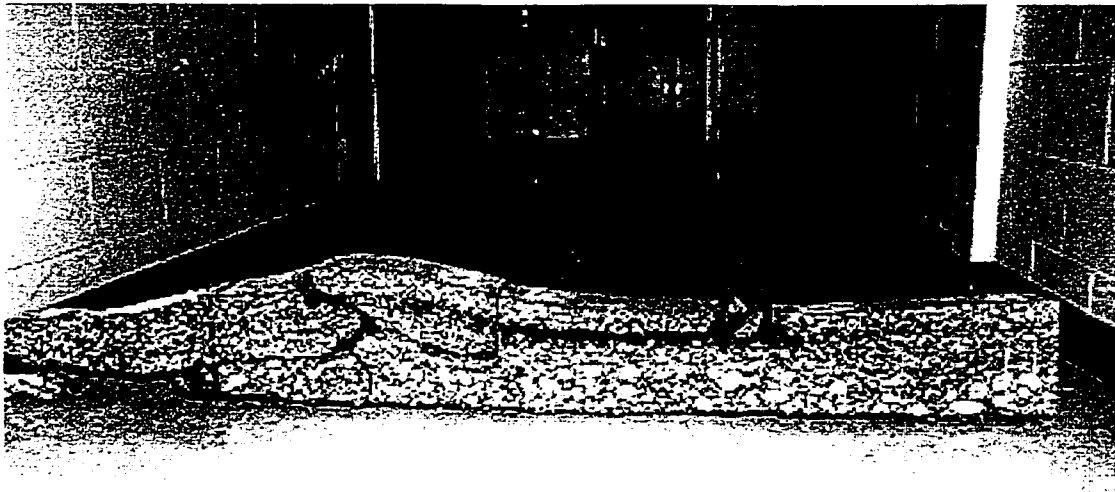
Figure 7: Illustration of Surface Rutting
(from Gervais and Abd El Halim 1990)

2.3.2 Surface/Overlay Rutting Mechanism # 1 - Traffic Induced Densification

With the exception of wear rutting caused by studded tires, surface or overlay

rutting is caused by two main mechanisms. The first is called "traffic-induced," or

"post" densification. Initial densification of the various pavement layers, including

the asphalt concrete, occurs during the construction phase in the form of

compaction. During compaction, the layers are compacted to form a dense,

consistent structure to resist traffic loading. However, layers that are not compacted

to a high degree retain significant void space. Under subsequent traffic loading, the

layers continue to consolidate as the excess voids are removed. This process is

known as traffic induced densification.

For properly constructed pavements, US-SHRP (1994) reports that traffic

induced densification is generally not considered to be the cause of substantial

rutting.

2.3.3 Surface/Overlay Rutting Mechanism # 2 - Shear (Plastic) Flow

The second and more critical rutting mechanism is shear or "plastic" flow of

the asphalt concrete mix under traffic loading. Shear flow involves lateral

movement of the asphalt cement and reorientation of aggregate particles under

traffic loading to a new or more stable equilibrium. The movement (strain) incurred

by the asphalt concrete is not recovered once unloaded, resulting in permanent

deformation. For properly constructed pavements, shear deformations caused

primarily by large shear stresses in the upper portions of the asphalt/aggregate

layers are dominant (US-SHRP 1994).

The shear flow phenomenon was the underlying reason for the development

of the InSiSST™. It is hypothesized that increasing the resistance of the asphalt

mix to shear deformation will reduce rutting and improve long-term pavement

performance significantly.

2.3.4 The Rutting Cycle

The two rutting mechanisms mentioned above are not mutually exclusive.

Indeed, a rutting cycle is observed in most instances during the design life of a

properly constructed asphalt pavement. The three stages of permanent deformation

with traffic loading are listed below (Carpenter 1993):

1. Primary – initial compaction and traffic induced densification

2. Secondary – stable shear period

3. Tertiary – rapid unstable shear failure

Rutting is initiated with continued densification of the asphalt layer under

traffic loading. Kandhal et. al. (1993) explain that during this stage, rutting is

directly proportional to traffic.
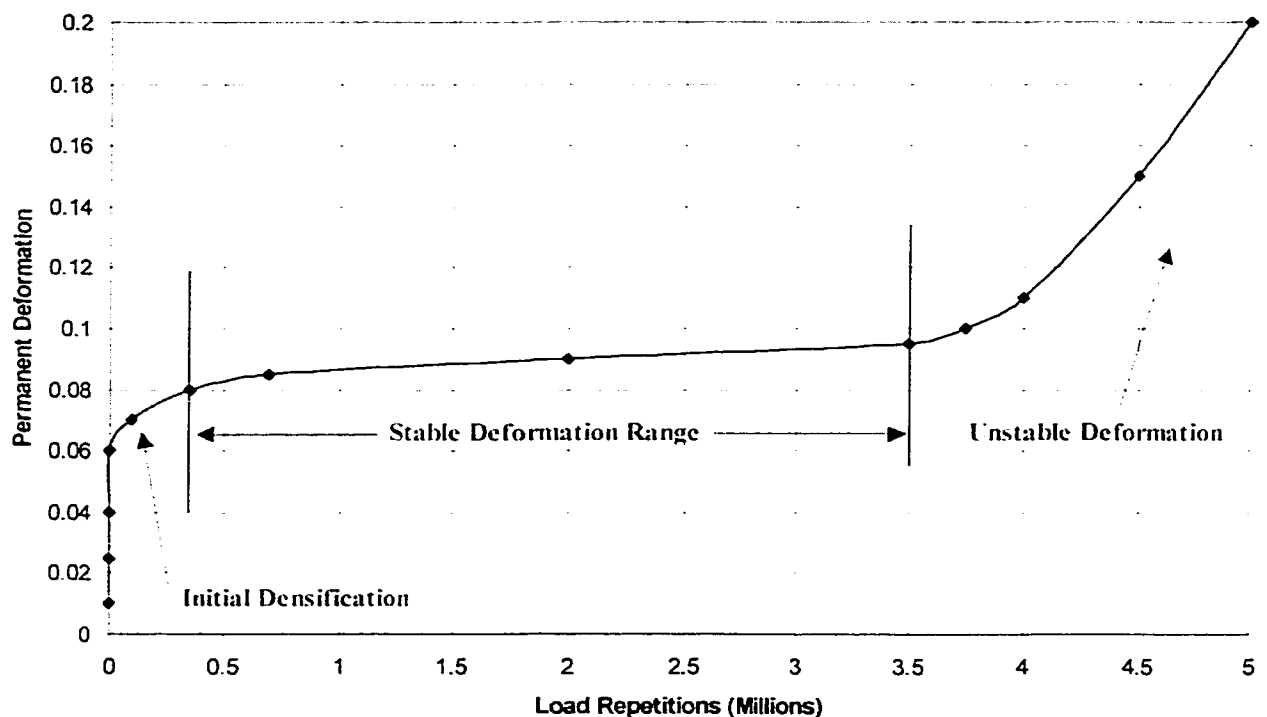
**Figure 8: The Progression of Rutting with Traffic Loading (Rutting Cycle)
(from Carpenter 1993)**

The second phase involves a stable shear period during which the rate of rutting decreases with increasing traffic until a condition of plastic flow occurs and the rate of rutting again increases (rapid unstable shear failure). Therefore, prevention of the onset of the tertiary flow stage should increase pavement life considerably with respect to permanent deformation.

2.4 Quantification (Measurement) of Rutting

Rutting is quantified using various methods and measures for evaluation and modelling purposes. Perhaps the most common measures are *average rut depth* or *maximum rut depth* in millimetres or inches as measured transversely across the pavement width using straightedges, profilometers, or other depth measuring devices.

A second commonly used measure is *average rutting rate*; the rut depth divided by the amount of traffic to which a particular pavement has been subjected. This measure allows different pavements to be compared directly. Previous work by Brown and Cross (1998), and Parker and Brown (1990) has shown that expressing the rate of rutting as a function of the square root of total traffic yields higher correlation with observed pavement behaviour when compared to other expressions (such as the log of traffic).

As previously presented, Simpson et. al. (1995) quantified rutting by determining the total area of deformation from transverse profiles obtained for the US-LTPP Project.

2.5 Categories for Rutting Variable Classification

The rutting phenomenon is very complex. At present, there is no single independent variable that completely captures or predicts rutting. In addition, Kandhal et. al. (1993) emphasized that a single "bad" property, such as excessive asphalt content, can nullify other good properties, such as coarse aggregate with 100% fractured faced count. Furthermore, there are also numerous interactions between the independent variables, making analysis or modelling more difficult.

For this investigation, the factors affecting permanent deformation were classified into eight unique categories and a ninth category encompassing combinations of the first eight. The categories are listed in Table 2 in no particular order of importance.

Table 2: Categories for Rutting Variable Classification

Category	Variable Grouping
A	Bituminous Materials and Additives
B	Mineral Aggregates
C	Mix Design Parameters
D	Strength/Resistance Properties of Mix
E	Pavement Structural Design
F	Construction-Related
G	Environmental
H	Traffic-Related
X	Combinations of Above Categories

A breakdown of the individual categories and their variables is presented in the following sections.

2.6 Category A – Bituminous Materials and Additives

As defined by the TAC (1997), bituminous materials are petroleum-based products of oil refining or naturally occurring asphalts. Asphalt is a dark brown to black solid or semisolid cementitious material that softens and liquefies when heated. Asphalt cement (AC) receives further refinement to meet specifications for paving and related purposes.

Although liquid asphalts (made from asphalt cement) are available, asphalt cement is the only material used for the production of hot-mix asphalt concrete (HMAC). Liquid asphalts are used primarily for cold-mix asphalt concrete, a less durable material not regularly used for road construction in Canada. Therefore, only asphalt cement and HMAC-related variables were considered during this investigation.

2.6.1 Effect of Chemistry

Asphalt cement consists of asphaltenes, oily constituents and asphaltic resins (TAC 1997). At present, data that conclusively relates the chemical properties of asphalt cement to permanent deformation is relatively limited.

A 1983 study performed on Interstate 90 in Montana compared the performance of asphalt cements from each of that state's oil refineries. Reports by Bruce (1987) and Jennings et. al. (1988) showed that asphalt cements containing lower levels of asphaltenes and saturates were more susceptible to rutting. No conclusive relationships were observed for other constituents such as polar aromatics or naphthene aromatics. However, the authors cautioned that mix design asphalt content could have been an overriding factor for that investigation.

2.6.2 Effect of Penetration/Viscosity

Penetration is an empirical measure of asphalt cement hardness. In theory, the greater the penetration, the more susceptible the asphalt concrete pavement is to permanent deformation. However, the penetration test is performed at a standard temperature of 25°C whereas rutting typically occurs at more elevated temperatures between 40°C and 60°C. Therefore, while various asphalt cements may yield similar penetration values, their high temperature performance may be markedly different. This has been the case to date since little data conclusively relates penetration to permanent deformation.

Viscosity is a measure of the resistance of the asphalt binder to flow (shear) at a specified temperature. Unlike penetration, viscosity measurements are often made at high temperatures to better capture the asphalt cement properties at temperatures more indicative of rutting (see Category G for the effect of temperature on pavement rutting).

Results of Bruce (1987) and Jennings et. al. (1988) did indicate that higher penetration and viscosity numbers seemed to result in greater rutting. However, this trend may have been influenced by the asphalt content in the mixes.

The NCAT National Rutting Study completed by Cross and Brown (1992, 1991) indicated that higher penetration values were correlated with increased rutting for mixes with more than 2.5% air voids in-place. However, the degree to which penetration correlated with rutting was much lower than that observed for aggregate properties. Conversely, a rutting study completed in Saskatchewan by Huber and

Heiman (1987) concluded that penetration and viscosity did not demonstrate a significant effect on rutting performance.

Nievelt and Thamfld (1988) concluded that asphalt cements with higher viscosity values produced asphalt mixes with greater rutting resistance as tested using wheel-tracking tests on samples at multiple test temperatures.

It should be mentioned that the new Superpave performance-graded (PG) binder specification has been implemented in Ontario (MTO 1998). This new specification does not rate asphalt cements based on penetration at a standard test temperature. Indeed, a rigorous testing regime using a combination of the Dynamic Shear Rheometer and Dynamic Viscometer measure viscosity at medium and high temperatures to better characterize high temperature binder performance (Asphalt Institute 1997a). However, penetration has been included in this investigation as the vast majority of existing roads were designed using the Marshall method, not the Superpave mix design system. Clearly, the effect of PG Binder properties would be applicable to new roads designed using Superpave.

2.6.3 Effect of Modifiers

As will be discussed further in Category G, asphalt cement properties are highly temperature sensitive. As temperature of the asphalt cement increases, its stiffness decreases, thereby increasing the potential for permanent deformation, as a larger deflection of the asphalt layer is incurred under the same load. The high temperature susceptibility of asphalt cement may be reduced through the addition of polymer modifiers. Terrel and Epps (1988) list a number of modifiers in Table 3.

Table 3: Various Asphalt Cement Modifiers
(from Terrel and Epps 1988)

Polymer Type		Example
Rubber	Natural latex	Natural rubber
	Synthetic latex	Styrene-butadiene (SBR)
	Block copolymer	Styrene-butadiene-styrene (SBS)
	Reclaimed rubber	Recycled Tires
Plastic		Polyethylene
		Polypropylene
		Ethyl-vinyl-acetate (EVA)
Combination		combination of above

2.6.4 Effect of Other Additives

In addition to polymer modifiers, other additives such as liquid anti-stripping agents or hydrated lime are used to improve the bond between the asphalt cement and the aggregate particles. Krutz and Stroup-Gardiner (1990) investigated the influence of moisture damage on rutting for the Nevada Department of Transportation (DOT). The loss of asphalt cement from stripping allowed the aggregates to shift, causing severe rutting of the pavements analysed. Therefore, the use of anti-stripping additives should reduce rutting by reducing the loss of asphalt concrete through moisture damage.

2.7 Category B - Mineral Aggregates

2.7.1 Effect of Source Properties

Aggregate source properties include soundness, toughness and deleterious materials. These properties are empirical in nature and are usually used only to evaluate local aggregate sources on a comparison basis.

While studying the effect of gradation on permanent deformation for the Nevada DOT, Krutz and Sebaaly (1993) compared source properties of various aggregates. A test regime utilising standard triaxial and repeated triaxial tests revealed that rutting performance of mix gradations containing substantial amount of fine material (i.e. finer overall gradations) was directly linked to source properties.

While not targeting any individual pavement distress, Wu et. al. (1998) subjectively compared source properties to pavement performance. The Micro-Deval (toughness) and Magnesium Sulphate Soundness (soundness) tests were more strongly correlated with the subjective pavement performance ratings compared to other source property tests such as the Los Angeles Abrasion and Freeze-Thaw Soundness tests.

2.7.2 Effect of Consensus Properties

Aggregate consensus properties include coarse aggregate angularity, fine aggregate angularity, flat and elongated particles and clay content.

The NCAT National Rutting Study concluded that the effect of aggregate angularity on rutting was dependent on in-situ air voids (Cross and Brown 1992, 1991). For in-situ air voids above 2.5%, the angularity of the coarse aggregate (two or more crushed faces) and the National Aggregate Association uncompacted voids for the fine aggregate (now referred to as "fine aggregate angularity") were highly correlated with rate of rutting. If the in-situ voids were less than 2.5%, rutting was likely to occur regardless of aggregate properties.

Marks et. al. (1990) concluded that the percentage of crushed aggregate strongly influenced creep resistance factors. As the percentage of crushed material

increased, creep resistance factor also increased. The relationship of creep to rutting is presented in Category D.

Button et. al. (1990) observed the relationship between aggregate properties and permanent deformation as the amount of manufactured (crushed) sand was replaced with rounded natural sand in the mix. The first observation was that the texture, shape and porosity of the fine aggregate were major factors related to plastic deformation. Second, permanent deformation increased significantly as the percent of rounded natural sand increased (i.e. as manufactured sand was replaced).

No information was found for flat/elongated particles or clay content at this time. However, it is well known that flat and elongated particles tend to break under compactive effort, altering the gradation of the mix. Clay is a compressive soil that can potentially change volume with time and moisture causing localized swell or settlement in the pavement structure.

2.8 Category C – Mix Design (Volumetric) Parameters

2.8.1 Introduction to Volumetric Parameters

A comprehensive historical review (and reinterpretation) of mix design volumetrics was presented by Coree (1999). Coree divided volumetric parameters into two main categories - Primary and Secondary as detailed below.

Primary Volumetric Parameters

The primary volumetric parameters are those relating directly to the relative volumes of the individual components:

- Air Voids, V_v - the volume of air voids

- Binder Volume, V_b - the volume of the bituminous binder

- Aggregate Volume, V_s - the volume of the mineral aggregate

Figure 9, commonly referred to as a "phase diagram," displays the various volumetric components.
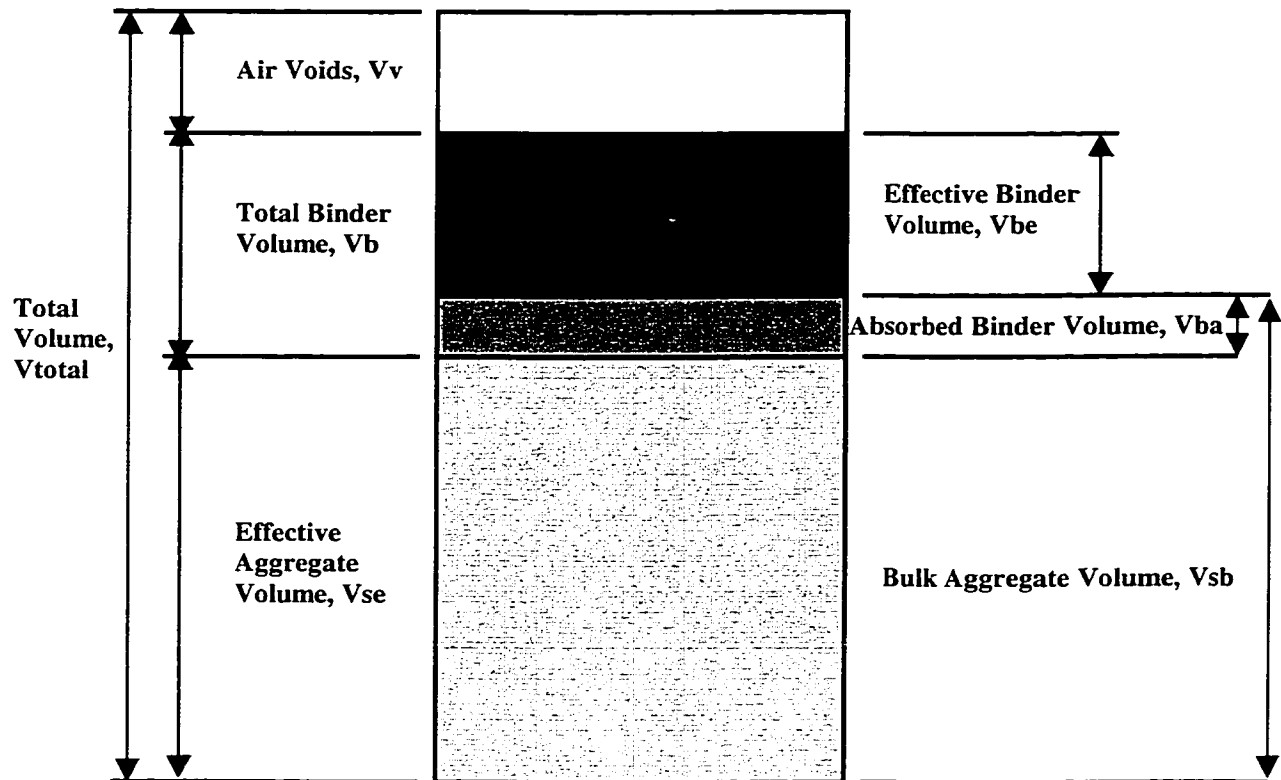
Figure 9: Phase Diagram of Mix Constituents in Compacted Specimen (from Coree 1999)

As shown, the bituminous binder is absorbed into the external pore structure of the aggregate such that a portion of the aggregate and bituminous binder share space. Therefore, the sum of the individual volumes ($V_b + V_s$) is greater than their combined volume (V_{b+s}). This situation allows further sub-division of the primary parameters given above:

- Effective Binder Volume, V_{be} - the volume of bituminous binder *external* to the aggregate particles, i.e., that volume *not* absorbed into the aggregate

- Absorbed Binder Volume, V_{ba} - the volume of bituminous binder *absorbed* into the internal pore structure of the aggregate

- Bulk Aggregate Volume, V_{sb} - the total volume of the aggregate, comprising the "solid" aggregate volume, the volume of the pore structure permeable to water but not to bituminous binder and the volume of the pore structure permeable to the bituminous binder

- Effective Aggregate Volume, V_{se}, - the volume of the aggregate comprising the "solid" aggregate volume and the volume of the pore structure permeable to water but not to bituminous binder.

- Apparent Aggregate Volume, V_{sa} - the volume of the "solid" aggregate, i.e., that volume permeable to neither water nor bituminous binder.

Secondary volumetric parameters

Three additional parameters have been widely used, and at various times, have formed critical design thresholds. These are the Percent Air Voids, V_a, the Voids in the Mineral Aggregate, VMA, and the Voids Filled with Asphalt, VFA.

- Percent Air Voids, V_a - simply V_V expressed as a percentage of the total volume of the mixture.

- Voids in the Mineral Aggregate, VMA - the sum of V_V and V_{be} expressed as a percentage of the total volume of the mixture. This parameter is directly analogous to "porosity" in soil mechanics.

• Voids Filled with Asphalt, VFA - the degree to which the VMA are filled with the bituminous binder, expressed as a percentage. This property is directly analogous to the "degree of saturation" in soil mechanics.

It is important to recognize that V_a, VMA and VFA are highly dependent on the degree of compaction and, according to Coree (1999), secondary parameters should never be quoted without referencing the degree of compactive effort used.

The following relationships may be derived from the above definitions and Figure 9:

$$VFA = \frac{V_{be}}{V_v + V_{be}} * 100 \qquad V_a = \frac{V_v}{V_{total}} * 100 \qquad VMA = \frac{V_v + V_{be}}{V_{total}} * 100$$

Simple algebraic manipulation reveals that the above equations are not mutually exclusive, since:

$$VFA = \frac{VMA - V_a}{VMA} * 100$$

Coree (1999) explained that in the process of mixture design, it is frequently necessary to seek to change the magnitude of one or more of these parameters. For example, upon analyzing a mixture, it may appear desirable to increase the VMA (a relatively common problem), or to manipulate the air voids. Various recommendations and techniques exist to achieve this. However, it is neither clear what effect such a change might have on the other parameters, nor whether that change might, in itself, compromise compliance in another direction. Indeed, no such change in any one parameter should ever be contemplated without checking the effects on the other two.

Although the interaction of volumetric properties is complex and greatly affects pavement performance, the effects of individual properties have been noted by numerous studies and are presented below.

2.8.2 Effect of Air Voids

In-situ air void content has been identified as perhaps the most critical parameter affecting rutting. Furthermore, the range of air voids identified for good rutting resistance is well known. Indeed, it was observed that for the roads selected during the NCAT study, none of the 50 or 75-blow mixes displayed unacceptable rutting rates if in-situ air voids remained greater than 4%.

Brown and Cross (1990) provide the following explanation:

> *An asphalt mixture with low voids acts very much like a saturated soil. It has no shear strength. When the voids are reduced to a very low level (2 to 3 percent), pore pressures tend to build up under traffic, the effective stress on the aggregate is reduced, and shear or plastic flow takes place.*

Therefore, pavements which retain 4% air voids or greater after years of traffic loading show excellent performance with respect to rutting.

Both Huber and Heiman (1987) and Kandhal et. al. (1993) concluded that pavements begin to exhibit plastic deformation when the air voids reached threshold values (usually 3% or less).

2.8.3 Effect of Asphalt Cement Content

Asphalt cement content refers to the amount (percentage) of asphalt binder in the asphalt mixture by weight. Effective asphalt content does not include the asphalt binder absorbed in the mineral aggregate. For rutting resistance, asphalt cement content should be relatively low to prevent shear flow under loading and

elevated temperature. However, enough asphalt cement must be present to bind the aggregate particles in place.

Huber and Heiman (1987) concluded that asphalt content and voids filled with asphalt were the most basic parameters affecting rutting, while Abd El Halim et. al. (1995) indicated that rutting decreases with increasing asphalt content to a maximum value, after which rutting increases with increasing asphalt content.

The Montana study, while not exploring the effect of asphalt content specifically, indicated indirectly the importance of asphalt content by cautioning that mix design asphalt content could have been the overriding factor for that investigation (Bruce 1987 and Jennings et. al. 1988).

Cross and Brown (1992, 1991) indicated that asphalt cement content was extremely important to rutting resistance. Kandhal et. al. (1993) echoed the importance of asphalt cement content by indicating that excessive asphalt content could effectively nullify other good properties of a mix such as crushed aggregates.

2.8.4 Effect of Gradation

A study of 32 asphalt concrete overlays placed over rigid pavements completed by Carpenter and Enockson (1987) indicated that the majority of rutting problems could be attributed to gradation. The tender mix phenomenon associated with a "hump" in the 0.45 power gradation chart was associated with rutting. Furthermore, the percent passing the No. 40 sieve and retained on the No. 80 sieve was found to influence rutting.

As previously mentioned, the effect of gradation on permanent deformation was studied by Krutz and Sebaaly (1993) for the Nevada Department of Transportation (NDOT). A second conclusion from this study was that rutting

resistance of finer gradations was influenced by binder characteristics more so than for more coarse gradations. Conversely, the performance of coarse gradations is more dependent on aggregate properties and less sensitive to binder type.

Work completed by Anani et. al. (1990) in Saudi Arabia indicated that a finer gradation of coarse portion of the aggregate (No. 4 and above) improved rutting resistance. This conclusion is in general disagreement with conventional (North American) mix design, however, as indicated by Krutz and Sebaaly (1993), finer gradations are more sensitive to binder type than more coarsely graded mixes. The binder used for the coarse mixes may have been different from that used for the finer graded mixes (or a different asphalt content). Furthermore, the loading condition of the selected roads was not reported. The effects of loading conditions on rutting resistance are explored in Category E.

Brown and Bassett (1990) indicated that increasing the maximum aggregate size of the mix increased the mix quality with regard to creep performance, resilient modulus and tensile strength. Each of these properties has an important relationship to rutting performance as will be presented in Category D.

2.8.5 Effect of VMA and VFA

The use of VMA and/or VFA to predict pavement performance has been debated for almost 100 years. Specifications for VMA and VFA were originally developed to provide a minimum asphalt content in the mix for durability and a minimum voids content for rutting.

While various researchers argue which parameter better predicts performance, most agree that increasing VMA and VFA (to maximum values) are good methods

to reduce rutting. Some investigations concerning VMA and VFA with respect to rutting are as follows.

Anani et. al. (1990) indicated that VMA was a primary variable with regard to rutting for the surface coarse. VMA of the unrutted sections was higher than that of the rutted sections.

Huber and Heiman (1987) indicated that VFA was one of the most basic parameters affecting rutting. Increasing VFA to a maximum value decreased rutting, while Carpenter and Enockson (1987) expressed that VMA was a significant variable for rutting.

The NCAT study indicated that VMA was more significant for the base coarse than the surface coarse (Cross and Brown 1992, 1991).

2.8.6 Effect of Dust Content

Coarsely graded asphalt mixes often include a relatively high proportion of dust to increase the stiffness of the asphalt binder. This is particularly true of Stone Mastic Asphalt (SMA) mixes that require stiff mastics to prevent the large aggregate particles from moving under load. As with polymer modification, increasing the stiffness of the asphalt cement by increasing dust content reduces susceptibility to rutting (at the expense of fatigue resistance). However, mixes with too much dust may display poor adhesion between the asphalt cement and the aggregate particles (stripping).

2.8.7 Effect of Laboratory Density and Compaction

One basic assumption underlying the mix design process is that prepared laboratory specimens will have the same density (and air voids) as the mix in the field after years of traffic (typically 4 percent). Insufficient laboratory compactive

effort results in low in-situ air voids since primary (construction) and secondary (traffic) compactive effort will be greater. As previously discussed, low air voids (below 3%) are a major cause of rutting in asphalt pavements. Conversely, excessive laboratory compaction leads to in-service pavements with high air void contents (10% or even higher). This situation results in excessive traffic induced compaction. Furthermore, continuous air voids are formed at high voids content, increasing permeability, which can reduce durability through accelerated ageing and/or stripping.

For the Marshall method, the NCAT study observed that stronger relationships between mix properties and rate of rutting were found for 75-blow mixes than with 50-blow mixes (Cross and Brown 1992, 1991). This result is expected since 75-blow Marshall mixes are designed specifically with rutting resistance as the primary design criteria. Fifty-blow mixes are designed for lower volume roads, whose primary design criteria are likely fatigue and thermal cracking resistance as opposed to rutting.

Kandhal et. al. (1993) found that mixtures are generally compacted to a higher degree by traffic than that provided by laboratory (Marshall) compaction. It was therefore recommended that laboratory compactive effort be increased for pavements designed specifically for heavy traffic.

Particle orientation under compactive effort also contributes to rutting as indicated by varying performance observed with Marshall compaction, gyratory compaction and roller compaction. Kandhal et. al. (1993) concluded that a Marshall compactor with rotating base and slanted foot gave the highest density overall when compared to standard Marshall and gyratory compaction. However, the gyratory

compactor achieved densities greater than the standard Marshall compactor for large

aggregate gradations. Additional research concerning laboratory compactor type

was completed by SHRP. Studies by Harvey and Monismith (1993), and Sousa et.

al. (1991) have concluded that gyratory, rolling wheel, and kneading compaction

produced specimens with significantly different permanent deformation responses

to repeated shear loading. This indicated that each compaction method caused a

particular type of aggregate structure and binder-aggregate film. It has also been

shown that fatigue behaviour of a compacted mix is influenced by the mixing and

compaction viscosities of the binder (Harvey et. al. 1994).

It should be mentioned that the Superpave system has adopted gyratory

compaction, as the specimens are much smaller and easy to handle. Unfortunately,

gyratory compaction does not produce the same aggregate and void structure as

field compaction, therefore, permanent deformation response of gyratory compacted

specimens will not be representative of an in-service pavement.

Finally, consistency of laboratory specimen preparation is another important

consideration. A round-robin test program completed by Lai (1993) investigated

the variation in laboratory compacted specimens tested using the Georgia Loaded

Wheel Tester by six different laboratories. Each laboratory prepared test specimens

using materials provided by Georgia DOT. Lai observed that although the variation

in density among specimens prepared within each laboratory was very low, the

variation among individual laboratories was very large. This indicated that different

laboratories used different preparation techniques, which in turn affected the

performance of the laboratory specimens. Indeed, rutting observed from the LWT

was significantly different among the different laboratories for the exact same mix.

The results clearly indicate that improvement and standardisation of laboratory

preparation specifications is required.

2.9 Category D – Strength/Resistance Properties of Mix

2.9.1 Effect of Marshall Testing

Like penetration, the Marshall stability and flow tests are empirical in nature.

Not surprisingly, results from Marshall tests have not yielded consistent information

regarding rutting resistance. Huber and Heiman (1987) concluded that Marshall

stability and flow values did not show an independent effect on rutting performance.

Similarly, the NCAT National Rutting Study concluded that Marshall

recompacted mix properties (stability and flow) did not correlate well with rate of

rutting (Cross and Brown 1992, 1991).

Conversely, Anani et. al. (1990) concluded that Marshall stability was

generally higher for unrutted sections and was a significant variable for rutting in

the base asphalt coarse.

It should be noted that Hveem stability has been directly correlated with

rutting since the test assesses the shear capability of the mix. However, since the

Hveem method is not used in Canada, it will not be pursued further for this project.

2.9.2 Effect of Shear Strength and Stiffness

Shear properties of an asphalt pavement are achieved through both aggregate

particle contact to form a tight, load-bearing skeleton and the asphalt binder that

holds the particles in place. At elevated temperatures, Alavi and Monismith (1994)

concluded that the influence of the aggregate skeleton is more pronounced than

binder properties. However, the influence of the binder on shear strength/stiffness increases dramatically at the onset of plastic failure as the in-situ air voids decrease below 2.5%.

During the NCAT study, gyratory testing machine (GTM) specimens were tested for shear properties and showed that the gyratory shear index (GSI) had higher correlation with rutting than the Marshall stability and flow (Cross and Brown 1992, 1991). The best relationship found was between rutting and GTM shear strength. As the shear strength decreased (GSI increased), the rate of rutting increased as well.

Kandhal et. al. (1993) also confirmed that GSI values were directly proportional to rutting performance. Pavements displaying high GSI values indicated high potential for rutting.

The importance of shear strength and stiffness has been emphasised by the United States Strategic Highway Research Program (US-SHRP 1994). US-SHRP research has identified that rutting appears to be more closely related to shear stress than normal or horizontal stresses. The SHRP research also referenced work by Célard (1977), who emphasised that based on the results of dynamic creep tests, the rate of permanent deformation was strongly related to shear stress. For example, Célard increased the shear stress from 0.1 MPa to 0.25 MPa (at constant normal stress of 0.1 MPa) and observed a 100-fold increase in the rate of permanent deformation. However, varying the normal stress did not appear to change the rate of permanent deformation.

Laboratory analysis of asphalt concrete cores by Abd El Halim et. al. (1995) indicated that increasing the shear strength of any asphalt mix can reduce surface rutting significantly.

2.9.3 Effect of Resilient Modulus and Indirect Tensile Strength

The resilient modulus M_r, is defined by Huang (1993) as the elastic modulus based on *recoverable* strain under repeated loads. Although asphalt pavements incur some permanent deformation after each load, if it is assumed that the load is small compared to the strength of the asphalt and is repeated a large number of times, the deformation under each load is almost completely recovered and can be considered as elastic (Huang 1993). The resilient modulus is determined through the indirect tension apparatus, and is considered a non-destructive test, allowing the same sample to be used a number of times under different loading and environmental conditions. The indirect tensile strength test, however, fails the sample.

The strength tests completed by Carpenter and Enockson (1987) showed that resilient modulus and indirect tensile strength bore a strong relationship to rutting for asphalt overlays placed over concrete bases.

Anani et. al. (1990) indicated that resilient modulus was inversely related to rutting for both the surface and base asphalt layers. Unrutted sections generally displayed higher M_r values than rutted pavements, however, threshold values were not given in the investigation.

Abdel Nabi (1995) observed a linear relationship between the laboratory shear strength and indirect tensile strength of asphalt cores. This finding indirectly

suggested a relationship between indirect tensile strength and rutting through the relationship to shear strength.

2.9.4 Effect of Creep

Because asphalt concrete is a viscoelastic material, its properties are temperature and time dependent. One method to characterize this behaviour is through creep compliance at various times. Huang (1993) noted that at constant stress, the creep compliance is the reciprocal of Young's Modulus. Creep compliance is determined through a creep test, involving either static or dynamic creep loading.

Van de Loo (1974) analysed the relationship between rutting and creep testing. Data from static and dynamic creep tests indicated that mix stiffness decreased as the number of load applications increased (likely due to strain softening). During the same study, Van de Loo also developed a method of estimating rut depth based on his results, often referred to as the "Shell Method."

2.10 Category E - Pavement Structural and Geometric Design

2.10.1 Effect of Order of Rigidity of Pavement Layers

Structural design of asphalt pavements is a critical component to rutting performance as the state of stress and strain under traffic loading is directly related to the structural system. Typical newly constructed pavements (asphalt concrete or PCC) are constructed such that the quality and strength of the pavement layers decreases with depth. For example, the asphalt concrete (or PCC) is of higher quality and strength (rigidity or stiffness) than the granular base layer(s), which in

turn is of higher quality and strength than the natural subgrade. Under this condition, the compressive load applied by the tires causes beam action in the asphalt layer subjecting the top of the granular base and subgrade to vertical compressive stress while the bottom of the asphalt layer is subjected to tensile stress. The actual stresses experienced in the pavement structure are dependent on the modular ratios of the constituent layers. Huang (1993) shows that, as the modular ratio increases, the vertical compressive stresses applied to the top of the subgrade are lowered significantly. A high modular ratio is therefore desirable to minimise rutting of the subgrade layer. Rutting of these pavements typically occurs over longer time as the granular layers and/or subgrade consolidate under the asphalt layer.

However, in the early 1980's, observations made in Ontario and Nova Scotia showed that rutting of asphalt overlays was occurring after only a few years in service. It was apparent that this new type of rutting was not described using the conventional theory. Gervais and Abd El Halim (1990) used the concept of relative rigidity and field observations to explain this phenomenon. The premature rutting for these cases was a result of the low modular ratio between the overlay and the underlying mature asphalt (or PCC) layer. Even after compaction, the new overlay remains relatively soft, producing a low relative rigidity between the asphalt layers. Under this condition, they showed that the asphalt overlay was in a state of compressive stress. The compressive stresses measured were small and not considered to be the rutting failure criterion. However, the resulting strain condition revealed that high tensile strains were produced within the asphalt overlay causing lateral flow of the soft overlay material. The compressive stress condition acted to

confine the deformations such that only the overlay deformed, much like a sandwich.

2.10.2 Effect of Pavement Layer Thickness

Pavement layer thickness also plays a major role in determining the stress and strain distributions throughout the pavement structure. In general, increasing asphalt layer thickness causes the same effect as increasing the modular ratio of the pavement layers, that being a reduction in the vertical compressive stress applied to the underlying base, sub base and subgrade layers. This in turn reduces rutting.

Kandhal et. al. (1993) concluded that the underlying layer conditions (modulus and thickness) contributed to the surface rut depth in the majority of cases. This is not surprising since that investigation examined asphalt overlays on top of PCC pavements. Although not referencing the relative rigidity concept in that report, the findings of Kandhal et. al. (1993) appear to confirm the explanation of premature rutting presented by Gervais and Abd El Halim (1990).

2.10.3 Effect of Surface (Wearing) Course vs. Base Coarse

Anani et. al. (1990) completed separate analyses for the surface (wearing) course and the base asphalt course. Regression analysis indicated that different variables were significant for the individual asphalt layers. This observation is not surprising since applied stresses and strains are significantly different depending on location in the pavement structure.

The NCAT study also completed separate analyses for surface and base asphalt layers (Cross and Brown 1992, 1991). As with Anani et. al. (1990), different variables were significant for the respective asphalt layers, however, the

strongest rutting relationships were observed in the surface layer. This is not surprising since almost all of the rutting was observed in the surface layer.

2.10.4 Effect of Pavement Alignment

Abdel Nabi (1995) demonstrated that route alignment significantly influences rutting performance. Pavement sections on hills and curves often display increased rutting due to two (additive) mechanisms. First, traffic speed is reduced for these sections, thereby reducing the asphalt layer modulus and increasing rutting. Second, the asphalt layers for these sections are subjected to sustained loading through the force of gravity. This gravity-induced creep was shown to dramatically reduce the shear strength of the asphalt, again increasing rutting under traffic loading.

2.11 Category F - Construction-Related Factors

2.11.1 Effect of Compaction and other Construction Practices

Field compaction must achieve specified in-situ density and air voids to ensure adequate pavement performance. In addition to density/void specifications, field compaction must strive for consistency throughout the pavement construction. Inconsistent compaction causes localized areas containing too little or too many air voids, allowing shear flow or traffic induced densification, respectively.

Pavement surface permeability is an area of construction that is commonly overlooked. A watertight surface prevents the infiltration of moisture that can cause surface stripping of asphalt. Furthermore, infiltration of moisture into the base and subgrade layers can cause hydraulic scour under traffic loading. However, in

addition to a watertight surface, adequate drainage must be provided for the granular layers to prevent stripping from below. Good construction and compaction can provide both adequate drainage and a watertight surface if completed properly.

Interestingly, the affect of aggregate particle contact has not been investigated until very recently. Particle contact is essential to transmit traffic loading through the asphalt layer and into the base and subgrade layers. A study underway at the Turner-Fairbank Highway Research Center (FHWA 1998b) involves analysing particle contact in asphalt cores using computerized tomography, as known as "CT" scanning. Initial results indicate that current compaction practices produce aggregate skeletons for which only 15% of aggregates carry over 50% of the applied load and 50% of the particles carry over 80% of the load. These striking results clearly indicate room for improvement concerning the in-service contact of aggregate particles under compactive effort.

The round-robin investigation concerning laboratory compaction variability completed by Lai (1993) also has application to field compaction. Clearly different paving contractors use different techniques to compact asphalt concrete, leading to significant variability between various sites and even along individual sites. Field compaction has long been touted as the most significant variable toward pavement performance (including rutting), however, little resources have been allocated toward improvement in the current compaction techniques or equipment.

Carpenter (1993) reported that the mix parameters produced during the initial construction of the pavement will influence how much permanent strain occurs when the limiting voids develop. In more simple terms, initial mix properties

produced during field compaction determine how much rutting occurs prior to the onset of plastic flow.

Of course, significant work has been completed by Abd El Halim in the field of asphalt compaction. Numerous field tests with the AMIR compactor have conclusively shown that improved compaction techniques reduce variability of density throughout the pavement structure, reduce permeability and improve pavement fatigue life by up to 50 percent (Abd El Halim et. al. 1995).

2.11.2 Effect of Quality Control/Quality Assurance (QC/QA)

Consistency during construction is critical to pavement performance. Poor QC allows areas with varying parameters and promotes localized deformation. Poor QA allows global permanent deformation if critical rutting variables are poor.

The NCAT study recommended that the most important QC/QA test that can be conducted during construction is to compact plant produced material in the laboratory and evaluate the air voids of the specimens (Cross and Brown 1992, 1991). This recommendation makes a strong case to provide on-site evaluation for QC/QA purposes.

Kandhal et. al. (1993) indicated that asphalt content measured from field cores was generally deficient from the value specified for the job-mix formula (laboratory mix design). Clearly, improved control over asphalt content is required for plant production since asphalt content is one of the primary factors governing rutting performance of pavements.

2.12 Category G - Environmental Factors

2.12.1 Effect of Temperature

Asphalt cement (and therefore asphalt concrete) is highly temperature

sensitive. Anani et. al. (1990) noted that, because asphalt concrete is black, solar

energy is readily absorbed and then retained due to its low thermal conductivity. As

the temperature of the pavement increases, the stiffness of the asphalt layer(s)

decreases. Reduced asphalt cement stiffness allows aggregate particle movement

and reorientation under traffic loading causing permanent deformation. Therefore, a

strong aggregate skeleton is required to resist rutting at elevated temperatures.

An excellent illustration of the effects that temperature can impose on asphalt

binder stiffness was published by Rickards (1998). Using the Shell Bands program,

asphalt binder stiffness was plotted versus temperature in response to the

compactive effort of three different compaction devices as shown in Figure 10.
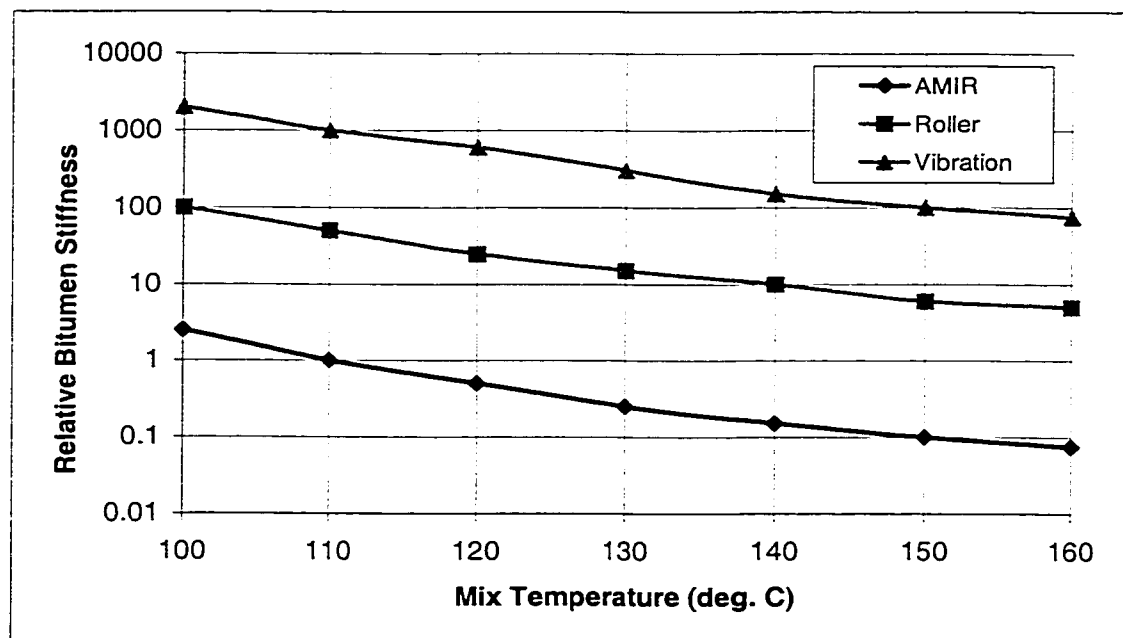
Figure 10: Bitumen Stiffness vs. Mix Temperature for Three Compaction Devices (from Rickards 1998)

Figure 10 clearly displays the reduction in binder stiffness with increasing temperature for each of the compaction devices. As an example, an increase in temperature of 40°C (110°C to 150°C) caused a 10-fold reduction in stiffness.

While such elevated temperatures are not usually encountered during normal operating conditions, extrapolation of Figure 10 suggests similar relative changes in stiffness could be experienced for more typical operating temperatures. This statement is supported by Hofstra and Kolomp (1972) who observed the significant effect that normal operating temperatures can have on asphalt mixes. During their investigation, a change in temperature from 20°C to 60°C reduced the modulus (stiffness) of the asphalt concrete by a factor of 60, while rutting increased by a factor ranging from 250 to 350 times. Clearly, temperature has a significant effect on asphalt pavement rutting.

A final example of the significant effect that temperature (and direct sunlight) have over rutting performance was noted by Anani et. al. (1990) in Saudi Arabia where rutting was significantly reduced, or even non-existent, under bridges where the pavement is shaded by the bridge deck.

2.12.2 Effect of Ageing

Over time and environmental conditioning, asphalt cement loses some of its flexibility (i.e. its stiffness increases). Therefore, the oxidation of asphalt cement actually increases the pavements resistance to permanent deformation so long as the bond between the asphalt cement and aggregate particles is maintained.

Kandhal et. al. (1993) explained that during early stages of a (newly constructed) pavement life cycle, rutting is directly proportional to traffic.

However, after this initial densification, the rate of rutting decreases with increasing traffic until finally a condition of plastic flow occurs and the rate of rutting again increases.

The importance of separating the rutting cycle into distinct periods was further held by Carpenter (1993). According to Carpenter, two vital criteria to judge the long term performance of a mixture are how quickly a critical rut depth is reached in the mixture, and the "rapidity" with which the mixture reaches the failure point at the onset of plastic flow. These criteria are not mutually inclusive as a mixture may reach critical rutting before the mixture becomes unstable, or it may become unstable before it reaches the critical rut depth.

2.12.3 Effect of Moisture Damage (Stripping)

Stripping involves the removal of asphalt cement from the mineral aggregates through moisture infiltration. Stripping can occur on the surface of the pavement causing loss of surface aggregate (ravelling) or can occur from below the asphalt layers due to poor drainage conditions or sealing of the asphalt surface. The loss of bond between asphalt and aggregate allows the aggregate particles to move or shrift under traffic loading, promoting permanent deformation.

As previously mentioned, Krutz and Stroup-Gardiner (1990) investigated the influence of moisture damage on rutting of chip-sealed pavements for the Nevada DOT. They found that sealing of the surface with the chip-seal accelerated stripping by trapping moisture under the asphalt layers. The loss of asphalt cement allowed the aggregates to shift, causing severe rutting of the pavements analysed. Drainage conditions of the pavements were likely insufficient in those cases.

2.13 Category H - Traffic (Load) Related Factors

2.13.1 Effect of Tire Contact Pressure (Load Magnitude)

The size of the tire contact area depends on the contact pressure between the tire and the pavement surface. Huang (1993) indicates that pavement contact pressure is greater than the tire pressure for low-pressure tires, because the walls of the tire are in compression and the sum of the vertical forces due to wall and tire pressure must be equal to the force due to contact pressure. Contact pressure is smaller than the tire pressure for high-pressure tires, because the tire walls are in tension. For simplicity, most pavement designs assume that the contact pressure is equal to the tire pressure, which is consistent with the findings of Gerrard and Harrison (1970).

Kandhal et. al. (1993) have reported that tire pressures have increased substantially in recent years. Tire pressures average 661 kPa (96 psi) and 689 kPa (100 psi) in Illinois and Texas surveys, respectively. Therefore, increased pressures are applied to the pavement, which will cause increased pavement damage.

Substantial finite element modelling of the effect of tire pressure was also completed during the SHRP research. Model runs were completed with tire pressures of 690 kPa (100 psi), 1380 kPa (200 psi) and 3450 kPa (500 psi), respectively. Results indicated that rut depth increased almost linearly with increased maximum permanent strain, which was directly related to increased tire pressure (US-SHRP 1994).

2.13.2 Effect of Tire Material

The concept of relative rigidity is also applicable to the modular ratio between the tire and the asphalt surface. Tires composed of different rubber/steel combinations produce different modular ratios between the tire and the asphalt surface, which affects the contact stresses. Gervais and Abd El Halim (1990) proposed that the switch from bias-ply to radial tires by the automotive industry represented a fundamental increase in rutting damage to asphalt pavements.

2.13.3 Effect of Number of Load Applications (ESAL's)

Rutting usually occurs over an extended period of time with numerous load applications according to the rutting cycle outlined by Kandhal et. al. (1993) and Carpenter (1993). With each applied load, a small amount of permanent deformation is introduced within the asphalt layer. The magnitude of this deformation is dependent on the stage of rutting.

Therefore, the number of applied ESAL's is directly proportional to rutting in asphalt pavements, at least during the traffic densification stage. Many rutting models incorporate ESAL counts, whereas some investigations such as Anani et. al. (1990) do not incorporate traffic effects directly, considering traffic to be an uncontrollable variable.

Other researchers have converted the total amount of rutting into a rutting rate by normalizing with traffic such as Cross and Brown (1992, 1991) during the NCAT National Rutting Study as well as Kandhal et. al. (1993). Other studies by Brown and Cross (1988) and Parker and Brown (1990) indicated that expressing the rate of rutting as a function of the square root of total traffic better models pavement behaviour than other expressions such as the arithmetic sum or log of total traffic.

2.13.4 Effect of Rate of Loading

Being a viscoelastic substance, the stiffness of an asphalt concrete pavement is dependent on load duration as well as temperature. Loads applied slowly cause a reduction in layer stiffness thereby increasing rutting by allowing asphalt to flow (similar effect to increasing temperature). Again, a strong aggregate skeleton is required to minimise rutting under these conditions.

Generally, the greater the speed, the larger the (asphalt concrete) layer modulus, and the smaller the strains in the pavement (Carpenter and Enockson 1987). Therefore, higher travelling speeds actually cause less rutting than lower travelling speeds (all else equal). The effect of load rate is apparent at areas of reduced speed such as intersections, hills and curves that exhibit increased rutting.

The effect of load application rate is also apparent in Figure 10 (Rickards 1998). The three separate lines in Figure 10 simulate three asphalt compactors applying different load rates to the asphalt concrete. As shown, the higher loading rate of the vibratory compactor invokes a greater stiffness response of the asphalt binder than the static steel roller or AMIR roller, respectively.

2.14 Category X – Combinations of the Other Categories

Variables listed in the above eight categories have been reviewed independently. However, many of these variables are strongly colinear and therefore work together (or against each other) to provide resistance to rutting. The interaction of aggregate angularity and in-situ air voids towards rutting was observed during the NCAT National Rutting Study. For in-situ air voids above 2.5%, the angularity of the coarse

aggregate (two or more crushed faces) and NAA uncompacted voids for the fine aggregate (aka fine aggregate angularity) are highly correlated with the rate of rutting. If the in-situ voids were less than 2.5%, rutting is likely to occur regardless of aggregate properties (Cross and Brown 1992, 1991).

The interaction between asphalt cement and gradation towards rutting was studied by Krutz and Sebaaly (1993). They concluded that rutting performance of finer gradations is influenced by binder characteristics more so than more coarse gradations. Conversely, the performance of coarse gradations is more dependent on aggregate properties and less sensitive to binder type.

The effect of asphalt-aggregate interaction was also completed during the SHRP research (US-SHRP 1994). Regression analysis of rutting induced by wheel-tracking devices displayed that asphalt-aggregate interaction accounted for upwards of 15% of the observed rutting. Finally, the interaction of volumetric properties such as air voids, VMA and VFA was well examined by Coree (1999) as presented in Section 3.3.

2.15 Summary of Rutting Variable Relationships

Table 4 summarizes the qualitative relationships between the categorized variables and permanent deformation. An entry of "Increase" indicates that rutting resistance increases with an increase in that particular variable, while an entry of "Decrease" indicates that rutting resistance is reduced with an increase in that variable (i.e. rutting increases all else equal). The inclusion of a question mark "?" indicates that the general trend is not well defined or questionable. The use of the word "max" indicates an upper limit, above which rutting resistance is reduced.

Table 4: Summary Table of Rutting Variables and Qualitative Relationships

Category A - Bituminous Materials and Additives					
Chemistry		Penetration	Viscosity	Use of Modifiers	
Asphaltenes	Saturates	Decrease?	Increase	Polymer	Antistrip
Decrease	Decrease			Increase	Increase?

Category B - Mineral Aggregates						
Source Properties			Consensus Properties			
Toughness	Soundness	Deleterious Materials	Coarse Angularity	Fine Angularity	Flat/ Elongated	Clay Content
Increase?	Increase?	Decrease?	Increase	Increase	Decrease?	Decrease?

Category C - Mix Design Parameters						
Gradation	Air Voids	Asphalt Content	VMA	VFA	Lab Compaction	Dust Content
see section 2.8.4	Increase (max)	Increase (max)	Increase (max)	Increase (max)	Increase (max)	Increase (max)

Category D - Engineering Properties of Mix				
Marshall Testing		Shear Strength/Stiffness	Resilient Modulus/ Indirect Tensile	Creep
Stability	Flow			
Increase?	Increase?	Dramatic Increase	Increase	Decrease

Category E - Pavement Structural Design	
Asphalt Layer Stiffness and Deflection	Asphalt Layer Thickness
Increase	Increase

Category F - Construction-Related	
Field Compaction	Quality Control and Assurance (QC/QA)
Increase (max)	Increase

Category G – Environmental		
Temperature	Aging	Moisture Damage
Decrease	Increase	Decrease

Category H - Traffic-Related		
Contact Pressure (Load)	Number of ESAL's	Rate of Loading (Speed)
Decrease	Decrease	Increase

Category X - Combinations of Above Categories

2.16 State-of-the-Practice: Asphalt Rutting Testers

Pavement rutting testers are currently attracting much attention from the asphalt industry. While some of these devices have been used for years, the widespread adoption of Superpave in the United States (more slowly in Canada), has re-ignited the search for a device that can both separate poor and good performing mixes, and also predict the long term field performance of pavements prior to construction. As mentioned, Superpave currently is based solely on volumetrics, binder and aggregate selection criteria.

At this time, there are numerous asphalt rutting tests in use by various agencies. Some are empirical tests, not based on engineering properties or analysis. Examples include the French Rut Tester, the Hamburg Wheel-Tracking Device, the Asphalt Pavement Analyzer (formerly Georgia Loaded Wheel Tester) and the Accelerated Load Facility (ALF). Other rutting tests, such as the Superpave Shear Tester (SST) measure engineering properties such as the shear strength or modulus (stiffness) of an asphalt mix. It is believed that these performance-based tests hold the most promise for modelling and predicting long term performance of pavements since engineering properties can be directly related to performance.

The objective of this section is to review some of the existing devices, which will lead into the following section that discusses their benefits and weaknesses with respect to performance prediction.

2.16.1 LCPC (French) Rut Tester

The LCPC Rut Tester was developed at the Laboratoire Central des Ponts et Chaussees (LCPC) in France. As shown in Figure 11, the device uses two

reciprocating pneumatic tires with diameter of 415 mm and width of 110 mm to assess the rutting resistance of mixes. Test slabs are 500 mm long, 180 mm wide and either 50 mm or 100 mm in thickness. A standard tire pressure of 0.60 ±0.03 MPa is applied approximately 67 cycles per minute (about 1.1 Hz). One cycle consists of a forward and backward pass of the loaded wheel; therefore, 134 individual passes are completed per minute (Romero and Stuart 1998). Test air temperature of 60°C is maintained without regard to the environment where the pavement is located or the depth at which the mixture is located within the pavement structure (Huber 1999). A LCPC Rut Tester costs about $125,000 CAD.

Interestingly, the developers of the French Rutting Test do not believe that statistical correlation between rutting observed in the test and that observed in the field can be developed since the rut tester simulates extremely severe rutting conditions (Huber 1999). However, LCPC reports that roads meeting the LCPC rut tester specification do not exhibit rutting in service.

Figure 11: LCPC Rutting Tester

Extensive work has been completed in Colorado using the LCPC device to correlate laboratory and field rutting performance by Aschenbrener (1994). The study investigated 33 pavement sections with satisfactory or poor performance in rutting resistance. Test slabs taken from the sites were tested with the LCPC Rut Tester and indicated that the French specifications were too severe for Colorado conditions. To reduce the severity, the test temperature was modified based on the actual field temperatures associated with Colorado conditions. Test data was also separated into high, medium and low categories. Regression analyses yielded high correlation (R^2 of 0.87 for high traffic and 0.68 for medium traffic) between field rutting and the slope of the rutting curve observed with the French device.

LCPC Tests were also completed on specimens recovered from the Westrack experiment. Good correlation (R^2=69.4%) between laboratory values and rutting observed at the test track was achieved through regression analysis (FHWA 1998c).

2.16.2 Hamburg Wheel Track Tester and Couch Wheel Track Tester

Esso AG developed the Hamburg Wheel Tracking Device in Hamburg, Germany in the 1970's (Romero and Stuart 1998). A solid steel wheel with a diameter of 204 mm and width of 47 mm rolls across an asphalt concrete slab immersed in water kept at 40°C or 50°C as shown in Figure 12. Immersion of the test specimens in water allows for the simultaneous testing of rutting and moisture damage (stripping) resistance of various mixes. Test slabs are 320 mm long, 260 mm wide and may be 40, 80 or 120 mm thick. A fixed load of 0.69 kN is applied to the wheels producing an average contact stress of 0.73 MPa (although actual contact pressure varies due to variable contact area during the test). This contact stress approximates the stress produced by one rear tire of a double axle truck.

Approximately 53 passes per minute (26 cycles per minute) are applied and the original test was performed to 9500 wheel passes. However, it was later discovered that some mixes could deteriorate due to moisture damage shortly after 10,000 passes. The number of test passes was subsequently raised to 19,200 to observe moisture damage. A Hamburg Wheel Tracking Device costs about $90,000 CAD.
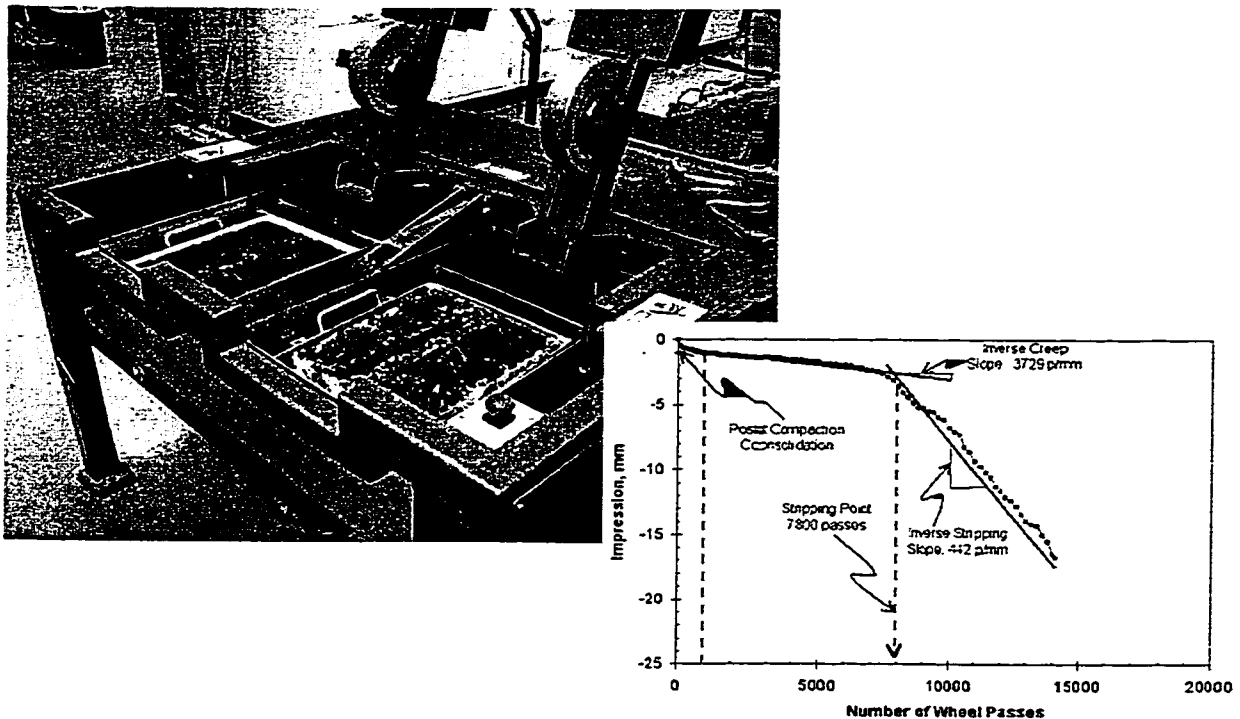
Figure 12: Hamburg Wheel Tracking Tester

Performance correlation between field performance and results from the Hamburg Wheel Tracking Device was also completed at the Colorado DOT by Aschenbrener (1995). Although the Hamburg stripping slope and stripping inflection point were able to distinguish between good and poor field stripping performances, the moisture conditioning system used by the device appeared too severe for rutting determination. However, regression analysis between the

Hamburg device and rutting at Westrack yielded good correlation (R^2=75.6%) (FHWA 1998c).

The Couch Wheel Track Tester is a variation of the Hamburg test. A single solid rubber wheel with an approximate contact pressure of 950 kPa (140 psi) is used to rut an asphalt slab. As with the Hamburg test, specimen temperature is controlled through submerging the specimen in a heated water bath. The number of wheel passes is counted with a digital counter while the rutting profile is measured with a linear variable differential transducer (LVDT). The LVDT measures the rut depth at the centre of the specimen and sends the signal to a linear graphing printer which provides continuous output during the test. An automatic cut-off switch terminates the test if a specimen prematurely fails or reaches the complete test cycle of 20000 passes of the rutting wheel. From the graph of rut depth versus number of cycles, the average rutting rate may be determined from the slope of the tangent from the consolidation point (typically measured 10 minutes after the start of the test) to the stripping inflection point. The stripping inflection point (if present) indicates a change in the rate of rutting with time due to loss of bond between the asphalt binder and the mineral aggregates. If no stripping inflection point occurs, the average rutting rate is simply the slope of the tangent from the consolidation point to the 20000 cycle mark. The graph provides much additional information including the stripping inflection point, as well as the rut rate prior to, and after the inflection point (Aschenbrener 1994).

2.16.3 Georgia Loaded Wheel Tester and Asphalt Pavement Analyzer

As the name implies, the Georgia Loaded Wheel Test (GLWT) was originally developed at the Georgia Institute of Technology in the mid 1980's for the Georgia

Department of Transportation to test rutting resistance of asphalt mixes (Lai 1986).

Unlike the French or Hamburg devices, the GLWT assesses rutting resistance by

rolling a concave steel wheel across a pressurized rubber hose placed along a test

beam. The 29 mm diameter hose is pressurized to 0.69 MPa. The device operates

at 67 passes per minute for 8000 cycles (16000 passes).

In 1995, the rights to commercially manufacture and market the GLWT were

purchased by Pavement Technology Inc. (Prowell and Schreck 2000). Numerous

improvements were introduced to the original design and the resulting device was

renamed the Asphalt Pavement Analyzer (APA). Unlike the GLWT, the APA

includes a water storage tank for testing specimens under water, and is capable of

testing both beam and gyratory specimens as shown in Figure 13.
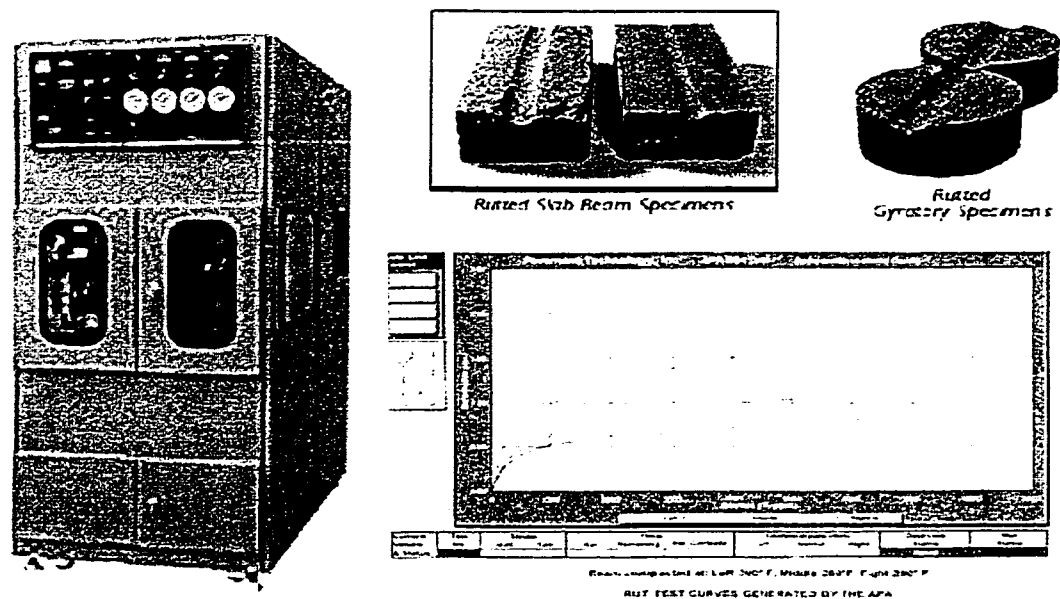
Figure 13: Asphalt Pavement Analyzer

As with the French and Hamburg devices, good correlation between field rutting performance and the GLWT/APA has been observed. For example, regression analysis between the APA rut depth and field rutting observed at Westrack has yielded R^2=79.7% (FHWA 1998c).

2.16.4 Accelerated Load Facility

The Accelerated Load Facility (ALF) is a full scale wheel tracking device incorporating one half of a single truck axle travelling along a 29 metre frame over a full scale pavement test section approximately 10 metres in length. Loads between 44.5 to 100.1kN may be applied. Unlike laboratory wheel tracking tests, the ALF applies loads in one direction only and can impose lateral distribution of the load to better simulate truck traffic loading (wander). ALF can simulate 20 years of cumulative traffic in six months or less. The ALF is shown in Figure 14.
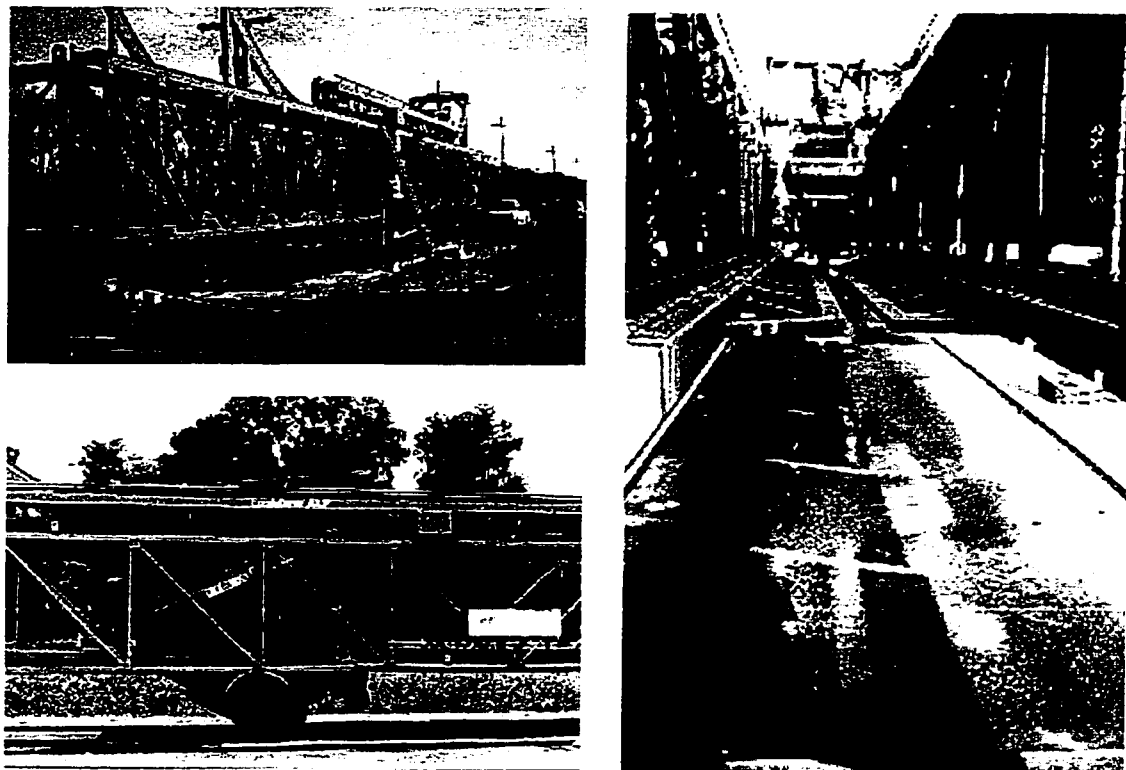
Figure 14: Accelerated Load Facility (ALF)

2.16.5 Superpave Shear Tester

One of the major products developed during SHRP research in the US was the

Superpave Shear Tester (SST). SHRP researchers identified that rutting appears to

be more closely related to shear stress than normal or horizontal stresses (SHRP

1994). As previously mentioned, the SHRP research also referenced work by

Célard (1977), who emphasised that, based on the results of dynamic creep tests, the

rate of permanent deformation was strongly related to shear stress. During SHRP, it

was anticipated that the SST would provide input to the Superpave performance-

based models, although development of the performance models is not expected

until 2005. The SST is illustrated in Figure 15.
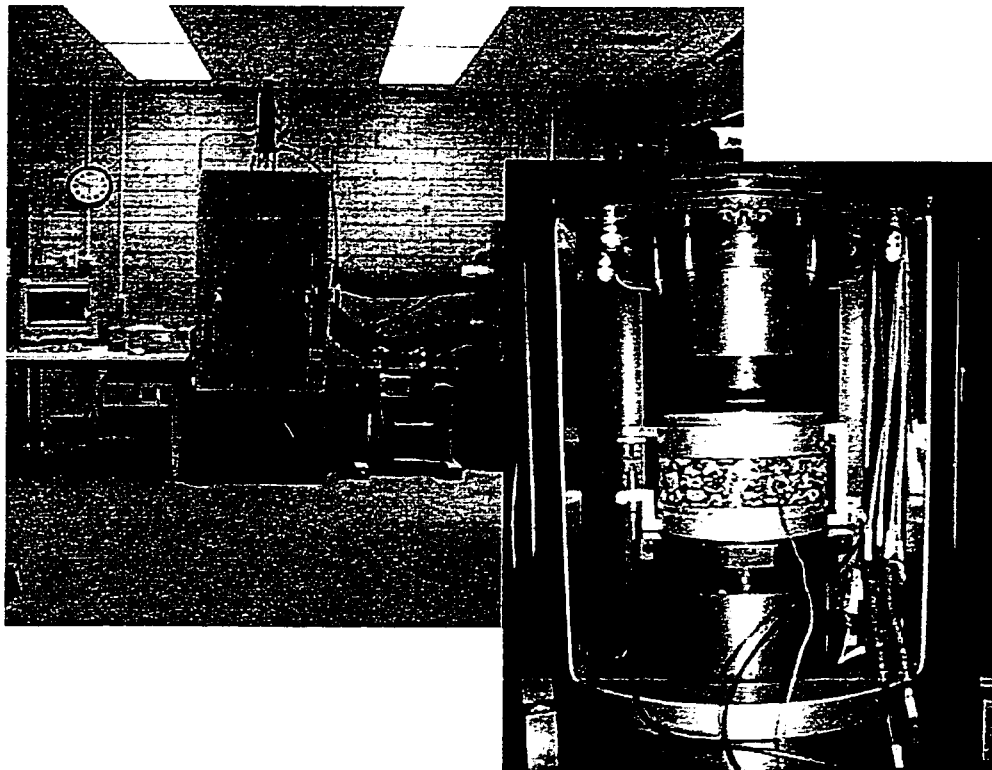
Figure 15: Superpave Shear Tester

Performance testing with the SST to date has produced acceptable correlation between shear properties and field rutting. At Westrack, correlation coefficients (R^2) of 0.55, 0.4 and 0.26 were observed for repeated shear at constant height, frequency sweep at constant height and simple shear at constant height, respectively (FHWA 1998c). While these values are significantly lower than those achieved with wheel tracking tests, it is important to note that the shear properties measured by the SST are not specifically meant for regression analysis, but are to be input into performance-based prediction models that have yet to be developed.

A second device known as the Field Shear Test (FST) was subsequently developed by Endura-Tec Systems as a field quality control device for Superpave (NCHRP 1998). The primary difference between the SST and FST are specimen orientation and the fact that the FST is a portable test and that the specimen is tested diametrally with the FST (similar to the indirect tensile test). Both the SST and FST are under investigation as simple performance tests under NCHRP 9-19.

2.17 Deficiencies with Current Testing/Modelling Practices

2.17.1 Discussion of Empirical Rut Testers

Table 5 compares the characteristics of the LCPC, Hamburg, GLWT/APA and ALF devices. With the exception of the ALF, all wheel tracking devices incorporate a small rolling wheel across a prepared specimen or core of known dimension. It is known that these tests can effectively rank asphalt mixes in terms of relative rutting resistance and, as previously mentioned, they have even displayed good correlation to observed field rutting. However, there are numerous

characteristics of these tests that preclude them from accurately predicting rutting performance of field pavements. First, laboratory wheel tracking tests do not have proper boundary conditions. The test specimens are surrounded by steel molds and are resting on a steel base, which is never the case with the testing of real pavements (Romero and Stuart 1998). Furthermore, stress development in laboratory rut testers is never representative of real life conditions because the size and pressure at the test wheel are unlikely to be representative of real wheels.

Table 5: Characteristics of Rut Testers
(compiled from Huber 1999; Romero and Stuart 1998; Prowell and Schreck 2000)

	Laboratory Wheel Tracking Tests				Full Scale
	French LCPC	Hamburg	Georgia-Type		ALF
			GLWT	APA	
Wheel Load (N)	5000	705	700	533 to 700	44500 to 100100
Contact Pressure (kPa)	600	730 to 1500	690	690 to 833	Variable
Loading Rate (cycles per minute)	60 to 67	26 to 60	33 to 45		6.3
Load Mechanism	Pneumatic Tire	Steel Wheel	Steel Wheel on Pressurized Hose		Full Size Pneumatic Truck Tire
Load Wheel Dimensions (mm)	400 (diameter) 110 (width)	200 (diameter) 47 (width)	29 (hose diameter)		
Test Environment	Air	Water	Air	Air or Water	Air
Specimen Dimensions, (mm)	500 (length) 180 (width) 50 or 100 (thick)	320 (length) 260 (width) 40, 80, 120 (thick)	300 (length) 125 (width) 75 (thick)	Beam or 150 (diameter) Core/Gyro specimen	Full Scale Section 9800 (length)
Test Temperature (C)	60	40 or 50	40	49 to 60	Ambient or 60
No. of Cycles in Specification	30000	9500 to 19200	8000		N/A
Max. Allowable Rut Depth (mm)	10	4 (10000 cycles)	7	N/A	N/A
Cost	$125,000 CAD	$90,000 CAD	$15,000 CAD (minimum)	$130,000 CAD	Variable ($ millions)

Specimen size may also contribute to lack of correlation since the relative size of the wheel compared to material constituents (such as aggregates), is not consistent with in service pavements. Finally, for any test to be valid, the load applied to a specimen should always be in proportion to the specimen size (Romero and Stuart 1998). This is not the case with most of the devices with the exception of the ALF.

However, although the ALF addresses the problems of dimensional incompatibility due to its full-scale nature, the resulting properties (rut depth or rate) do not represent fundamental engineering properties that can be input into a mechanics of materials model for performance prediction. Furthermore, the ALF is extremely expensive ($ millions) and not feasible for field QC/QA.

2.17.2 Discussion of Existing Shear Tests

Although the development of the SST and the FST represented an important step toward measuring asphalt shear properties, neither test is ideally suited for widespread implementation. The SST does provide a great deal of information with regard to mix shear properties, however, it is very expensive (approximately $250,000 USD), confined to the laboratory, and requires a great deal of training to use correctly.

While the FST is a portable device, the diametral loading condition is not representative of field loading conditions. Furthermore, Sousa et. al. (1991) have reported that diametral loading (from the indirect tension test) is inappropriate for permanent deformation characterization because the state of stress is non-uniform and strongly dependent on the specimen.

Finally, both tests require the preparation of cylindrical specimens either through gyratory compaction or coring of in-service pavements. As has been discussed at length throughout this thesis, these preparation methods are either non-representative of the mix in the field, or damage the specimen to a large degree. The development of an in-situ test will both provide an excellent complimentary test device to existing laboratory tests, as well as better represent the performance in the field.

CHAPTER 3: REVIEW OF PREVIOUS WORK AND ANALYTICAL MODELLING

3.1 Introduction and Chapter Overview

Two previous research efforts formed the foundation for the current investigation. The first was a comprehensive laboratory investigation of asphalt shear properties and pavement rutting completed at Carleton University by Zahw (1995). This chapter begins with a review of that investigation, followed by the results of a new study to investigate the relationships between asphalt mix characteristics, shear properties and pavement rutting, using data collected during his research.

The second underlying research effort involved the construction of a first generation in-situ shear strength test device, also at Carleton University by Abdel Naby (1995). A review of the device, known as the Carleton In-Situ Shear Strength Test (CiSSST), is provided including its main benefits and the results of his research concerning in-situ shear strength and its relation to pavement performance.

The chapter concludes by introducing an improved analytical approach to derive asphalt pavement shear properties from the surface plate loading condition developed using closed form equations and the finite element method.

3.2 Review of Previous Work - Laboratory Torsion Testing of Asphalt Concrete

3.2.1 Introduction

A comprehensive laboratory study of asphalt pavement rutting and shear strength and stiffness was completed at Carleton University in 1995 (Zahw 1995). The testing program involved the mixing, compaction and testing of over 1200 standard Marshall specimens representing a total of 58 different asphalt mixes. Mix shear strength and modulus were determined through laboratory torsion testing of cylindrical specimens to failure. The Tinius-Olsen torsion test machine is shown below in Figure 16.
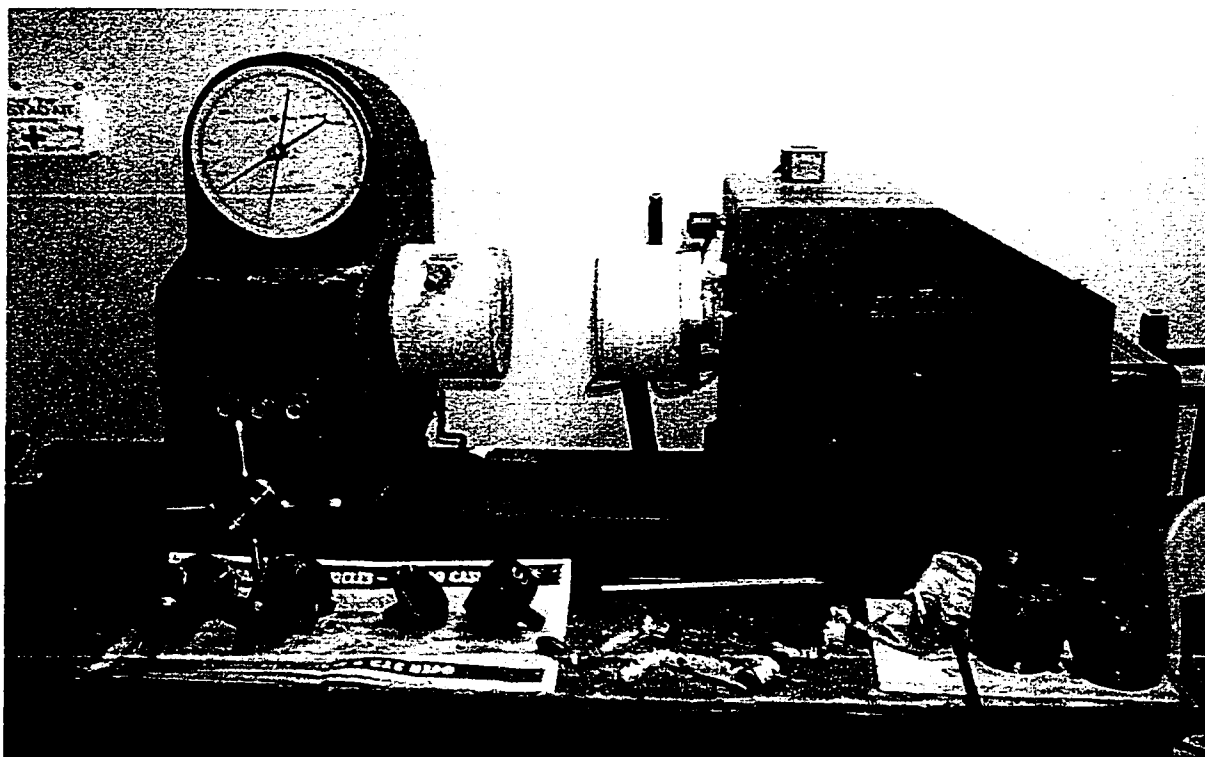
Figure 16: Torsion Test Equipment at Carleton University

Cylindrical Marshall specimens or cores were glued to steel plates using an epoxy and loaded horizontally into the device. All testing was completed at 25°C. Torque and twist angle at failure were recorded by the device and the specimens failed in shear with a characteristic 45° failure surface as highlighted in Figure 17.
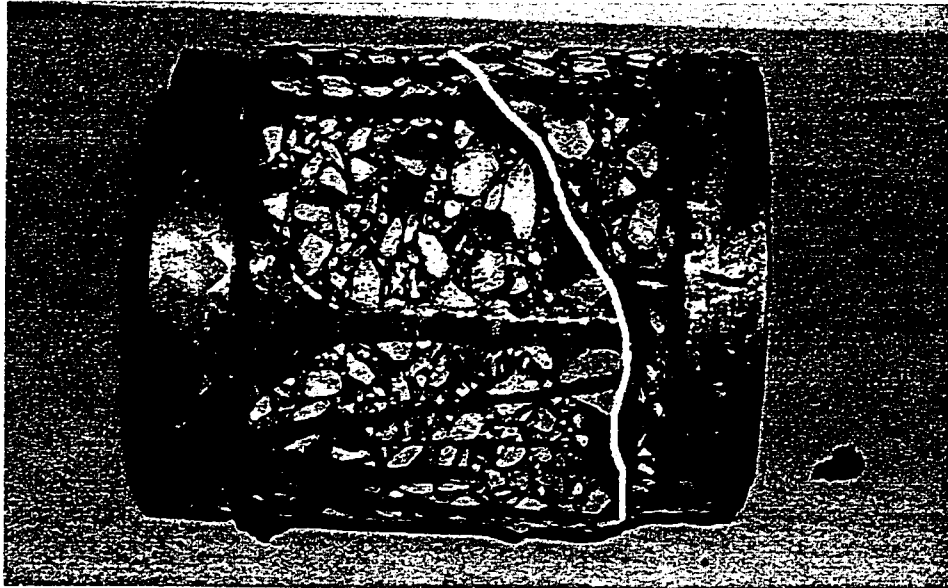
Figure 17: Typical Failure of Asphalt Specimen in Torsion Test Device

Permanent deformation characteristics were determined through the Shell Pavement Design method utilizing uniaxial unconfined static creep tests at three stress levels (0.1 MPa, 0.3 MPa and 0.6 MPa).

3.2.2 Deriving Shear Properties from Laboratory Torsion Tests

By definition, fundamental engineering properties of materials such as tensile or compressive strength, shear strength and stiffness, elastic modulus, etc. are unique to individual materials and not dependent on boundary conditions. However, there are few testing procedures (if any) that directly measure

fundamental properties. In most cases, a given load is applied to a test specimen and the desired fundamental property is then determined knowing the specimen dimensions. For example, compressive strength (f'_c), which is a fundamental property of Portland Cement Concrete, is determined by applying an axial load to failure, and then using that failure load and the cross sectional area of the specimen to calculate f'_c. However, the measured values of the fundamental properties can be strongly dependent on the test conditions such as load rate, confining pressure, temperature etc. With PCC (and many other materials including asphalt concrete), the faster the applied load, the greater the resulting strength response. Therefore, various standards (CSA, ASTM, etc.) have been developed so that a single set of test parameters is used to produce comparable results.

Under similar test conditions, alternative methods may be used to determine fundamental properties. For example, the Superpave Shear Test (SST) measures shear properties of asphalt concrete by applying a force across an asphalt core or gyratory specimen. Given the specimen dimensions (cross sectional area), the shear properties of the mix are easily calculated. The same shear properties of the core or gyratory specimen may be determined using a torsion test as well. Again, given the specimen dimensions, the shear properties may be determined from the applied torque. A comparison of the mechanics behind the SST and torsion test is shown in Figure 18.

While the method of force application is different, the differential elements (dA) within the specimens are subjected to shear in both cases, thereby allowing the calculation of the shear properties independent of the test method or boundary conditions.
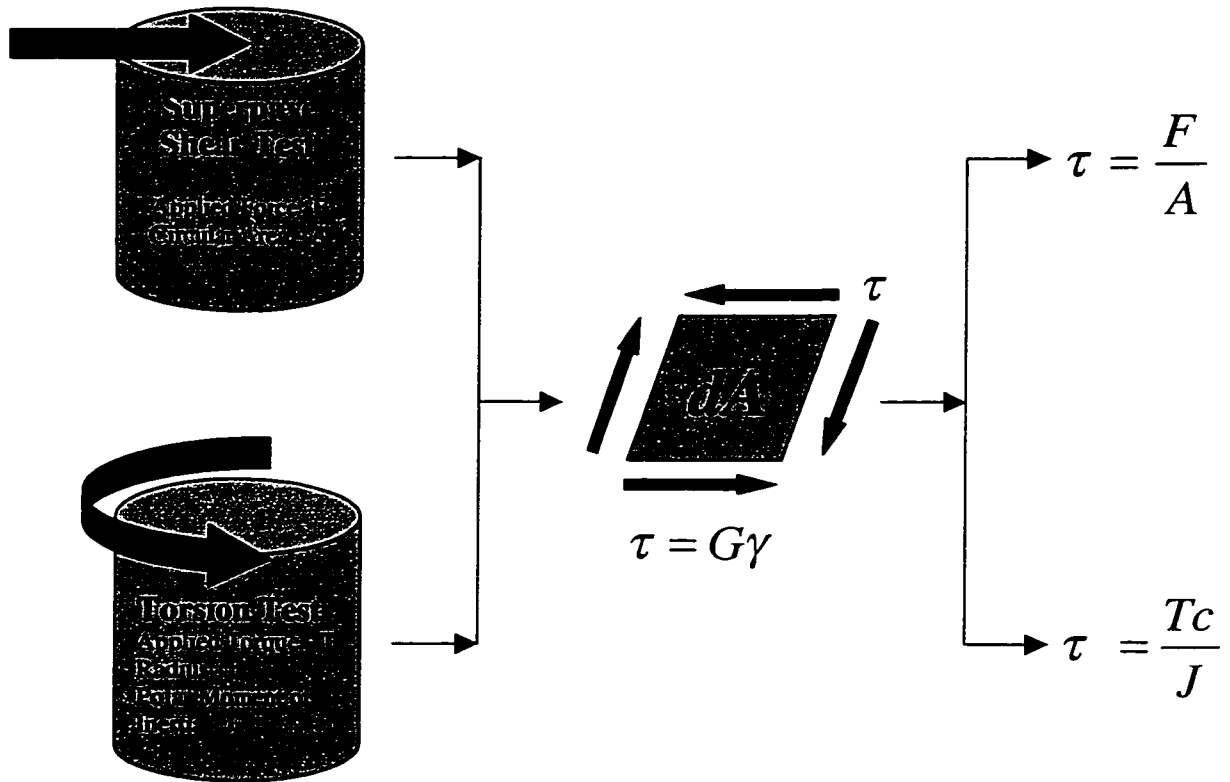
Figure 18: Determination of Shear Properties from Different Test Methods

As shown in Figure 18, the shear strength of the asphalt mix may be determined

using Equation 1:

$$\tau = \frac{T * c}{J} \qquad (1)$$

where:

τ = the shear strength (MPa)

T = the maximum applied torque (N*m)

c = the radius of the test specimen (mm)

J = the polar moment of inertia (mm^4)

3.2.3 Major Findings of Laboratory Torsion Testing

The work of Zahw (1995) represented new and extensive research toward a better understanding of the rutting phenomenon and its underlying causes. One of the main findings was that conventional asphalt design criteria such as density alone do not provide a reliable indicator of high rutting resistance, whereas the use of shear properties better characterized the mix performance. This finding was supported by research completed during the Strategic Highway Research Program (US-SHRP 1994), which was being completed concurrently by Zahw (1995).

In addition to the development and verification of a shear testing framework using laboratory torsion testing, Zahw also generated a large volume of data including mix properties, measured shear properties and mix performance as determined through unconfined static creep tests. This database was utilized during the current investigation to produce new and valuable models relating mix properties to shear properties, as well as shear properties to calculated rutting. The results of this analysis are presented in the following section.

3.3 Analysis of Laboratory Mix, Shear and Rutting Database

3.3.1 Relation of Mix Characteristics to Shear Properties

Sixteen asphalt mix properties were available in the Zahw database for the analysis as listed below in Table 6. These properties were subsequently grouped into three main categories – Asphalt Binder Properties, Mineral Aggregate Properties and Mix Design Properties.

Table 6: Mix Properties Available from Zahw (1995) Database

Asphalt Binder Properties	Mineral Aggregate Properties	Mix Design Properties
• Penetration @ 25C • Ring and Ball Softening Point • Kinematic Viscosity • Penetration Index • Viscosity @ 25C • Binder Stiffness, Sbit	• Coefficient of Uniformity • Coefficient of Curvature • Percentage of Coarse Material • Presence of Crushed Stone Present in Mix • Percentage of Mineral Filler	• No. of Blows with Marshall Hammer • Final Specimen Density • Asphalt Cement Content • Voids in the Mineral Aggregate • Dust to Binder Ratio

Table 7 displays the measured engineering properties including shear stress, strain and modulus, as well as the estimated rutting from unconfined uniaxial static creep testing at 0.1, 0.3 and 0.6 MPa stress levels.

Table 7: Engineering Properties Available from Zahw (1995) Database

Measured Shear Properties	Estimated Rutting Properties*
• Average Shear Strength • Average Shear Strain • Average Shear Modulus	• Rut Depth at 0.1 MPa Stress • Rut Depth at 0.3 MPa Stress • Rut Depth at 0.6 MPa Stress

*Estimated rutting properties based on unconfined static creep testing (Shell Method)

The first step in the analysis involved relating the asphalt mix properties to the measured laboratory shear properties. A correlation matrix was developed for all 16 variables using the statistical features of Microsoft Excel. The seven mix variables yielding the greatest correlation coefficients are displayed in Table 8.

Table 8: Mix Properties Yielding Greatest Correlation to Shear Properties

Mix Property	Correlation Coefficients		
	Shear Strength (MPa)	Shear Strain (%)	Shear Modulus (MPa)
Penetration @ 25C	-0.67	-0.80*	-0.49
Viscosity @ 25C	0.44	0.66**	0.18
Coefficient of Uniformity	0.59	negligible	0.70
Presence of Crushed Coarse Aggregate	0.41	0.22**	0.48
No. of Blows with Marshall Hammer	0.07	-0.35	0.22
Density	0.57	negligible	0.71
Voids in Mineral Aggregate	0.21	-0.07	0.26

* coefficient should have positive relationship
** coefficient should have negative relationship

Examination of the correlation coefficients indicated that the effect of each mix characteristic on the shear properties made rational sense, with the exception of some of the relationships between the mix properties and shear strain. Intuitively, a parameter that causes an increase in shear strength or modulus should have a negative effect on shear strain. However, in the cases of penetration, viscosity and the presence of crushed coarse aggregate, the correlation coefficients for shear strain did not display the correct sense (positive or negative). Relative to the shear strength and modulus, however, much lower correlation was displayed between shear strain and many of the mix properties. Therefore, as the shear strain is inherently contained within the shear modulus, further analysis of shear strain was not completed in this investigation. A brief discussion of the resulting relationships is now presented.

Until the Superpave performance-graded binder specification was developed, penetration was the primary criterion for the selection of asphalt binders for road construction in North America. Therefore, although it is an empirical measure of binder stiffness, it was not surprising to see that penetration was well correlated with mix shear properties. Less correlation was observed with viscosity than penetration.

The coefficient of uniformity is a measure taken from soil mechanics to describe the shape of the gradation curve of the mineral aggregates used in each mix. As indicated in previous sections, the aggregate skeleton is critical for rutting resistance, therefore, the shape of the gradation curve and its associated packing configuration would likewise be highly correlated with shear properties. The high correlation with shear strength and modulus clearly indicated the importance of aggregate skeleton to transfer the load to the underlying layers of the pavement.

The variable referred to as "Presence of Crushed Coarse Aggregate" was simply a binary choice of whether or not the coarse aggregates in the mix were crushed (i.e quarried stone) or not (i.e. river gravel). If the aggregate was crushed, a value of "1" was assigned, whereas a value of "0" was assigned if the aggregates were not crushed. Although it may have been desirable to have a more descriptive measure of aggregate angularity such as fractured face count, this information was not recorded during the initial investigation by Zahw. Interestingly, the binary choice variable proved to be well correlated with shear strength and stiffness and was therefore kept in the analysis.

The number of blows with the Marshall hammer is a measure of compactive effort. Marshall mixes designed for high truck traffic applications are usually

designed as 75-blow mixes, indicating that 75 blows with the Marshall hammer are applied per side of the specimen during mix design. Mixes designed for regular traffic levels usually are designed with 50 blows per side. Therefore, the greater number of blows required to achieve the design mix properties, the stronger the mix.

Final specimen density has long been the primary measure of mix adequacy, therefore, it was not surprising to see a high correlation between density and shear properties. Finally, voids in the mineral aggregate (VMA) is a measure of the void space within the compacted mix. Volumetric properties are the foundation of mix design, therefore good correlation was expected. It should be mentioned that asphalt cement content was not selected as an independent variable, despite its well-known effect on rutting resistance. This decision was largely made based on the greater correlation observed between VMA and the shear and rutting properties when compared to asphalt content, as well as the fact that asphalt content information is contained within the VMA parameter.

Based on the correlation matrix, the dependent variables listed above in Table 8 should have provided the best input for regression models to explain the measured shear properties. However, some of the properties were highly correlated to one another, referred to as collinear dependent variables. Such variables could not be used for regression in their current form. While one option would be to simply remove the collinear variables, the information associated with those variables would then be lost in the model. Another technique involves the use of combination variables. For example, Penetration and Viscosity @ 25C were highly correlated (-0.66) and therefore could not both be incorporated into regression analysis. However, instead of discarding the variable displaying the lower correlation to the

shear properties (in this case Viscosity), the two variables were combined into a single variable referred to as Penetration-Viscosity Ratio (PVR) as shown below in Equation 2:

$$PVR = \frac{Pentration\ @\ 25C}{Vis\cos ity\ @\ 25C} \qquad (2)$$

A second combination variable was also created from the original seven – Average Rate of Densification (ARD), which was defined as the ratio of final specimen density to the compactive effort as expressed by the square root of the number of blows applied by the Marshall hammer as shown in Equation 3:

$$ARD = \frac{Density}{\sqrt{\#\ Blows}} \qquad (3)$$

It should be stressed that combining correlated dependent variables should not be completed haphazardly; the combined variable must make rational sense. In the case of PVR, the resulting correlation coefficient for shear strength was -0.67, indicating that as PVR increases, shear strength decreases. Examining the ratio itself, PVR will increase with either an increase in penetration or a decrease in viscosity, or both. Therefore, according to the ratio, shear strength will decrease with an increase in penetration or a decrease in viscosity (i.e. a softer asphalt is used). This relationship makes sense since softer asphalts have a higher tendency to rut – all else equal.

By dividing the final density by the square root of the number of Marshall hammer blows, the ARD variable represented an average slope of the densification curve. In other words, ARD provides an indication of the amount of compactive effort needed to achieve the final density. Asphalt mixes that have strong aggregate

91

skeletons typically require more compactive effort to obtain specified density since it is more difficult to rearrange the aggregates during compaction. Therefore, it was expected that lower values of ARD would result in more rut resistant mixes. The square root of the number of Marshall hammer blows was selected as it has been shown that field rutting is better described by the square root of traffic when compared to arithmetic or logarithmic functions (Brown and Cross 1988, and Parker and Brown 1990).

A second correlation matrix was developed for the resulting 5 selected mix variables as shown in Appendix A. Note that this matrix displayed both acceptably low correlation between the individual dependent variables, and very high correlation between the dependent and independent variables.

Equations 4 and 5 below were developed from multiple regression analysis of the five selected mix variables to model measured shear strength and modulus. The actual data used in the regression analyses is reported in Appendices B (mix variables) and C (shear properties). As shown by the coefficients of determination (R^2), the dependent variables within Equations 4 and 5 explain a high degree of the variability observed in the shear modulus and strength, respectively.

$$G = 560 - 2.7*PVR + 232*CU + 344*C_{bin} - 14135*ARD + 10680*VMA$$

(4)

$(R^2 = 0.83)$

$$\tau = -66 - 0.9*PVR + 50*CU + 65*C_{bin} - 2410*ARD + 2552*VMA$$

(5)

$(R^2 = 0.88)$

where:

G (kPa) = Shear Modulus (Stiffness) at 25°C;

τ (kPa) = Shear Strength at 25°C;

PVR (mm/Pa*s) = Ratio of Penetration (mm) to Viscosity at 25°C (Pa*s);

CU = Coefficient of Uniformity (D60/D10);

C_{bin} = Presence of Crushed Coarse Aggregate in Mix (Binary choice of 1

for Yes or 0 for No);

ARD = Average Rate of Densification (ratio of final mix density to the

square root of the number of blows with Marshall hammer); and

VMA = Voids in the Mineral Aggregate (%)

The use of the combination variables in Equations 4 and 5 maximized the

amount of information contained per variable without introducing collinear

dependent variables. Furthermore, the dependent variables utilized cover all of the

major areas governing mix performance; bitumen properties (PVR), gradation (CU),

angularity/roughness of the aggregates (Cbin), density and compactive effort (ARD)

and volumetric properties (VMA).

Tables 9 and 10 display the regression statistics for the shear modulus and

shear strength equations respectively. In both equations, the intercept term was

statistically insignificant as indicated by the low t statistic. All other variables

yielded high t statistics, indicating high significance.

Table 9: Regression Statistics for Shear Modulus (Equation 4)

	Coefficients	Standard Error	t Stat
Intercept	560	745	0.8
Penetration-Viscosity Ratio (mm^3/N @ 25°C)	-2.7	0.28	-9.7
Coefficient of Uniformity (D60/D10)	232	23.0	10.2
Presence of Crushed Coarse Aggregate	344	119	2.9
Average Rate of Densification [Final Density/Sqrt(#blows)]	-14135	2997	-4.7
Voids in Mineral Aggregate	10680	2938	3.6

Table 10: Regression Statistics for Shear Strength (Equation 5)

	Coefficients	Standard Error	t Stat
Intercept	-66	164.5	-0.4
Penetration-Viscosity Ratio (mm^3/N @ 25°C)	-0.94	0.062	-15.1
Coefficient of Uniformity (D60/D10)	50.2	5.0	10.0
Presence of Crushed Coarse Aggregate	64.6	26.2	2.5
Average Rate of Densification [Final Density/Sqrt(#blows)]	-2410	662	-3.6
Voids in Mineral Aggregate	2552	649	3.9

The individual coefficient of determination (R^2) for each individual variable was also investigated and the results are displayed in Table 11. As shown, the Penetration-Viscosity Ratio (PVR) alone could explain approximately 22% of the

variation in shear modulus and 44% of the variation in shear strength. Coefficient

of Uniformity accounted for 49% of the shear modulus and 35% of the shear

strength. Interestingly, the binary choice variable – "Presence of Crushed Coarse

Aggregate in Mix" – represented a large portion of the shear properties; 23% of the

shear modulus and 17% of the shear strength. The remaining variables, ARD and

VMA explained less of the variation in the shear properties; however, they were

highly significant in both equations.

The results of the individual regression analyses tended to confirm the results

found in the SHRP research; that binder properties contribute approximately 33%

toward rutting resistance, while the remaining contribution comes from the

aggregates and the asphalt-aggregate interaction [US-SHRP 1994].

Table 11: Contribution of Individual Variables Toward Shear Properties

Variable	Individual Coefficient of Determination for Shear Modulus $(R^2\%)$	Individual Coefficient of Determination for Shear Strength $(R^2\%)$
PVR	21.9	44.2
Coefficient of Uniformity	48.6	34.7
Crushed Coarse	22.8	16.8
ARD	7.7	9.8
VMA	6.8	4.6

3.3.2 Relation of Shear Properties to Rutting

Additional analyses were completed to investigate the relationship between

the shear properties of the mix and its rutting resistance as determined through the

Shell procedure. Figure 19 displays the graphs of rut depth versus shear modulus of the mix for each unconfined creep test stress level. As shown, a high degree of correlation was observed between shear modulus and rut depth with R^2 values ranging from 0.60 to 0.80 using a power relationship. Similar relationships were seen for shear strength as illustrated in Figure 20, although less correlation was observed than with shear modulus. The results of the analysis clearly indicated that shear strength and modulus are able to explain a large amount of the variability observed in the rutting as measured through laboratory creep tests, although shear modulus appeared to be a better indicator. The rutting models displayed in Figure 19 and 20 are also listed in Table 12 below. For reference, the actual shear and rutting data from the Zahw (1995) database are attached as Appendix C.

Table 12: Rutting Models for Shear Strength and Modulus

Creep Test Stress Level (MPa)	Laboratory Rutting Models	
	Shear Modulus @ 25C (kPa)	Shear Strength @ 25C (kPa)
0.1	$Rut = 245 * G^{-0.742}$ (R^2=0.80)	$Rut = 18.25 * \tau^{-0.515}$ (R^2=0.63)
0.3	$Rut = 4301 * G^{-1.037}$ (R^2=0.60)	$Rut = 62.92 * \tau^{-0.626}$ (R^2=0.47)
0.6	$Rut = 3E6 * G^{-1.820}$ (R^2=0.73)	$Rut = 11791 * \tau^{-1.383}$ (R^2=0.67)

Figures 19 and 20 contain much important information that necessitates further discussion. First, the graphs clearly show that as shear strength and modulus increase, the amount of rutting experienced during the test decreases significantly, particularly at higher test stress levels. For example, an increase in shear modulus

from 2500 MPa to 3000 MPa (20% increase) reduced the amount of rutting from 2 mm to 1.4 mm (a 30% reduction) for the 0.6 MPa test stress level. For the lower stress levels, the graphs become flatter, indicating a reduced benefit for increased shear modulus and strength for lower stress scenarios. Although beyond the scope of this investigation, the information can potentially be used to optimize mix design selection (based on modulus or strength) for a desired level of performance (rutting limit) and a given traffic loading scenario (stress level). Furthermore, the results of quality control and assurance testing (QC/QA) could be checked against the graphs to ensure that the finished pavement will perform as specified, with possible penalty or bonus implications to the contractor.
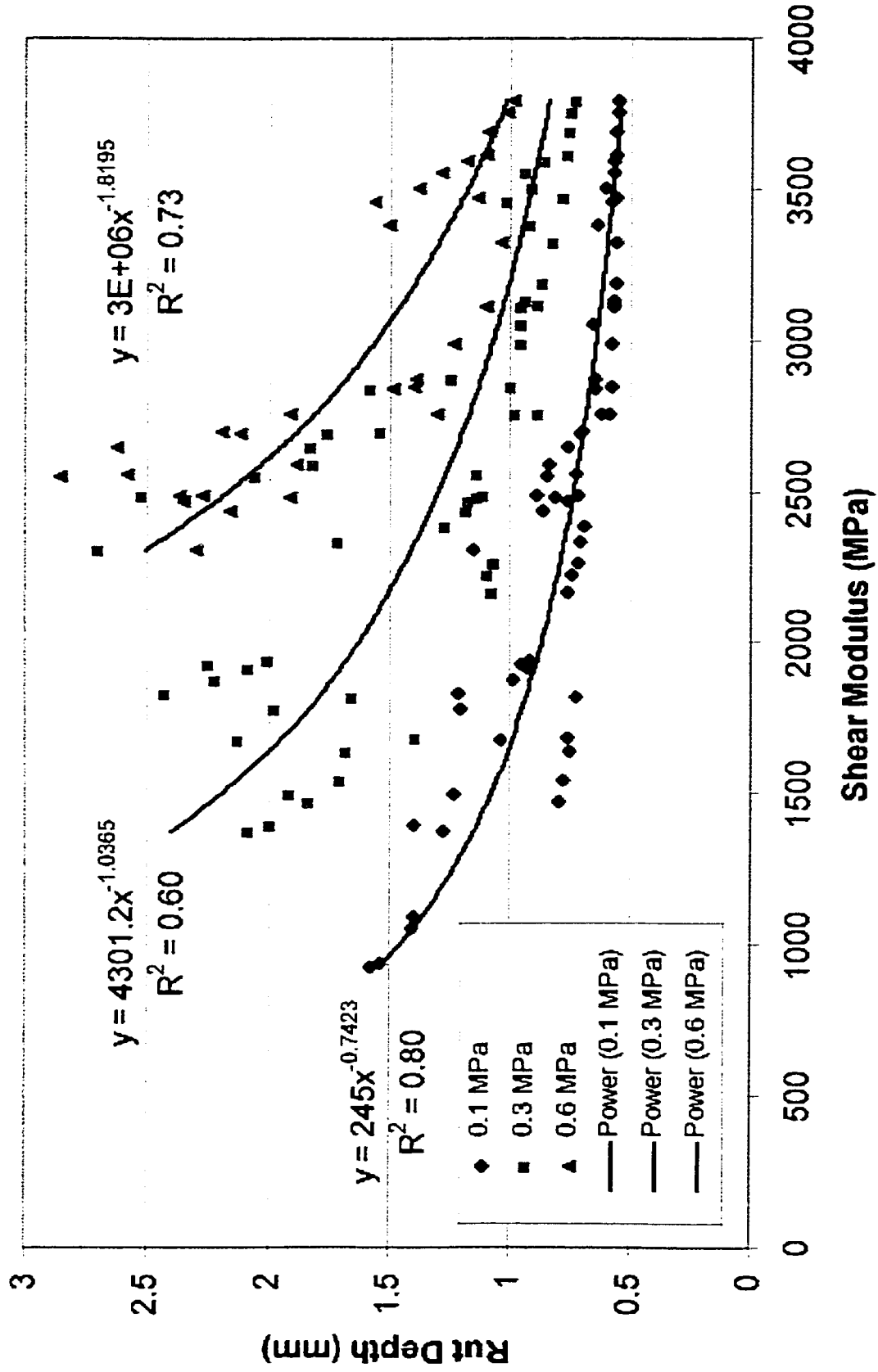
Figure 19: Laboratory Rutting vs. Asphalt Mix Shear Modulu
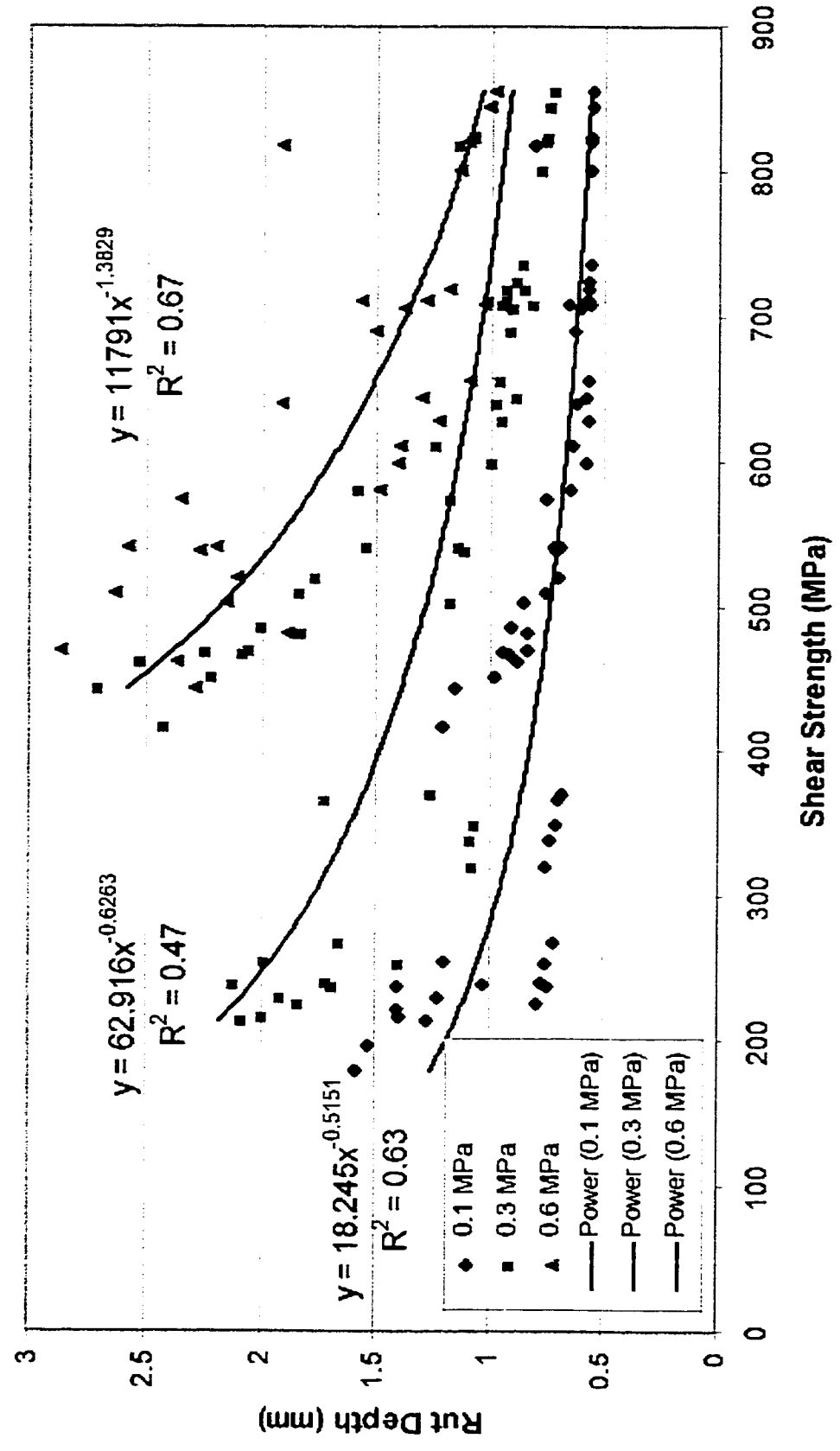
Figure 20: Laboratory Rutting vs. Asphalt Mix Shear Strength

3.4 Review of Previous Work - The Carleton In-Situ Shear Strength Test (CiSSST)

3.4.1 Introduction

The concept of testing the shear strength of asphalt pavement surfaces using a rotational load in the field was first conceived by Abd El Halim and Abd El Nabi in the early 1990's. To investigate the feasibility of this concept, the Carleton In-Situ Shear Strength Test (CiSSST) facility, shown in Figure 21, was constructed at Carleton University.
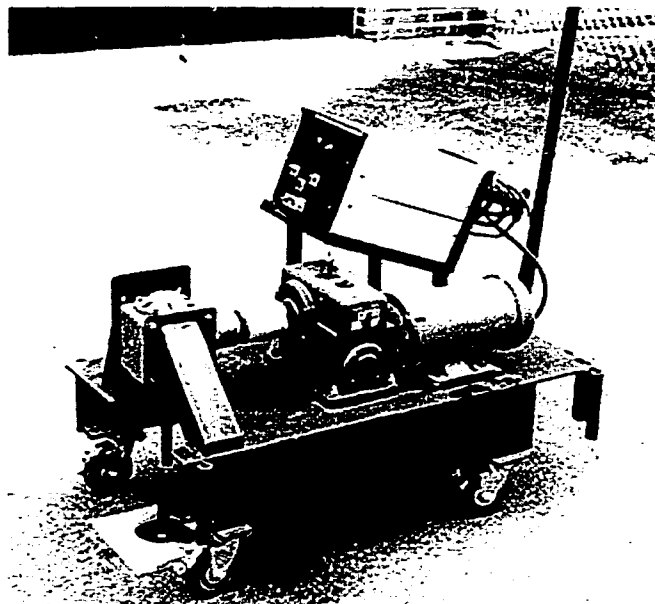
Figure 21: The Carleton In-Situ Shear Strength Test (CiSSST) Facility

The facility consisted of a cart-like chassis on small castor wheels for positioning. Force was applied via an electric motor coupled to a gear reducer and a right-angled gearbox. The gearbox transmitted the torque through a vertical drive shaft to a torque cell, which in turn was attached to a steel loading plate bonded to the asphalt surface with a strong epoxy resin. During the testing procedure, torque

was applied until failure of the asphalt surface occurred. The failure torque was measured with a torque cell and the failure strain was determined by measuring the angle of twist at failure with a protractor.

3.4.2 Deriving Shear Properties from Field Torsion Tests

The laboratory torsion specimens tested by Zahw (1995) had clearly defined boundary conditions that allowed the calculation of shear properties using simple closed form equations. However, deriving shear properties from torsion tests with the CiSSST was much more difficult due to the field boundary conditions. The method of testing with the CiSSST, known as the surface-plate method, utilized a steel plate attached to the pavement surface using epoxy resin. Therefore, torsion was being applied from a steel disc of finite dimension (100 mm diameter) onto a flat surface with (practically) infinite dimension, often referred to as a half-space. This loading condition is similar to the linear torsional shear stress/displacement conditions shown in Figure 5, and represented a completely different set of boundary conditions than the laboratory torsion test. Therefore, a different set of constitutive equations was required to determine the shear properties. The surface plate loading condition of the CiSSST device is illustrated in Figure 22.

Applied Torque (T)
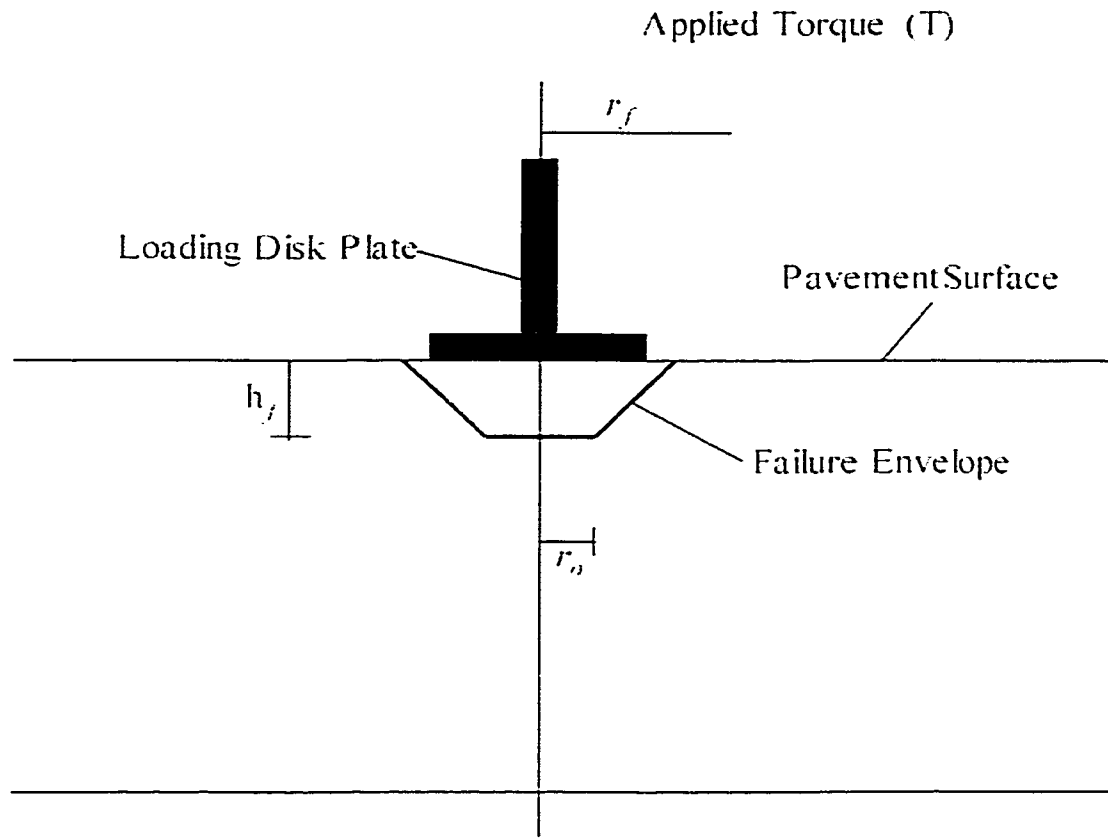
Figure 22: Loading and Boundary Conditions of CiSSST

In previous studies with the CiSSST device, Equation 6 was developed by

Abdel Naby (1995) for calculating the mix shear strength based on the assumption

that the failed surface formed the frustum of a cone as shown in Figure 22.

$$T = \frac{2}{3}\pi\tau\left[\left(\frac{r_f^3 - r_o^3}{r_f - r_o}h_f\right) + r_o^3\right]$$

(6)

where:

T = the maximum applied torque (N*m)

τ = the in-situ shear strength (MPa)

h_f = the failure depth (mm)

r_f = the upper radius of the frustum of the failed cone (mm)

r_o = the lower radius of the frustum of the failed cone (mm)

3.4.3 Main Results of Previous Experiment

The results of Abdel Naby (1995) provided two important conclusions. First, the CiSSST was able to differentiate between the shear properties of different mixes, as well as the differences within the same mix placed in different geometries (curved sections vs. straight sections). This indicated that the device was sensitive to changes in mix shear properties and could potentially differentiate between mixes with good or poor rutting resistance.

Second, greater variation between replicate specimen results was observed during laboratory testing than in-situ testing. As supported by Peck and Lowe (1960), it was hypothesized that the coring process used for laboratory specimen preparation damaged the specimens to such an extent that a greater variation was observed during laboratory testing than that experienced during field testing.

3.4.4 Advantages of CiSSST Prototype

The concept behind the CiSSST facility was quite simple, yet very effective. No special preparation of the asphalt surface was required and the test could be completed very quickly once the epoxy resin had cured. The applied rotational force produced a state of pure shear stress without complicated bending, tensile or compressive forces. The test was very repeatable as indicated by the low variation between tests (Abd El Nabi 1995) and measured actual field shear properties instead of attempting to simulate field conditions using laboratory analysis.

3.5 Improved Analytical Framework to Determine Asphalt Shear Properties from the Surface Plate Loading Method

3.5.1 Introduction

As previously presented, an equation for asphalt shear strength was developed by Abdel Naby (1995) during initial investigations with the CiSSST device. However, shear strengths calculated using Equation 6 were consistently greater than those determined by Zahw (1995) in the laboratory, often by as much as 300%. Notwithstanding the fact that laboratory and field compaction methods produce different aggregate particle orientation as outlined in previous sections, it was likely that Equation 6 did not fully represent the boundary conditions of the pavement, therefore, the calculated shear strength of the mix was not entirely correct. It should be stated that for comparative purposes, this did not present a problem to the analysis of Abdel Naby (1995). However, for accurate modelling of rutting resistance based on shear properties, new constitutive relationships between the surface plate method and field shear properties are currently under development at Carleton University by Bekheet et. al. (2000). Although not part of this thesis, these relationships are briefly presented in the following section for completeness.

3.5.2 Reissner-Sagoci Problem

As outlined in Section 3.4.2, the surface plate torsion test involves applying a torsional force through a steel test plate epoxied to the asphalt surface as shown in Figure 23. Torque is applied at a constant rate until failure of the asphalt surface in shear. The typical failure plain is shown in Figure 24.
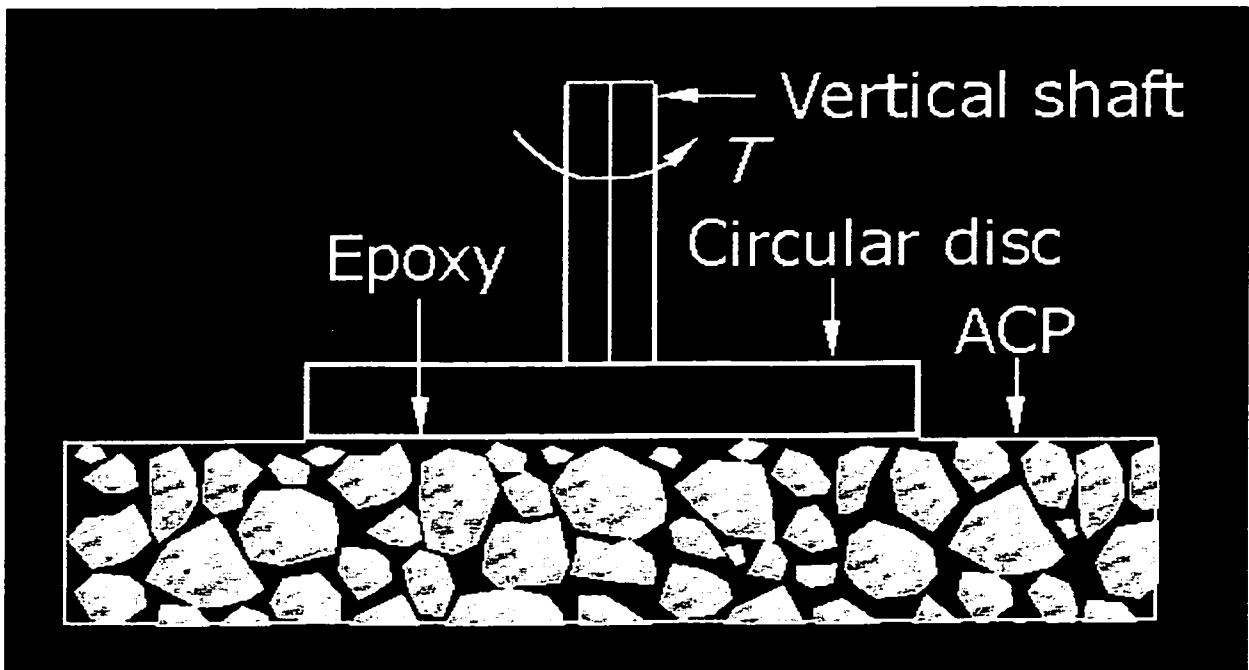
Figure 23: Load Plate Attached to Asphalt Concrete Pavement (ACP) Surface
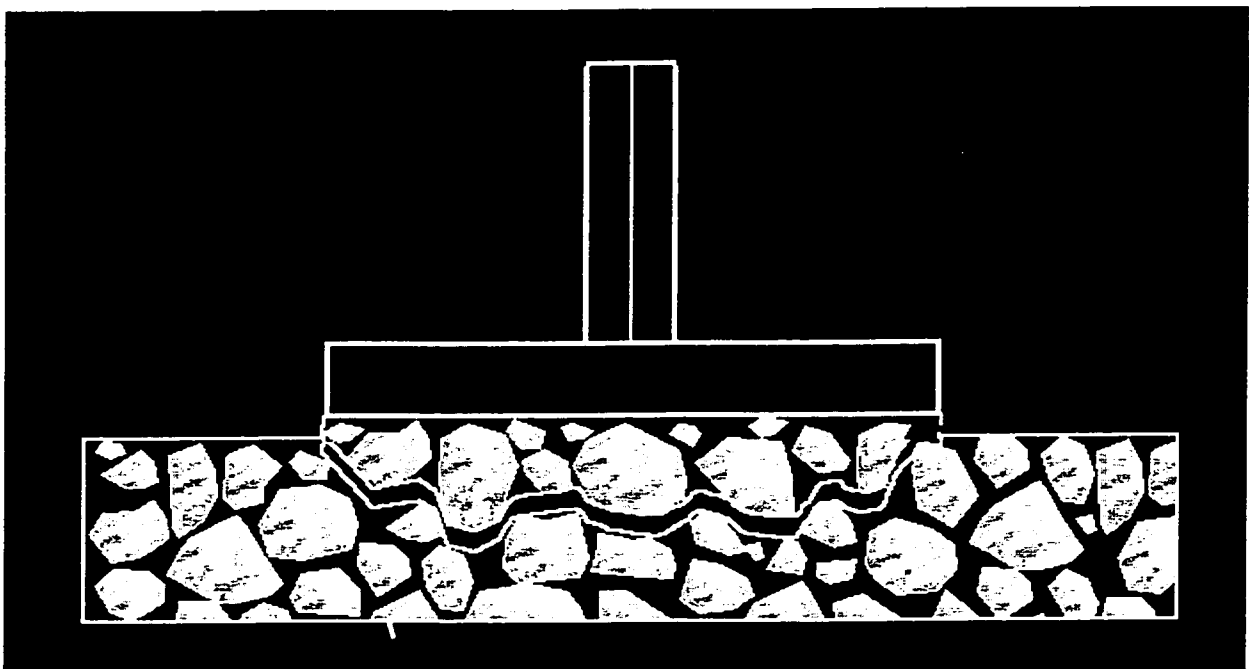
Figure 24: Induced Failure in Asphalt Concrete Pavement (ACP) Surface

The problem of applying a torsional moment on the surface of a half-space

was developed by Reissner and Sagoci (1944) and Sneddon (1946). For an elastic,

homogeneous and isotropic material in cylindrical coordinates (r, Ø), all stresses

vanish with the exception of shear stresses $\tau_{r\emptyset}$ and $\tau_{z\emptyset}$ as shown in Figure 25. A

simplified form of the shear stress $\tau_{z\emptyset}$ is available when z=0 (at the surface of the

half-space) as shown in Equation 7:

$$\tau_{z\theta} = \frac{4\Phi G}{\pi\sqrt{\left(\dfrac{a}{r}\right)^2 - 1}}$$ (7)

Where:

G = Shear modulus of the material

a = Radius of the loading plate

Φ = Angular displacement of the loading plate (radians)

r = Distance from the centre of the loading plate (r<a)
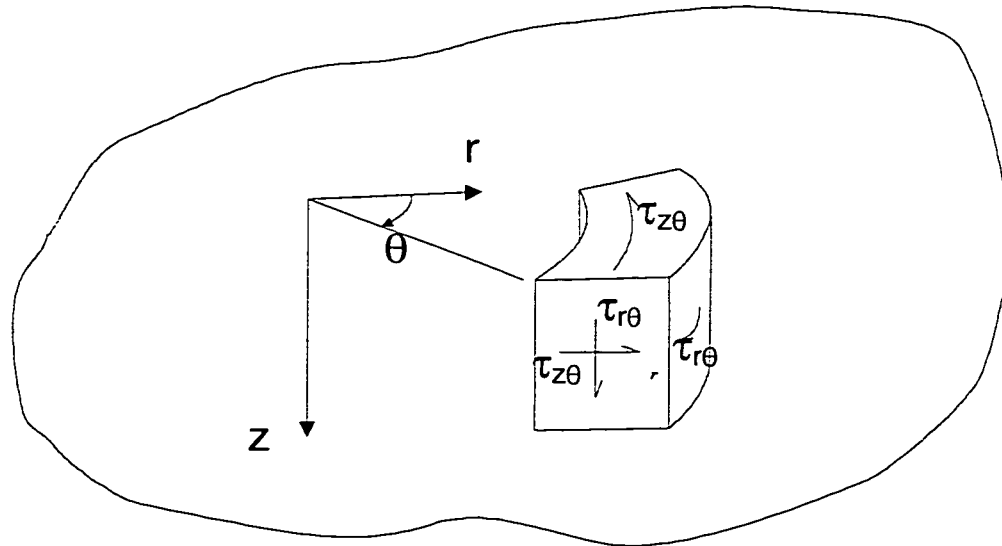
**Figure 25: Differential Element Shear Stresses from Reissner-Sagoci Problem
(from Bekheet et. al. 2000)**

It should be mentioned that Equation 7 is only valid within the radius of the loading plate (r<a). The relationship between the applied torque, T and the resulting angular displacement can be derived by integrating $\tau_{z\theta}$ over the area of the loading plate as shown in Equation 8 (Bekheet et. al. 2000):

$$T = \frac{16}{3}G\Phi a^3 \qquad (8)$$

As shown, the shear modulus may be calculated from the applied torque and angular displacement (twist angle). No closed form solution has been developed by Bekheet for shear strength to date. While such a relationship may be developed in the future, the modulus (stiffness) appears to better characterize rutting; therefore efforts were focussed on evaluating stiffness for this investigation.

3.5.3 Finite Element Modelling and Verification

Although Equation 8 provided the means to directly calculate the shear modulus of the pavement surface, the underlying assumptions of elastic, homogeneous and isotropic conditions do not always reflect the properties of asphalt concrete. Indeed, asphalt is a viscoelastic material depending on its temperature and rate of loading. Therefore, to further develop the Reissner-Sagoci equations for asphalt concrete, Bekheet et. al. (2000) investigated the use of the finite element method.

Briefly, a finite element mesh was constructed using 20-node, 3 dimensional brick elements to simulate the Reissner-Sagoci problem. Elastic, homogeneous and isotropic material properties were first entered into the model to compare the results of the model run with the closed form solutions provided by the Reissner-Sagoci equations. Results of this model verification are illustrated in Figure 26.

As shown, the results of the initial model verification were almost identical to

the closed form solutions, indicating that the finite element mesh modelled the

Reissner-Sagoci problem very well.
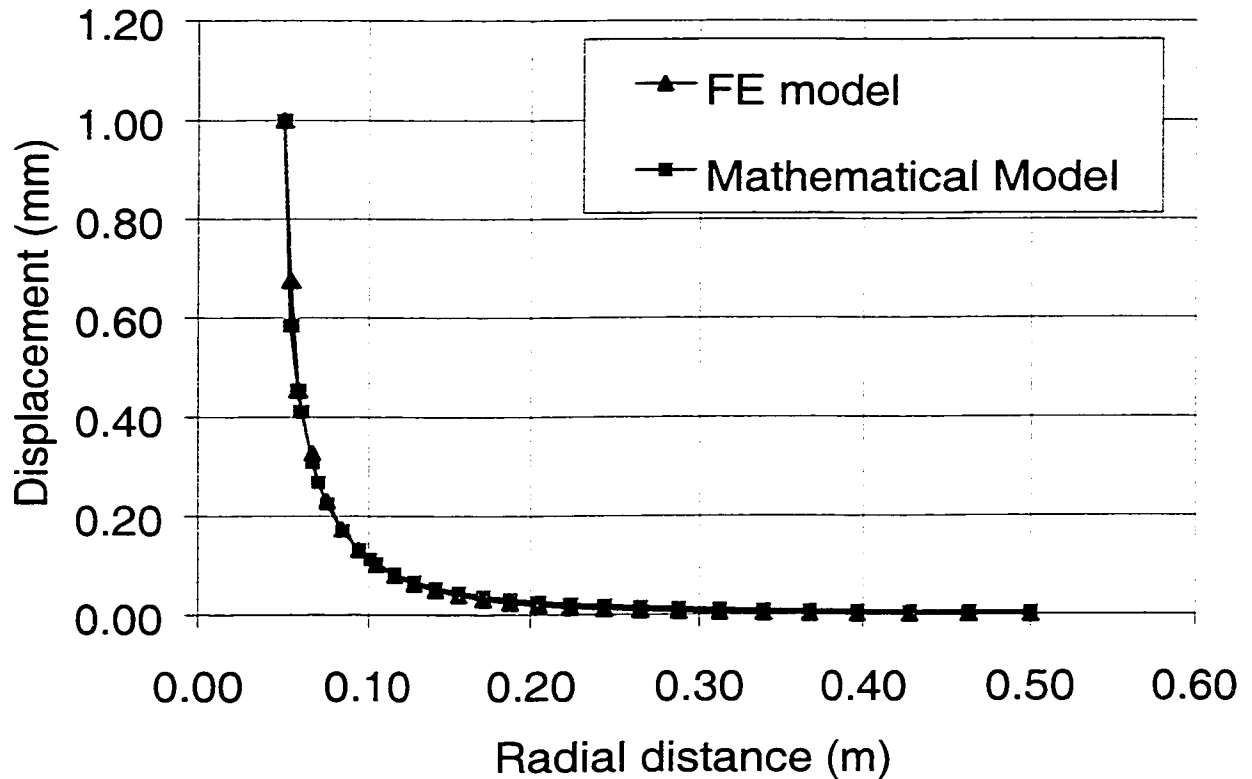
**Figure 26: Initial Finite Element Model Verification
(from Bekheet et. al. 2000)**

The next step, which is currently underway, will be to take the verified finite

element mesh and apply non-linear, viscoelastic material properties that better

characterize asphalt concrete. The finite element model may then be used both for

analyzing the effect of non-linear, viscoelastic properties on Equation 8, as well as

performance modelling through repeated loading.

CHAPTER 4: DEVELOPMENT OF THE IN-SITU SHEAR STIFFNESS TEST (InSiSST™)

4.1 Introduction and Chapter Overview

Based on the material presented in the Introduction (Chapter 1) and Literature Review (Chapter 2), it is hoped that the need for an advanced test device for measuring the in-situ shear properties of asphalt pavements is not only apparent, but also warranted and desirable. Chapter 3 "paved" the way for the development process by providing a sound analytical foundation for deriving shear properties from an in-situ test using the surface plate torsion method.

This chapter presents the process completed during the development of such a device, known as the In-Situ Shear Stiffness Test (InSiSST™). Development of the InSiSST™ took a logical, step-wise approach. This approach commenced by first reviewing previous work of other researchers, followed by an analysis of current deficiencies, which ultimately lead to the design and fabrication stages. Once fabrication was completed, a series of validation, debugging and shakedown exercises were completed to ensure ruggedness of the device. An initial set of field test procedures is also presented to enable others to use the InSiSST™.

4.2 Critical Analysis of CiSSST Prototype Deficiencies

Design of the InSiSST™ commenced with an analysis of the deficiencies observed with the CiSSST prototype. Although the CiSSST represented an important first step toward in-situ measurement of shear properties and yielded much important

information, a number of design-related and operational deficiencies were noticed during its use as outlined in the following sections.

4.2.1 Chassis Design and Weight

The chassis of the CiSSST device consisted of a metal cart mounted to small castor wheels. Transportation of the test device was very inefficient and dangerous due to its large weight, however, once on the pavement surface, the CiSSST was relatively easy to manoeuvre into position over the test plate. In total, the CiSSST device weighed approximately 50 kg (110 lbs.). During set-up and breakdown, the device had to be manually lifted into and out of the transport vehicle by at least four operators. Since only one or two operators were required during the actual test procedure, this was clearly an inefficient use of operator time and resources, commodities that are in increasingly short supply. Furthermore, lifting heavy equipment inherently compromises operator safety, another important consideration.

4.2.2 Stabilization of Test Device

A stable test device during the application of torque was critical to the accurate measurement of pavement shear strength/stiffness. Stabilization of the CiSSST was achieved through two methods. The first consisted of locking the castor wheels to prevent rolling. The weight of the device then acted to prevent movement during testing. This method proved unsatisfactory and a secondary stabilization system was incorporated. This system consisted of six large steel stakes that were fed through hollow tunnels welded vertically to each corner and midway along the sides of the test device. The stakes were then driven into the pavement surface using a sledgehammer. Although relatively effective, problems were identified with this method as well. In addition to the significant operator

effort required to drive the stakes into the pavement surface, the pavement surface was damaged through the use of the stakes. The most serious problem associated with this technique stemmed from the fact that the test device had to be attached to the test plate prior to stabilization. Therefore, the torque cell was already attached to the test plate as the stakes were driven into the pavement and the sensitive electronics within the torque cell were subjected to intense force as the hammering was applied. This may have eventually damaged the torque cell – the most costly component of the device. The hammering force may have also affected the epoxy bond between the steel loading plate and the asphalt surface in some cases where bond failure was observed.

4.2.3 Epoxy System Used for Loading Plate Attachment

The epoxy used for CiSSST testing required a relatively long cure period of 24 hours at temperatures above 10°C. This required the closure of the test site to traffic twice within a 24-hour period – once to epoxy the loading plates and once for actual testing. Closing roads to traffic at any time period increases congestion and driver stress, as well as presenting significant safety risk to highway personnel. Therefore, test preparation and execution must be completed in the shortest duration possible.

4.2.4 Data Collection, Control System and Available Test Program

Accurate data collection during testing was limited to applied torque only. Furthermore, although the datalogger recorded instantaneous torque readings, the data was not accessible for on-site viewing unless downloaded into a portable computer.

Angle of twist at failure was measured crudely with a protractor — instantaneous angle of twist was simply not possible with the CiSSST device. Due to this limitation, a graph of applied torque versus angle of twist (stress vs. strain) was not possible.

Control of the CiSSST was also limited. Only two test (rotation) speeds were available and there was no way of monitoring for constant stress or strain conditions.

4.2.5 Overall Test Device Performance

To its credit, the CiSSST device performed extremely well given its basic construction and control system. However, there were a number of general performance deficiencies that were observed during testing that required attention. The first concerned the overall "strength" or "capacity" of the test device. The motor and gearbox combination selected for the CiSSST was not able to provide torque sufficient to fail some pavements at all test temperatures. A limiting test temperature of 10°C was assigned to the CiSSST device to achieve failure. Secondly, the coupling used to transmit torque from the motor to the gearbox was under-designed and failed during one test program.

It must be again emphasised that the CiSSST performed extremely well for the purposes for which it was designed — a preliminary, research-oriented device. The results obtained with the CiSSST represented an all-important first step toward the development of a mainstream test facility.

4.3 Design Objectives for InSiSST™ Test Facility

4.3.1 Mitigation of CiSSST Deficiencies

Defining the design objectives represented the next step in the development process of the InSiSST™ facility. The objectives presented in this section were established largely through analysis of the CiSSST prototype deficiencies in addition to other common sense objectives essential for designing a widely used test device.

4.3.2 Reasonable Cost

If a test device is to be successful in any market driven economy, its cost must be reasonable as compared to its value to users. Also, it does not matter how much benefit the test will provide if the user is unable to afford its cost in the first place. Therefore, costs incurred by the end-user (purchasing cost, operating and maintenance, etc.) must be justified with regard to the benefits provided by the test. Furthermore, as the goal was to produce a platform for a widely used test device, these costs must be within a reasonable range for the average user.

4.3.3 Portability and Safety

As road systems span thousands of kilometres, the portability of an in-situ pavement test device to various test sites is of great importance. Furthermore, the device must be easily mobile within individual test sites since numerous tests are performed to ensure statistical significance. Operator safety is another important consideration as injuries cause employers to incur loss of productivity and increased compensation costs. Obviously injuries are also detrimental to the employees as well.

4.3.4 Number of Operators and Ease of Use

Employee salaries are usually the single largest expense that an employer will incur. Therefore, minimizing the number of operators required to perform the field test will greatly increase the attractiveness of the device to both end-users and their clients. Additional savings may be realized by developing a test that is simple to perform such that specialized training is not required for operators.

4.3.5 Minimal Test Time and Damage to Pavement Surface

Minimizing the time required to perform a field test produces two substantial advantages. First, more tests may be performed for a given time period, increasing the amount of data acquired by the researcher and the amount of money generated by the contractor. The second advantage concerns the disruption to traffic flow. As this is an in-situ test, sections of road must be closed to perform the test, which increases traffic congestion and the potential for worker injury.

Destructive pavement tests are becoming increasingly undesirable since the result is usually an acceleration of pavement deterioration. Tests that are non-destructive or that produce little disturbance (semi-destructive) to the pavement structure are favoured.

4.3.6 Correlate Results to Pavement Performance Indicators

Perhaps the most important consideration when developing the InSiSST™ facility was the need to correlate the field test results to both standard laboratory values and pavement performance indicators such as rutting and cracking. Achieving such correlation would yield significant and immediate benefits to the three primary areas of pavement engineering. The first area is mix design. An in-situ shear stiffness test in conjunction with laboratory testing would be a powerful

combination for analyzing the potential of proposed mix designs. Also, the results of such a test apparatus could be used to produce "shift" or "master" curves relating in-situ shear strength/stiffness to various factors such as loading rate, temperature and asphalt content to name a few. The second area is the quality control and quality assurance (QC/QA). Newly constructed asphalt pavements could be tested to verify acceptable construction practices through the measurement and comparison of in-situ strength parameters with code requirements. The final area is the long term pavement performance (LTPP). Monitoring of actual field shear strength/stiffness of pavements with time would assist in predicting future pavement performance. This, in turn, would allow for more efficient allocation of limited rehabilitation funds and also help determine the effect of real world conditions, such as environmental factors, on pavement performance.

4.4 Design of InSiSST™ Facility

4.4.1 Introduction and Overall Design

The design for the InSiSST™ facility was conceived based on the stated design objectives and noted CiSSST deficiencies. While complete adherence to the design objectives was the ultimate goal, trade-offs between objectives were necessary. Therefore, the InSiSST™ design represented an optimization of the individual design objectives into an integrated system.

The completed InSiSST™ device is shown in Figures 27 through 29. As shown, the components are mounted to a small A-frame trailer to provide exceptional portability. As with the CiSSST facility, the InSiSST™ utilises an

electric motor and gearbox to produce the required torque. The motor/gearbox combination is mounted vertically on a steel platform that is attached to a positioning system that incorporates two sets of worm-screw slides working in tandem, also referred to as an "X-Y table." The top set of slides allows positioning of the platform in the transverse direction (with respect to the trailer orientation). The transverse slides are in turn mounted to a second set of slides allowing positioning in the longitudinal direction. The entire positioning system is mounted to a box-tube frame occupying the space between the tow bar and the axle of the trailer. The test frame is attached to the trailer frame via four screw jacks, one at each corner of the test frame. During transportation of the InSiSST™, the jacks are retracted to hold the frame in the air to prevent damage. Once driven into position, the jacks are extended to lower the test frame to the ground and then continue extending until the weight of the trailer is supported solely by the test frame. As with the positioning system, an electric motor is used to raise and lower the jacks. A single motor is used to deploy all four jacks using mitreboxes and driveshafts. Control of the jacks and positioning slides is provided by commercially available electric motor controls. Control of the actual test procedure is provided by a laptop computer. Instantaneous torque and angle of twist measurements are collected on the computer during the test procedure. A large plastic storage box is mounted to the front of the trailer to house the electronic components. Finally, a generator is mounted to the rear of the trailer to provide electricity for the InSiSST™. A more detailed explanation of the individual systems is provided in the following sections.

Figure 27: Side View of InSiSST™
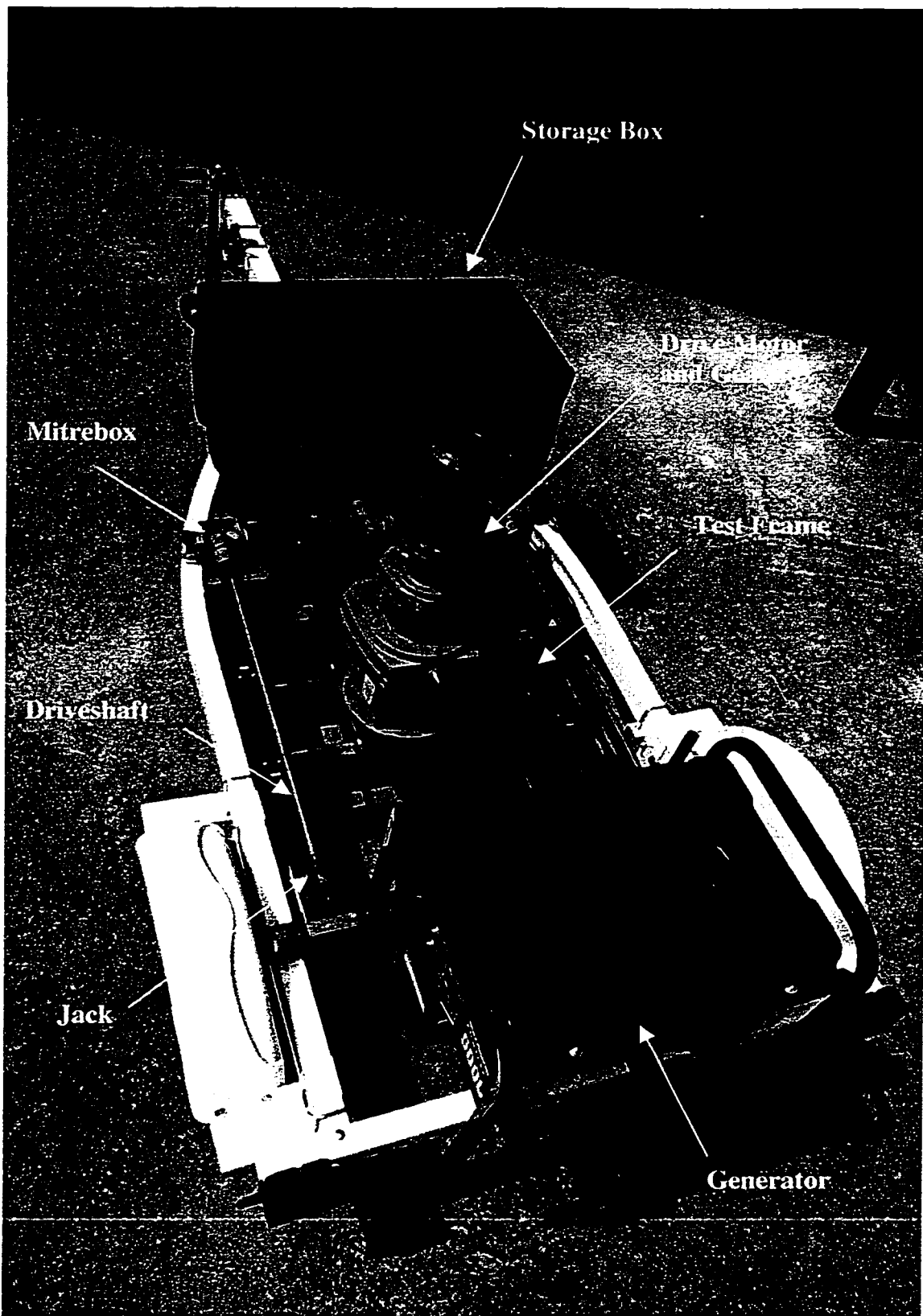
Figure 28: Top View of InSiSST™
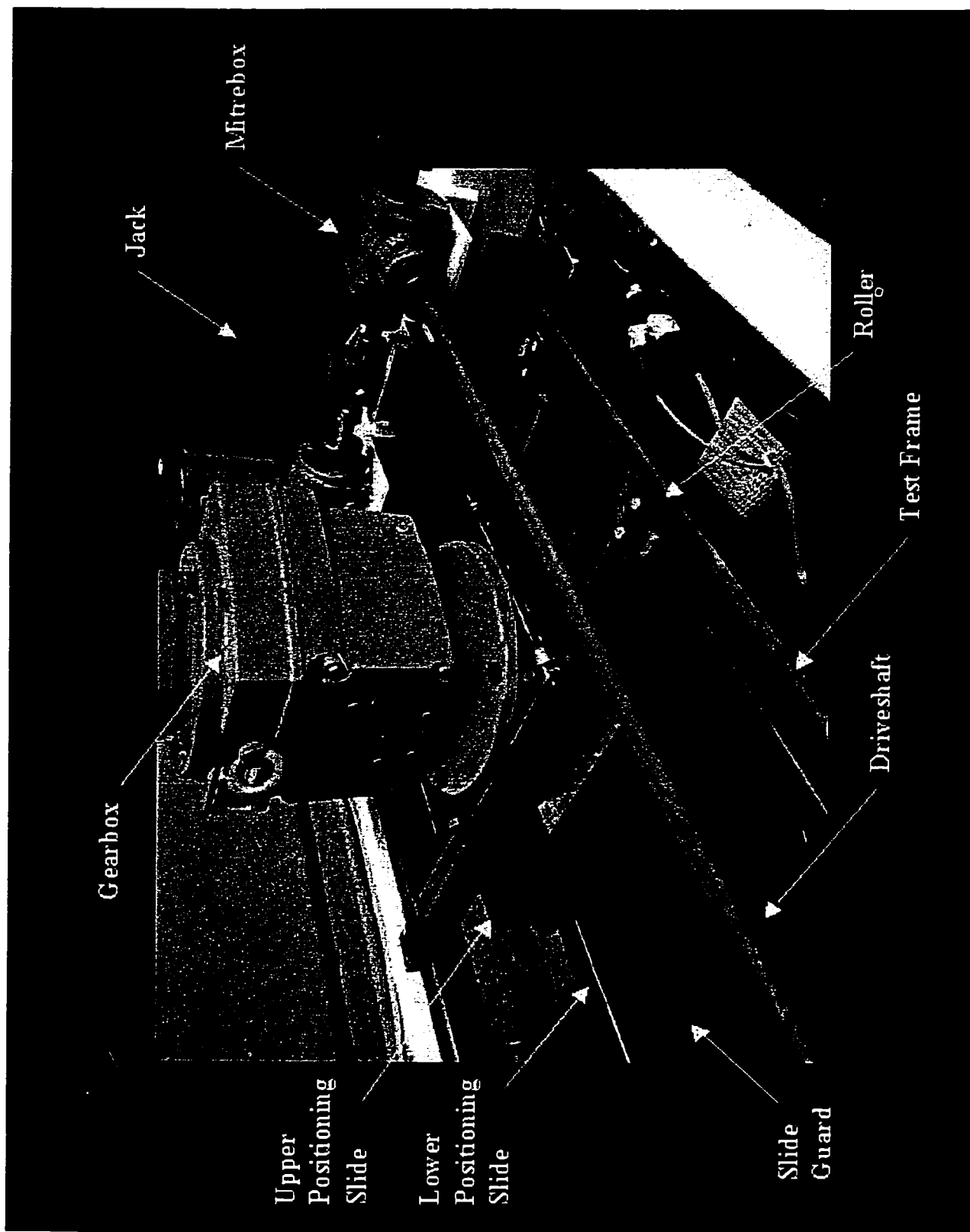
Figure 29: InSiSST™ Positioning System

4.4.2 The Primary Force Generation System (Powertrain)

After investigating alternative methods to produce the required rotational force (torque) for the test, it was concluded that, like the CiSSST, the use of a simple electric motor and gearing still represented the best choice for this application. Systems incorporating hydraulics or pneumatics would certainly produce acceptable, if not superior results. However, these systems were simply too expensive, at least at the concept exploration stage.

The first important improvement involved the vertical alignment of the main drive motor and gearbox. The vertical alignment saved a significant amount of space when compared to the CiSSST facility, which utilized a right-angled gearbox attached to a horizontally mounted motor. The straight gearbox arrangement provided increased capacity and reduced backlash compared to right-angled gearboxes.

The overall capacity of the motor and gearbox system was increased significantly to ensure failure of all asphalt surfaces encountered (over a reasonable temperature range). The gearbox is a triple reduction unit with a final ratio of 8101:1. Therefore, 8101 revolutions of the main drive motor are required to turn the output shaft of the gearbox a single revolution. This huge reduction was needed not only to reduce the test speed to reasonable levels, but also to increase the available torque to fail the asphalt surface. Whereas the CiSSST device produced a maximum torque of approximately 508 N*m (4500 lbf*in), the InSiSST™ can apply up to 1550 N*m (13700 lbf*in) of torque, an increase of over 200%.

Another significant improvement over the previous design was to mount the motor directly to the gearbox. As mentioned earlier, the CiSSST had a driveshaft

and coupling between the motor and gearbox which failed during one suite of field testing. The direct attachment also reduced power loss between the gearbox and the motor. A final benefit was that the direct motor/gearbox coupling provided a tight seal, thereby significantly reducing the likelihood of infiltration of water and/or dirt into the gearing.

One disadvantage of the vertically mounted gearbox and motor was a higher centre of gravity. However, a restraint system was developed using tie straps to prevent movement of the gearbox and motor during transportation.

4.4.3 The Transportation System

One of the greatest problems with the CiSSST facility was its lack of portability. The integration of the facility with a trailer allows exceptional portability from site to site. Furthermore, the facility no longer requires lifting or lowering by human effort. This drastically reduces not only the potential for injury, but also the number of operators required for testing, which will provide significant cost savings to the end-user. Another benefit of the trailer-mounted option is that any vehicle with a trailer hitch may tow the facility.

One disadvantage of the trailer-mounted option is that the facility is subjected to a much harsher environment, such as the infiltration of water, dust and dirt. However, judicious selection of rugged and/or sealed components reduced this concern.

4.4.4 The Test Frame and Positioning System

The test frame fills the space between the trailer axle and the front cross bar, providing the foundation for many of the essential InSiSST™ systems as shown in Figures 27 and 28.

There are two "levels" to the test frame and positioning system. The lower

level houses the lower sliding system, consisting of the 2 sets of tandem worm-

screw slides (i.e. 4 individual slides) mounted orthoganally to allow movement in

the longitudinal and transverse direction as shown in Figure 30. The bottom worm

screw slides are mounted within 150 mm wide steel channels that run the length of

the test frame to prevent damage during transportation.

Legend:
A - Transverse Slides
B - Longitudinal Slides
C - Drive Belt
D - Motor
E - Test Frame
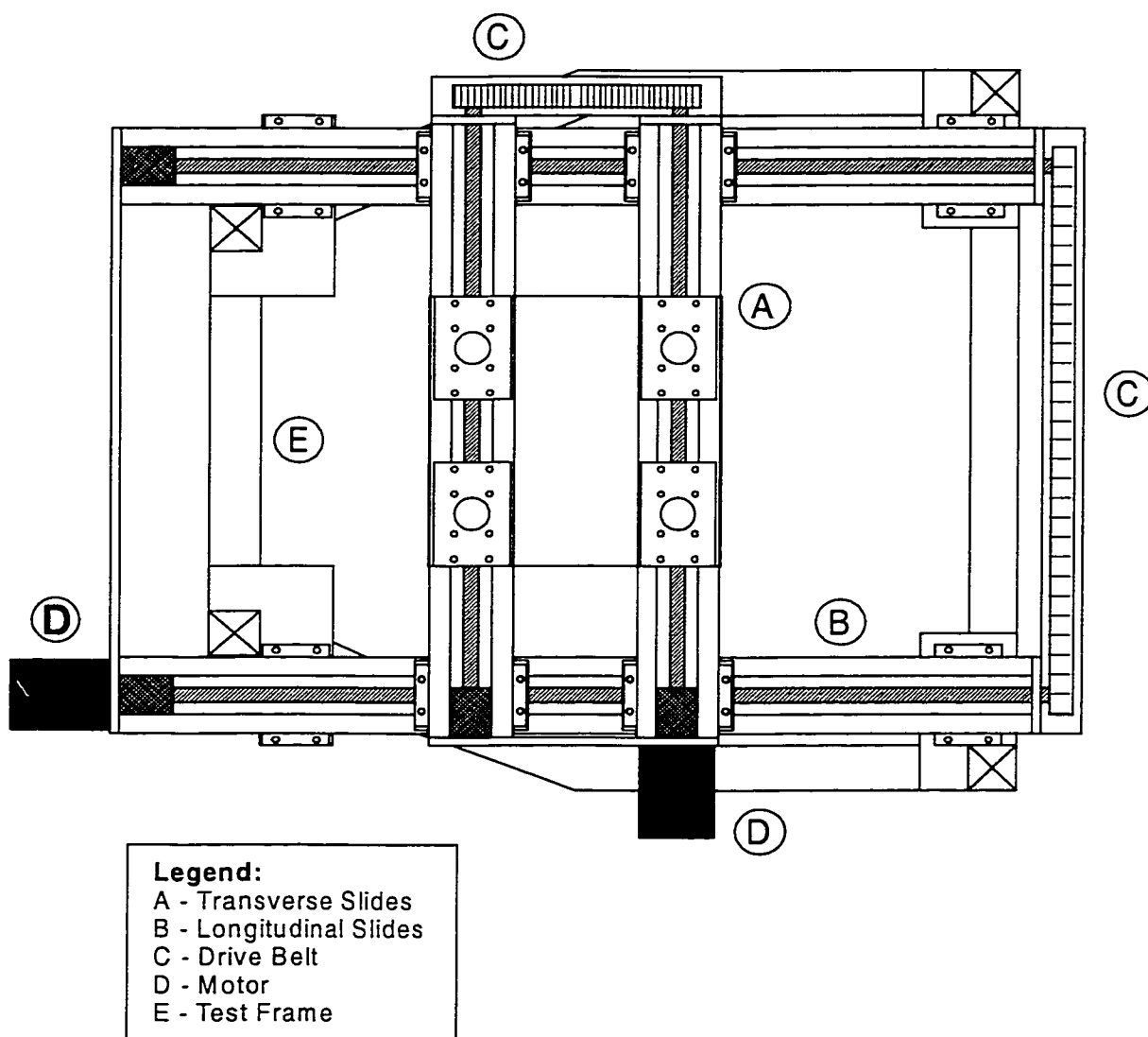
Figure 30: Plan View of the Lower Positioning System
(Protective Steel Channels not shown)

The upper test frame and sliding system were developed to isolate the gearbox from the worm screw slides for two main reasons. First, due to the large weight of the gearbox (136 kg or 300 lb), it could not be directly mounted to the worm screw slides according to the manufacturers specifications for static (dead) load. Second, if the gearbox was mounted directly to the slides, the reactionary force produced by the gearbox during an actual field test would be transmitted through the slides themselves. Even at low levels of applied torque, this reactionary force would greatly exceed the manufacturers specifications for dynamic load and would likely damage the slides.

The upper level of the test frame consists of 50 mm hollow structural sections that provide support for the upper sliding system. As shown in Figure 29, the gearbox is mounted to a steel plate 300 mm (12 in) square. This plate is mounted on rollers and slides transversely across a set of connected 50 mm HSS beams, which are also mounted on rollers and slide longitudinally along the upper test frame. The upper sliding system is attached to the worm screw slides below, thus allowing the slides to control the movement of the gearbox within the test frame. Before a test is initiated, the connection between the upper and lower sliding systems is removed by clamping the upper sliding system to the upper test frame. By isolating the upper and lower sliding systems, the large weight of the gearbox and reactionary forces are not applied to the worm screw slides.

A dedicated controller and control pad housed in the front storage box control the movement of the entire positioning system. In its current configuration, a net travel distance of 150 mm (6.9 in) in either direction from the centre position is capable with the transverse slides and a total longitudinal travel distance of 640 mm

(25.2 in) is capable with the longitudinal slides. Therefore, a total testing area of 0.1 m^2 (148 in^2) is available each time the test frame is lowered. If a 100 mm (4 in) diameter test plate is used, four plates can be placed inline with a minimum distance between tests of 80 mm (3.1 in). If larger load plates such as 125 mm (5 in) and 150 mm (6 in) plates are desired for larger aggregate mixes, 3 plates should be used to provide a minimum between plate distance of 88 mm (3.5 in) and 63 mm (2.5 in), respectively. Initial analytical modelling by Bekheet et. al. (2000) has indicated that strains experienced outside of the test plate drop to less than one percent at a distance of 50-mm (2 in) from the outer edge of the plate. Therefore, a statistically significant number of tests can easily be performed for a single test-frame deployment. Furthermore, the slides incorporate sealed motors and gearing to be protected from the elements.

4.4.5 The Stabilization System

A stable test platform was a critical design factor for the InSiSST™ facility. By lowering the test frame and lifting the trailer off its wheels using jacks, the full weight of the trailer is applied to the test frame. Stability against the rotational force applied to the test plate is therefore achieved through frictional force between the bottom of the test frame and the pavement surface.

The test frame used in the InSiSST™ facility presents a frictional condition very similar to that observed with thrust bearings or disk clutches called "disk friction". An applicable formula for disk friction may be derived by considering a rotating hollow shaft. For a hollow shaft whose end is bearing against a solid flat surface, the minimum torque required to keep the shaft rotating may be computed using Equation 9 below (Beer and Johnson 1988).

$$M = \frac{2}{3}\mu_k P \frac{R_2^3 - R_1^3}{R_2^2 - R_1^2} \qquad (9)$$

Where R_1 and R_2 are the inner and outer radii of the shaft respectively, M is

the required torque, μ_k is the coefficient of dynamic friction and P is the axial force

applied to the shaft. By replacing the dynamic friction coefficient μ_k with the static

friction coefficient μ_s, Equation 9 may be used to find the largest torque that may be

applied to the disk prior to slippage. For this application, the test frame itself is

analogous to the hollow shaft. The force P is applied by the gravitational force of

the trailer and test frame on the pavement surface while the couple M is applied by

the motor/gearbox during the test procedure. To find the magnitude of force P

sufficient to resist the rotational reaction, "equivalent radii" were determined for the

test frame. The test frame is rectangular in overall shape as shown in Figure 31.
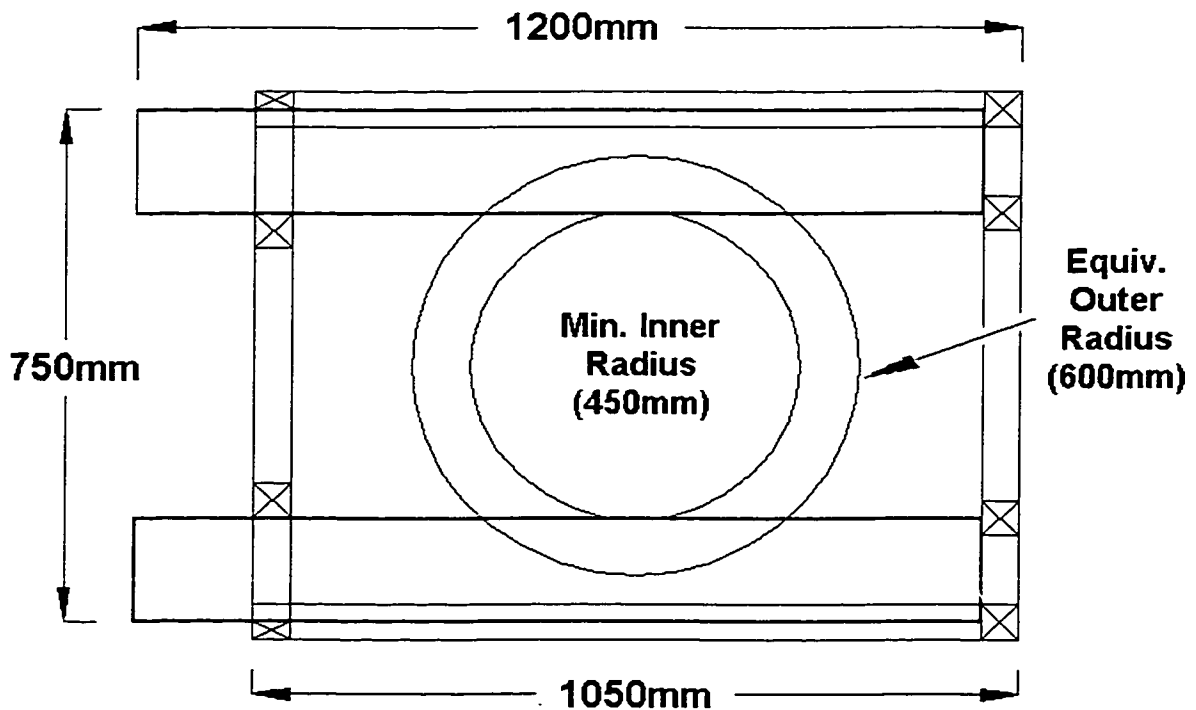
Figure 31: Plan View of InSiSST™ Test Frame

Based on previous testing regimes with the CiSSST device, the maximum failure torque applied to an asphalt pavement surface using a 100 mm (4 inch) diameter test plate was approximately 508 N*m (4500 lbf*in). It was reasonable to assume that the weight of the trailer will be evenly distributed at each corner of the test frame via the jacking system. Therefore, regardless of the position of the motor and gearbox within the test frame, the full frictional resistance of the interface between the test frame and the pavement surface should be mobilized assuming that the pavement surface is relatively flat.

The total contact area between the test frame and the pavement surface is 0.52 m^2 (5.6 ft^2) including the channels that protect the positioning slides. From the centre of the test frame, the minimum inner radius is 0.45 m (17.7 in). The "equivalent" outer radius was then calculated using the equation for the area of a 2-dimensional ring as shown in Equation 10.

$$A = \pi \left(r_{outer}^2 - r_{inner}^2 \right) \qquad (10)$$

where:

A = total contact area (0.52 m^2);

r_{inner} = minimum inner radius (0.45 m)

The resulting equivalent outer radius was found to be 0.60 m (23.9 in). Utilizing these radii with M = 508 N*m (4500 lbf*in), and assuming a coefficient of static friction of 0.5, the minimum weight (normal force, P) applied to the test frame must be approximately 1905 N. Therefore the load applied to the test frame must be 195 kg (428 lbs.) according to Equation 9.

Much of the required weight is provided by the trailer and test frame, as well as the equipment necessary for operating the test facility. This includes the jacking system and the data acquisition/control system.

A static coefficient value of 0.5 was selected for the analysis to ensure a reasonable factor of safety. The actual coefficient of static friction between the test frame and the pavement surface is likely to be 0.7 or greater as a neoprene (rubber) pad has been epoxied to the bottom of the test frame to increase the friction.

This system prevented movement during testing and eliminated the need to drive stakes into the pavement surface. Therefore, no damage is imposed on the pavement through stabilization and no operator effort is required. Furthermore, by having the stabilization completed prior to positioning and testing, the sensitive electronics of the torque cell are not subjected to unnecessary stress. To prevent the use of multiple motors, a set of custom driveshafts and mitreboxes was fabricated to connect all four jacks to a single motor, thereby reducing cost and ensuring that the jacks do not operate independently of one another.

The jacks themselves are coated with a plastic layer to resist corrosion, and accordion-like bellows cover the screws to prevent the infiltration of water and dirt into the gearing.

4.4.6 Epoxy System

As mentioned, the epoxy system used previously required 24 hours to cure prior to testing. This limitation required two visits to the test site, an inefficient and costly method of testing.

During the investigation, numerous adhesive systems were tested for suitability. Most systems either required cure times that were similar to the existing

system or did not provide suitable strength at all. For example, instant contact-type adhesives were not effective as they rely on direct contact between the asphalt surface and the steel plate. Due to the roughness of the asphalt surface, this contact was not provided.

At this time, the best performing product is a two-part epoxy system that provides adequate strength after 2 hours at room temperature. Therefore, curing time at elevated temperatures, such as those experienced in the field during testing will reduce this time. Two hours was deemed as an acceptably short time interval as the tests themselves can be completed in minutes once the epoxy has cured.

4.4.7 The Test Control/Data Collection System

The main drive motor is controlled by using a variable speed motor controller with a speed sensor connected directly to the motor shaft. The speed sensor provides a closed loop system and ensures that the motor does not deviate from the desired test speed. Therefore, the InSiSST™ is a strain-controlled test as the rate of displacement (twist angle) is controlled, while the resulting torque (stress) is measured by the torque cell. The accuracy of the motor controller is ±1 revolution per minute (rpm).

The variable speed motor controller also allows the selection of a variable test speed between zero revolutions per minute (rpm) and 1800 rpm. Table 13 displays pre-programmed strain rates and there associated drive motor speed. The strain rate of 0.0005 revolutions per second corresponds with the strain rate used in the Superpave Shear Tester during frequency sweep testing.

Table 13: Target Test Strain Rates and Associated Motor Speeds

Target Strain Rate (rev/s)	Required Motor Speed (rpm)
0.0005*	243
0.0010	486
0.0015	729
0.0020	972
0.0025	1215
0.0030	1458
0.0035	1701
0.0037	1800**

* Strain rate of SST for frequency sweep testing
**1800 rpm is the maximum available motor speed

Torque is recorded with a torque cell similar to that used with the CiSSST facility, although of higher capacity. Both the InSiSST™ torque cell and the motor controller have standard RS-232 (serial) connections for connection to a computer. However the laptop has only a single serial connection. To overcome this problem, a Universal Serial Bus (USB) adapter box was used. This device allows the connection of up to 4 individual serial connections into the adapter with a single USB output to the laptop. Therefore, the laptop computer is able to control and acquire data from up to 4 individual serial devices simultaneously. At present, only the torque cell and motor controller are attached to the laptop. The positioning system also has a serial connection and may be controlled with the laptop in the future.

This centralized control and data acquisition system allows the collection of instantaneous readings at user-defined sampling intervals. Results are saved directly to the laptop and other relevant information such as test site location,

weather conditions, temperatures, etc. may also be directly entered into a database for future analysis.

4.4.8 Overall System Integration

All of the separate components were selected and designed to work well together as a single unit. The result is a test facility that is portable, stable, and rugged. The test requires only a single operator, no heavy lifting or complex set-up, and can be completed rapidly. The test results are accurate and are available instantly. All of the individual components operate under the same power requirements as provided by the central generator.

4.4.9 Cost

As the InSiSST™ is still in its prototype form, the actual cost of the device is not representative of a final production model. The component costs of the InSiSST™ totalled approximately $37,500 CAD ($25,000 USD). However, there are many other costs such as labour, overhead, marketing, etc. that must be factored in when determining a final purchase price. Furthermore, the component costs would likely decrease if produced in larger quantities. However, based on the component cost, it is estimated that a final production model would be priced below $50,000 USD, which was identified by the National Asphalt Pavement Association (NAPA) as being a reasonable cost for such a performance test (FHWA 1998d).

4.5 Fabrication, Debugging and "Shakedown" Testing

All fabrication activities were completed at Carleton University in the Civil and Environmental Engineering Laboratories. As with any new or complex technology, a

number of interesting challenges were encountered during the development of the

InSiSST™ device. Perhaps the most frustrating were the long delays experienced

when ordering and acquiring the component parts for the InSiSST™. Although most

of the components were commercially available, they were not actually fabricated or

assembled until ordered, thus requiring up to 2 months to receive and in turn delaying

the fabrication of the InSiSST™ on multiple occasions.

4.5.1 Positioning System Debugging

When the positioning system was first installed and attached to the gearbox,

the system would often "stall" while moving the gearbox back and forth within the

test frame. It first appeared that the stepping motors of the positioning slides were

not powerful enough to move the gearbox. However, upon further examination, it

was discovered that the slides were not completely parallel and that the gearbox was

hitting the slides at certain spots along the slide length. Once adjusted, the

positioning system performed properly.

4.5.2 Jacking System Debugging

The jacking system itself presented no major problems during development,

although the rate of extension and retraction of the jacks is faster than anticipated.

The addition of a gear reducer to the jacking motor is expected to reduce the speed

at which the jacks rotated, although has not been completed to date.

4.5.3 Test System Debugging

Once constructed, the motor controller and torque cell were connected to the

laptop computer via the USB-to-Serial connection box to begin the software

development. Unfortunately, the test software conflicted with the USB adapter and

caused the computer to "crash" everytime the test software was initiated. A

software patch was obtained from the manufacturer of the USB adapter and the problem was solved.

4.5.4 Shakedown Testing

A series of shakedown exercises were completed with the InSiSST™ to ensure an acceptable amount of ruggedness prior to field testing. Most of the shakedown testing was completed in and around the Carleton University campus.

The most challenging test of ruggedness for the InSiSST™ was completed between July 16th and 18th of 2000 when the trailer was driven from Ottawa to College Park, Maryland and then to Washington, DC for a demonstration at the Transportation Research Board. The total trip distance was approximately 2000 km (1250 miles), most of which was along major Canadian highways (416, 401) and US Interstates (80, 95) at speeds ranging from 80 to 120 km/h (50 to 75 mph). While in College Park and Washington, the InSiSST™ was towed along city streets, many of which were in poor condition displaying potholes, extensive cracking, patching and rutting. The InSiSST™ traversed countless sharp bumps and dips during the journey and there was some concern for the health of the electronic equipment housed in the storage box. However, no damage whatsoever was observed upon return to Carleton University, with the exception of some very thin surface rust on the metal test frame. The test frame will be soon cleaned and painted to prevent future rusting. To ensure that the electronic equipment does not fail in future trips, bubble padding will be installed to protect the equipment from shock.

4.6 Field Test Procedure

The following is an initial draft of the field test procedures for effectively and safely using the InSiSST™. It is expected that more comprehensive versions of these procedures will be developed with the increased use of the device.

4.6.1 Equipment Checklist

Before leaving to the test site, the operator or technician should ensure that all necessary equipment is packed and in proper working order. Table 14 lists the equipment needed for field testing.

Table 14: Equipment Checklist

• Sufficient epoxy for field testing and associated mixing equipment
• Sufficient loading plates (cleaned and roughened)
• Fuel for the generator
• Infrared thermometer
• Stiff brush to clean dust from asphalt surface
• Callipers for measuring the depth of failure
• DipStick profiler (if rutting survey desired)
• Nuclear Density Gauge (if density survey desired)
• Laptop computer

4.6.2 Transportation Safety

The InSiSST™ is a trailer-mounted device that is towed behind a vehicle to various test sites. Therefore, safety must be an important consideration during the transportation of the InSiSST™. To help ensure a safe journey, users of the InSiSST™ should follow towing safety guidelines recommended by trailer manufacturers and/or government agencies. A comprehensive guide to towing safety is produced by Sherline Products Incorporated (Sherline 1999) and the

Ontario Ministry of Transportation (MTO 2000) has developed a quick checklist for trailer safety.

Prior to transportation with the InSiSST™, the jacking system should be completely retracted such that the test frame is in its uppermost position. Furthermore, the gearbox and drive motor must be secured to the test frame and/or trailer using the ratcheting nylon straps prior to transportation.

4.6.3 Securing the Test Site

Closing of a road section or lane always involves some risk. Therefore, traffic control should only be carried out by trained professionals with the proper equipment. If possible, traffic control measures should be initiated and completed by local or provincial transportation agency personnel to ensure the safest working conditions. However, if private traffic control is required (and permitted), the contractor should contact their local or provincial agency for appropriate traffic control procedures and equipment.

4.6.4 Preparation of Pavement Surface and Bonding the Loading Plates

Pavements are subjected to numerous types of dirt, oil and other chemicals that are introduced and tracked by automobiles, trucks and other vehicles. These chemicals will often adversely affect the quality of the bond between the asphalt surface and the steel loading plate, thereby, affecting the test results. To ensure the highest quality bond, the pavement surface should be free of deleterious substances. At a minimum, a stiff brush or broom should be utilized to remove fine particulate materials. In some cases, it may be also necessary to gently wash the asphalt surface with soap and water to remove more stubborn substances. Care should be

taken in these cases not to damage or strip excess asphalt from the pavement surface.

The surface should be completely dry prior to the placement of the loading plates. The epoxy must be prepared according to the manufacturers specifications to ensure maximum strength and bond. The epoxy should be spread evenly across the bottom of the loading plate with care such that air bubbles are not entrapped. Enough epoxy should be used such that when the plate is placed on the asphalt surface and compressed, a small amount of epoxy is displaced along the perimeter of the loading plate. The loading plates should be placed in either a straight line or staggered such that they will all fit within the test frame when lowered. Excess epoxy may be removed with a clean towel. If possible, a small weight such as a brick should be placed on the plate during the curing process. Pavement temperature is measured with the thermometer and the required curing time based on manufacturers information is assessed.

4.6.5 Rutting/Density Surveys (Optional)

While the epoxy is curing, a rutting and/or density survey of the test section may be completed to provide additional information for analysis. A grid system such as that illustrated in Figure 32 can be marked using a chalkline. Transverse and longitudinal profiles may be measured using the DipStick or similar profiler to provide rutting and roughness data. A nuclear density gauge may also be used to measure the density of the asphalt both in the wheelpaths and the midlane. An example pattern for in-situ shear testing for research purposes (white circles) and coring (grey circles) is also shown in Figure 32, although the pattern shown would require the movement of the InSiSST™ within the test site.
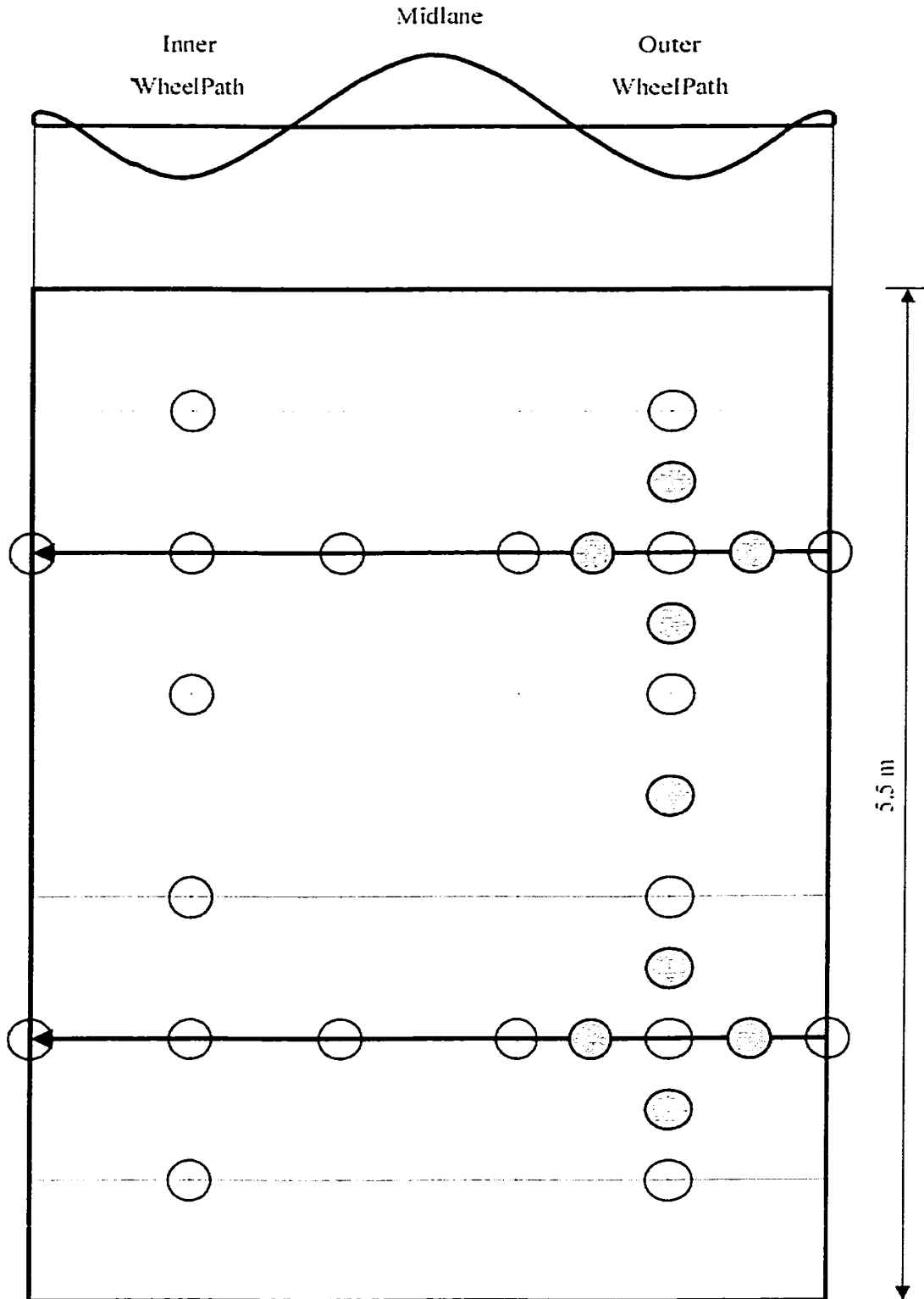
Figure 32: Outline of Rutting and Density Survey

4.6.6 InSiSST™ Test Procedure

Once the epoxy has cured, the field testing with InSiSST™ may commence.

The following steps should be completed in order:

1. Detach the InSiSST™ from the tow vehicle and manoeuvre it over the test plates such that all test plates will be within the test frame when lowered (Figure 33).

2. Chock the tires of the trailer once in position to prevent movement of the trailer. A brick or wooden wedge work well (Figure 34).

3. Attach the torque cell cable to the torque cell (Figure 35).

4. Install the torque cell and connecting collar onto the gearbox driveshaft.

5. Lower the test frame to the ground and ensure that the weight of the trailer has been transferred to the test frame (the trailer suspension will relax when this occurs).

6. Attach the USB connection to the laptop and turn the laptop on.

7. Turn on the slide controller.

8. Use the slide control pad to align the torque cell (and gearbox) over the first test plate (Figure 36).

9. Activate the motor controller software on the laptop and turn the torque cell until it is aligned with the load plate in the radial direction.

10. Lower the connecting collar on the torque cell into the load plate (connecting collar shown in Figure 37).

11. Measure the pavement temperature directly adjacent to the load plate and record it for future analysis (Figure 38).

12. With the torque cell firmly connected to the load plate, activate the torque cell software. The software will begin to take readings at the predefined sampling rate and record them in a text file. There should be very little load shown for these initial readings as the drive motor has not been restarted yet.

13. Press the red calibration button to calibrate the torque cell (Figure 36). Ensure that at least one calibration reading has been recorded in the text file.

14. Once calibrated, the test may be initiated. To do this, select the desired strain rate from the motor controller software. As the strain is applied, the torque readings should increase until failure of the asphalt surface.

15. When failure occurs, press the Escape key to stop the drive motor.

16. Inspect the failed asphalt surface and loading plate. Measure the depth of failure with the callipers and record it for later analysis.

17. Save the test file to the hard drive.

18. Repeat steps 8 through 16 for the remaining load plates.
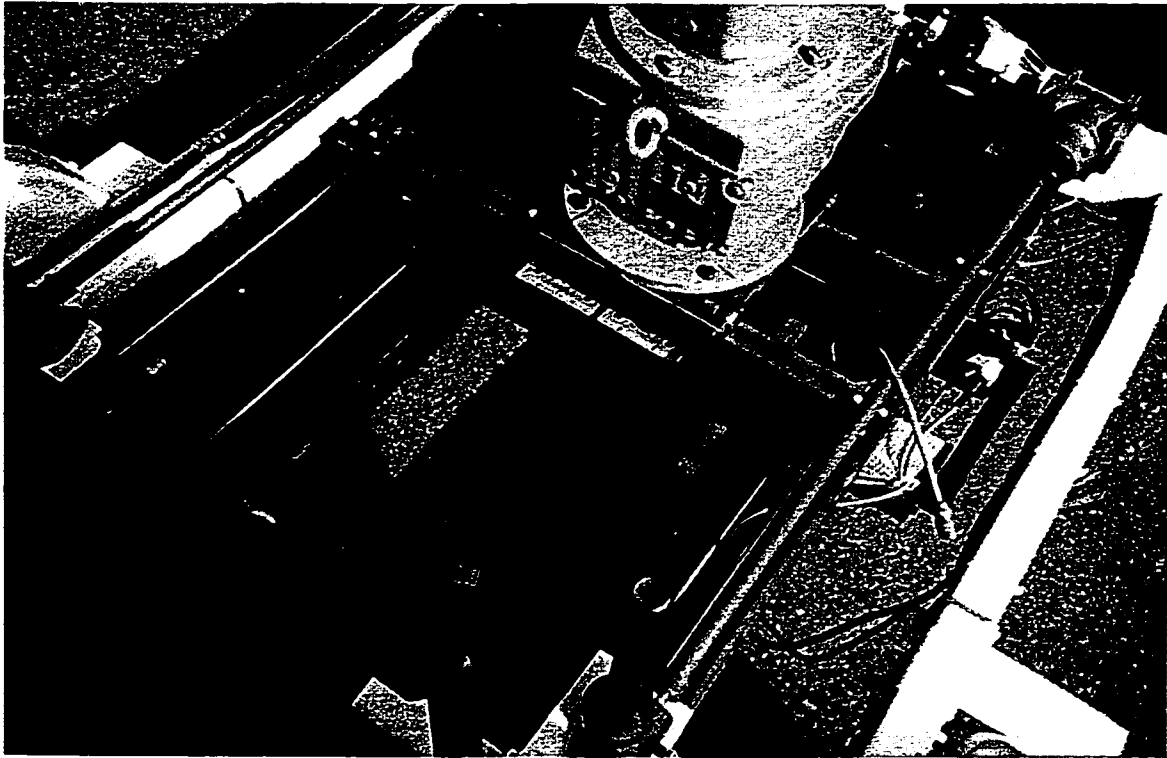
Figure 33: InSiSST™ Trailer over Test Plates
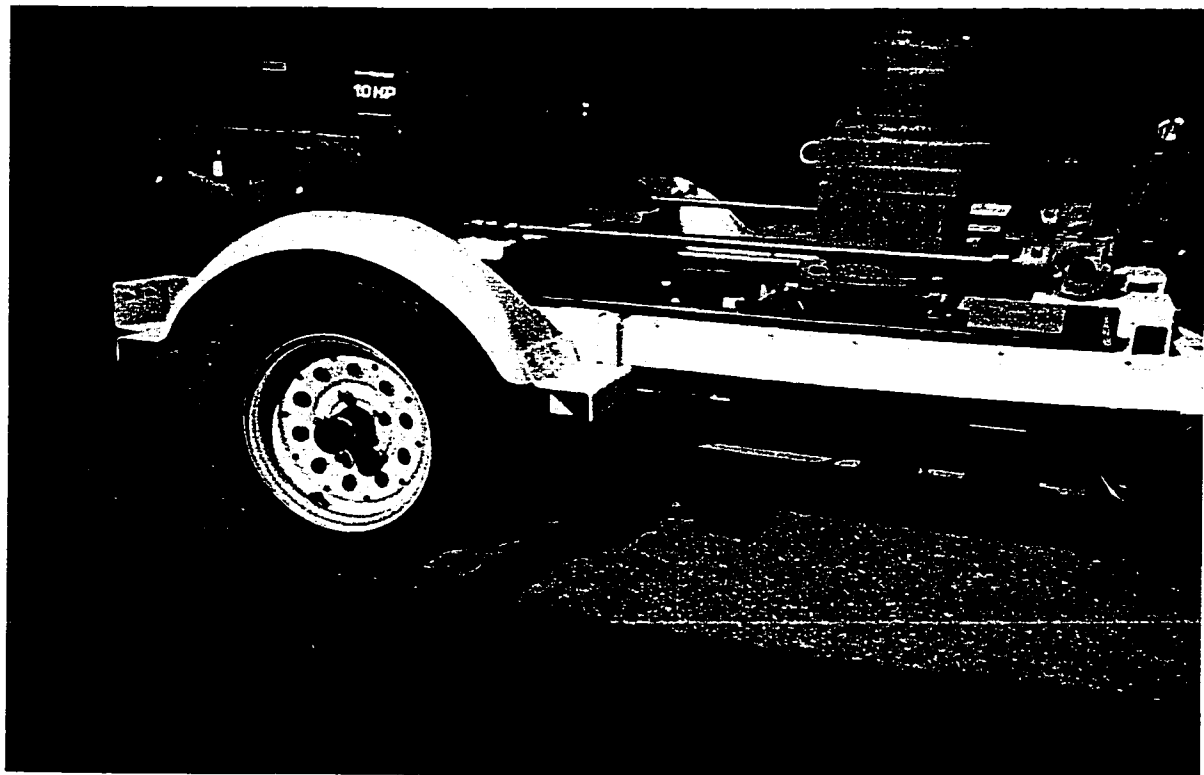
Figure 34: Chocking the Trailer Tire

Figure 35: Attach Torque Cell Cable to Torque Cell

Torque Cell
Calibration

Positioning
System
Controller

Slide Motor
Controller

Positioning
System
Control Pad
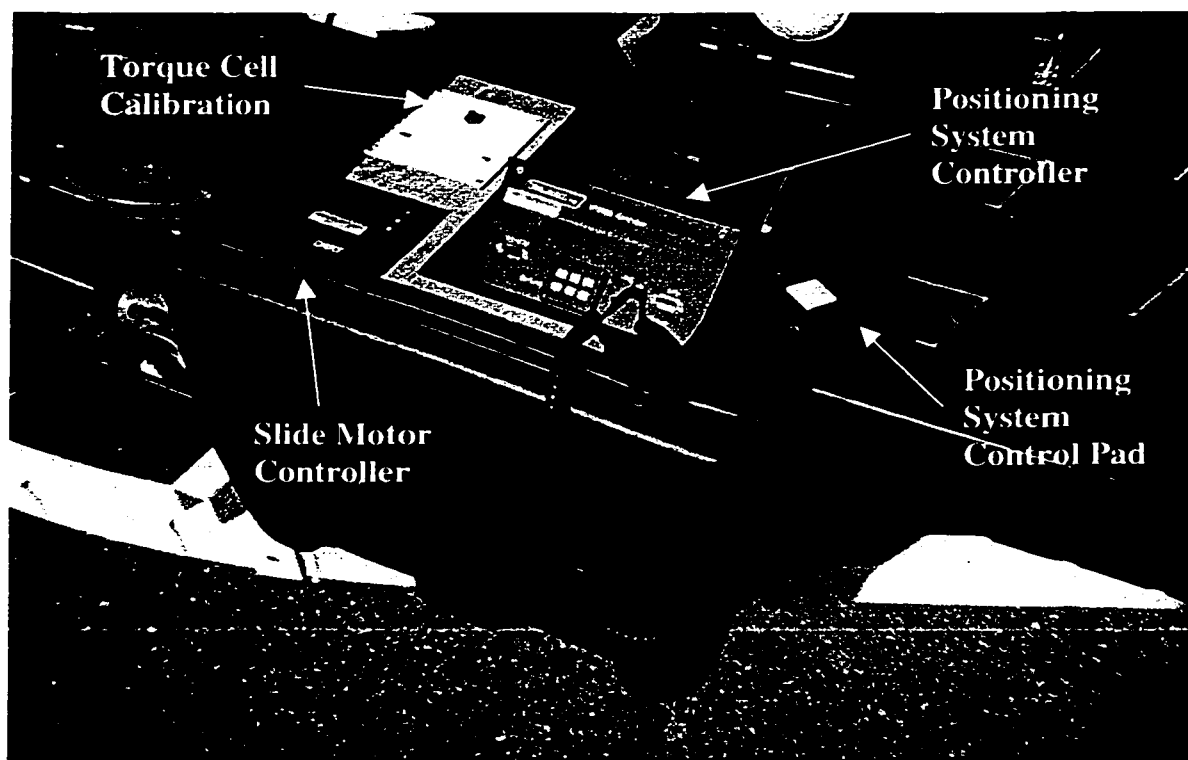
Figure 36: InSiSST™ Controls (Computer not shown)
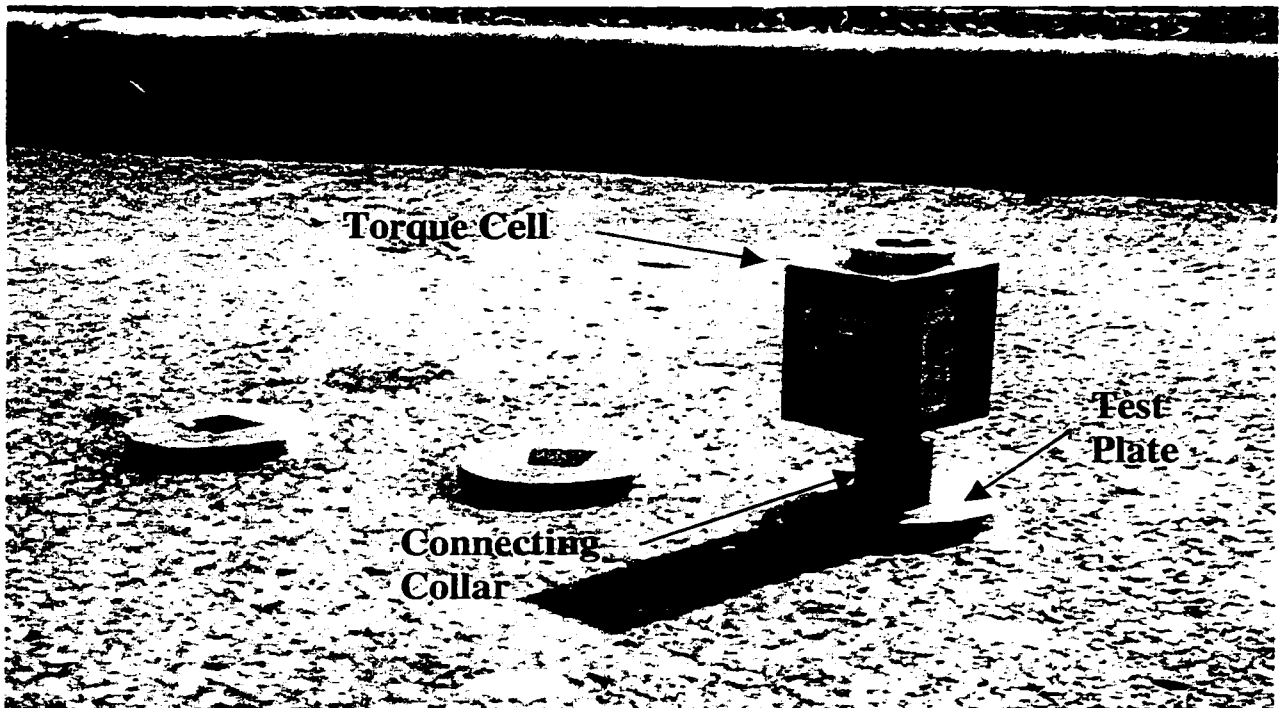
Figure 37: Connecting Collar from Torque Cell to Test Plate
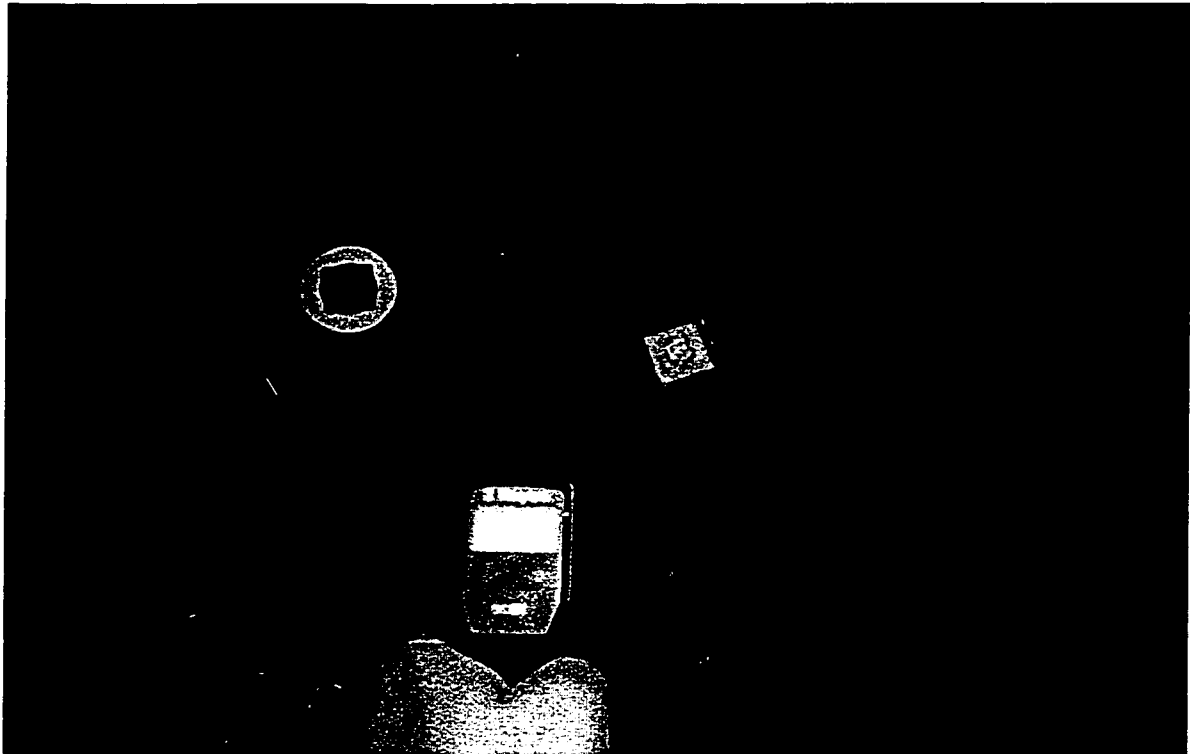
Figure 38: Taking Pavement Temperature with IR Thermometer

4.6.7 Leaving the Test Site

After all of the desired tests have been completed, all equipment should be collected and stored for transportation. The InSiSST™ test frame must be fully raised and the gearbox must be secured to the test frame and trailer using the ratcheting straps. Reattach the InSiSST™ to the tow vehicle as per the safety recommendations discussed previously. Ensure that the site is left clean and that the small divots removed by the InSiSST™ during testing are sealed with a slurry mix to prevent moisture infiltration.

CHAPTER 5: Preliminary Testing and Validation

5.1 Introduction and Overview

With the InSiSST™ facility constructed and the base analytical models available, the final stage of the investigation involved preliminary field testing for validation purposes. Chapter 5 first presents the results of an exercise to validate the linear elastic assumption made by the Reissner-Sagoci equations. Next, the results of comparison testing with the CiSSST and InSiSST™ devices are presented, including an interesting observation concerning the test plate diameter. Chapter 5 concludes with a comparison of field shear properties to those observed in the laboratory.

5.2 Analytical Models vs. Field Test Results

5.2.1 Verification of Linear Elastic Assumption

As reported by Bekheet et. al. (2000), preliminary field tests were conducted using the CiSSST with the objective of verifying the applicability of the linear elastic assumption used by the Reissner-Sagoci equations for asphalt concrete. To this end, pilot tests were completed at Carleton University with a modified test procedure to accurately measure the surface displacements (Bekheet et. al. 2000).

The angular displacement values from the tests were also compared to the expected values using Equation 8, as shown in Figure 39. While the number of data points from the field tests was low, they displayed high correlation with Equation 8 ($R^2=0.86$). This result implied that the linear-elastic assumption for asphalt pavement behaviour was reasonable in this case. However, the pavement

temperature during the test was close to room temperature (approximately 22°C or 72°F), which would have contributed to the linear elastic response.
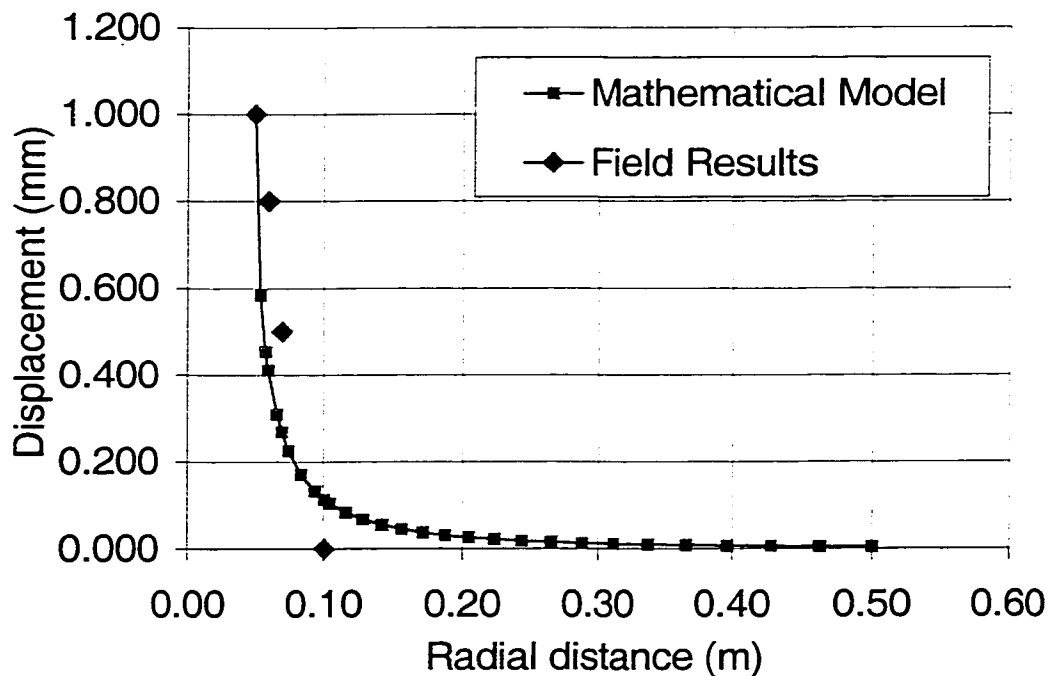
Figure 39: Comparison of Field Results with Reissner-Sagoci Model (from Bekheet 2000)

5.2.2 InSiSST™ vs. CiSSST

The surface plate method of testing is used for both the CiSSST and the InSiSST™, however, a set of comparison tests were completed to ensure that similar results were achieved. The tests were completed in a parking lot at Carleton University consisting of an HL3 asphalt concrete mix. HL3 is a standard surface mix used throughout Ontario for low to medium traffic volumes. Unfortunately, due to the age of the mix (8 years), the actual mix design data was not available for analysis.

Test plates of 92 mm (3.6 in) diameter were epoxied to the pavement surface

for each test device. The plates were placed in a straight line with a minimum clear

spacing of 65 mm (2.5 in) between each plate. Testing was completed the

following day to ensure full cure of the epoxy. Results of the CiSSST testing are

given in detail in Appendix D, and summarized in Table 15. One of the CiSSST

tests failed between the epoxy and the steel test plate, while the remaining 5 tests

produced failure of the asphalt surface. The pavement surface temperature for tests

C1 through C4 was 29°C, while test C5 was tested at a surface temperature of 27°C.

The average shear strength calculated through Equation 6 was 2058 kPa with a

relatively high coefficient of variation (COV) of 19.2%.

Table 15: Comparison of CiSSST and InSiSST™ Results

CiSSST Testing			InSiSST Testing		
Test No.	Ultimate Shear Strength (kPa)	Pavement Surface Temp. (°C)	Test No.	Ultimate Shear Strength* (kPa)	Pavement Surface Temp. (°C)
C1	1779	29	I1	2343	35
C2	1528	29	I2	2123	35
C3	2154	29	I3	2447	32
C4	2372	29			
C5	2455	27			
Average	2058		Average	2304	
STDev	395		STDev	166	
COV	19.2		COV	7.2	

*Ultimate Shear Strength calculated with Equation 6 (Abdel Naby 1995)

Once CiSSST testing was complete, the 3 InSiSST plates were tested –

however, each test yielded bond failure between the steel test plates and the epoxy.

As these test plates were newly machined, it was hypothesized that a thin layer of

grease or oil was present on the steel surface, which had compromised the bond.

The plates were placed in an oven for 2 hours, roughened with a circular grinder and then re-epoxied to the asphalt surface. When tested again, all 3 plates produced the desired failure in the asphalt surface.

Results of the InSiSST testing are shown in detail in Appendix E and also summarized in Table 15. Unfortunately, the pavement temperature at the time of InSiSST™ testing was higher than during the CiSSST testing. The surface temperature for tests I1 and I2 was 35°C, while I3 was tested at 32°C. To compare the results of the InSiSST™ to the CiSSST, the shear strength of the InSiSST™ tests were calculated using Equation 6. As shown in Table 15, the average shear strength was 2304 kPa, with a COV of 7.2%.

A two-sample t-test was used to determine whether or not the mean values were statistically the same. The null hypothesis assumed that the difference between the means was zero, and the resulting t statistic was calculated using Equation 11 (Miller et. al. 1990):

$$ t = \frac{(\overline{x}_1 - \overline{x}_2) - \delta}{\sqrt{(n_1 - 1)s_1^2 + (n_2 - 1)s_2^2}} \sqrt{\frac{n_1 n_2 (n_1 + n_2 - 2)}{n_1 + n_2}} \tag{11} $$

where:

x_1, x_2 = the sample means

δ = the desired difference between the means (zero in this case)

n_1, n_2 = the number of observations

s_1, s_2 = the sample standard deviations

The resulting t statistic was 3.36, which was less than the critical t of 3.707 for $(n_1+n_2-2) = 6$ degrees of freedom at the 1% confidence level. Therefore, the null

hypothesis was accepted and the difference between the mean values (δ) was statistically zero. These results indicated that both devices were measuring the same material property, although the InSiSST™ results were much more consistent (lower COV). However, it was expected that the InSiSST™ results would be lower than the CiSSST results as the asphalt temperature was greater and the CiSSST test had a faster loading rate. While more testing is clearly required, the high COV of the CiSSST tests (19.7%) could explain why the CiSSST strengths were lower in this case.

5.2.3 Practical Calculation of Shear Modulus Using Equation 8

As previously mentioned, the current analytical models were developed assuming linear elastic material properties. However, when actually measuring material properties in the field or laboratory using test equipment, the resulting data is often not strictly linear. Figure 40 displays a typical graph produced during testing with the InSiSST™. Although the graph is fairly linear, an "S" type curve is observed due to tolerances with the device at the beginning of the test, as well as non-linear yielding of the asphalt close to the failure point. Therefore, to determine the linear-elastic modulus using Equation 8, the strain (twist angle) was corrected by taking the tangent of the "S" curve. The equation of the tangent line was determined as shown in Figure 41. From the resulting equation, the intercept of the tangent line with the x-axis (twist angle) was then determined and used to shift the points of the torque-twist angle graph to zero. It should be noted that the torque values were not adjusted – ie. the maximum torque value observed during the test was used in Equation 8.
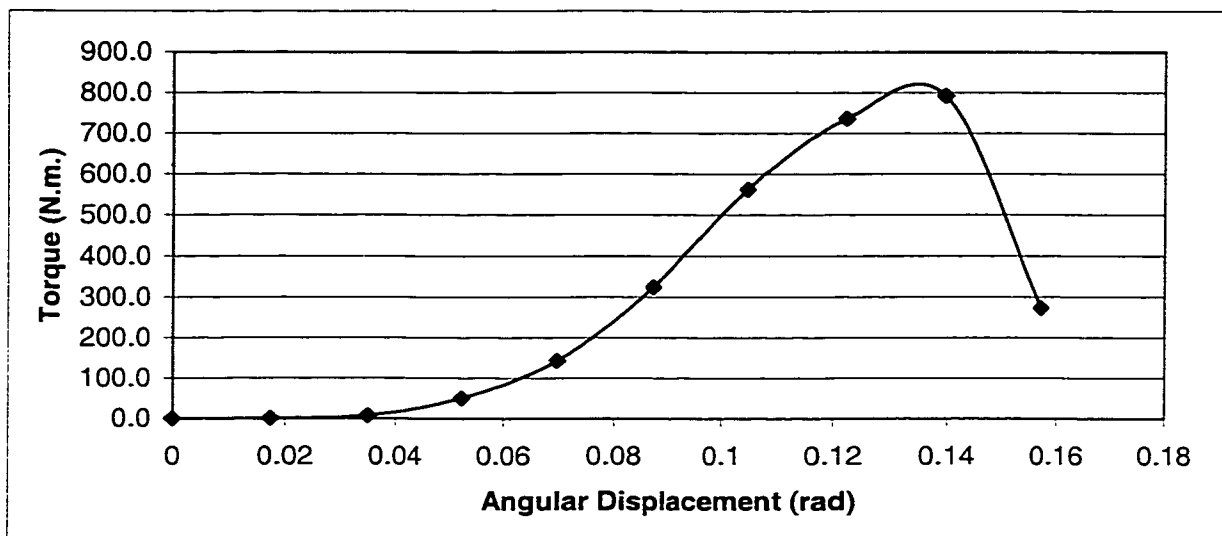
Figure 40: Typical Torque vs. Twist Angle Graph from InSiSST™
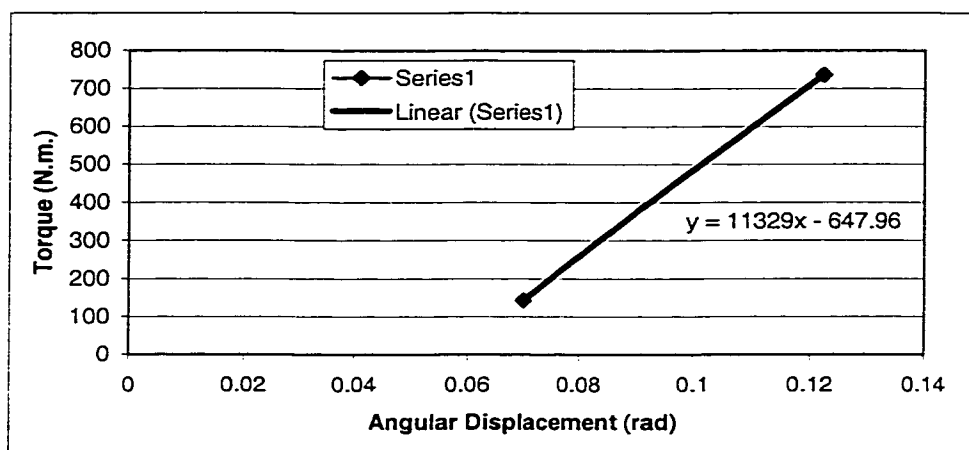
Figure 41: Determining the Tangent of the Torque-Twist "S" Curve

5.2.4 Asphalt Modulus vs. Torque Per Unit Twist

Using the technique presented in the previous section, the modulus of the asphalt pavement at failure was calculated for the 3 InSiSST™ tests as shown in Table 16. From the 3 InSiSST™ tests producing failure of the asphalt concrete, the average modulus was calculated at 20828 kPa using Equation 8, with a COV of 17.6%. Examination of the test results indicated that tests I1 and I2 had nearly

identical values for modulus (18909 and 18521 kPa, respectively), while test I3

yielded a higher modulus of 25056 kPa. Unfortunately, due to time and weather

constraints, additional testing with InSiSST™ could not be completed prior to the

completion of this thesis. However, an additional 8 tests had been completed

previously with InSiSST™ on the same asphalt concrete, although each of those

tests produced bond failure between the steel loading plate and the epoxy. While

the modulus of the asphalt concrete at failure could not be calculated for these tests,

there were enough data points prior to the bond failure to calculate the linear slope

of the torque-twist graph (Figure 41) for each test.

Table 16: Shear Modulus vs. Torque Per Unit Twist

Test No.	Failure Surface	Asphalt Temp. (deg C)	Ultimate Shear Modulus (kPa)	Torque Per Unit Twist (N*m/rad)
I1	Asphalt	35	18909	11100
I2			18521	11329
I3		32	25056	13148
		Average	**20828**	**11859**
		STDev	**3666**	**1122**
		COV (%)	**17.6**	**9.5**
BF1	Epoxy-Load Plate Interface	28	Not Applicable	10221
BF2				11964
BF3				11572
BF4				13311
BF5				11866
BF6				12512
BF7				13132
BF8				13827
		Average*		**12180**
		STDev*		**1104**
		COV (%)*		**9.1**

*includes test results for I1, I2 and I3

The resulting mix property, referred to as "Torque Per Unit Twist (N*m/rad)" was calculated for both those tests yielding failure in the asphalt concrete, as well as those producing bond failure. The results are also presented in Table 16. A number of interesting observations were made based on this measure. First, the Torque per Unit Twist (TUT) values for the tests yielding failure in the asphalt concrete were much more consistent than the ultimate shear modulus from Equation 8 as indicated by the low COV (9.5% vs. 17.6%). Furthermore, the TUT values were virtually identical for all 11 tests, regardless of whether asphalt failure or bond failure was observed.

5.2.5 Effect of Loading Plate Diameter

InSiSST™ testing was also completed with 125 mm (5 in) plates to observe the effect of test plate diameter on calculated material properties. Detailed test results are attached in Appendix E for reference. Two interesting results were observed with the 125 mm plates. The first concerned the shape of the torque vs. twist angle graph. As shown in Figure 42, the 125 mm plates displayed a rapid increase in torque to what appeared to be a yielding point, and then a much slower increase in torque over a large increase in strain to an ultimate failure point. Upon further inspection of the data and Figure 42, it was observed that the linear slope of the torque-twist angle graph (Torque Per Unit Twist) was almost identical for both the 92 and 125 mm plates as shown in Table 17. The results of Table 17 implied that the onset of failure was independent of plate diameter.

For the 92 mm plates, complete failure occurred at this point, whereas ultimate failure was not observed with the 125 mm plates until a much larger strain was imposed. Two potential hypotheses were developed to explain this behaviour.

First, it was hypothesized that the initial yield point represented the failure of the asphalt-aggregate interface along the failure plane, while the additional increase in torque required to fail the asphalt completely with the 125 mm plates was needed to overcome the aggregate interlock. It is not known at this time why the same behaviour was not observed with the 92 mm test plates since the failure surface imposed by both plates was the same shape (Figure 24). However, the larger failure surface of the 125 mm plate may have simply required additional torque to overcome the aggregate interlock.
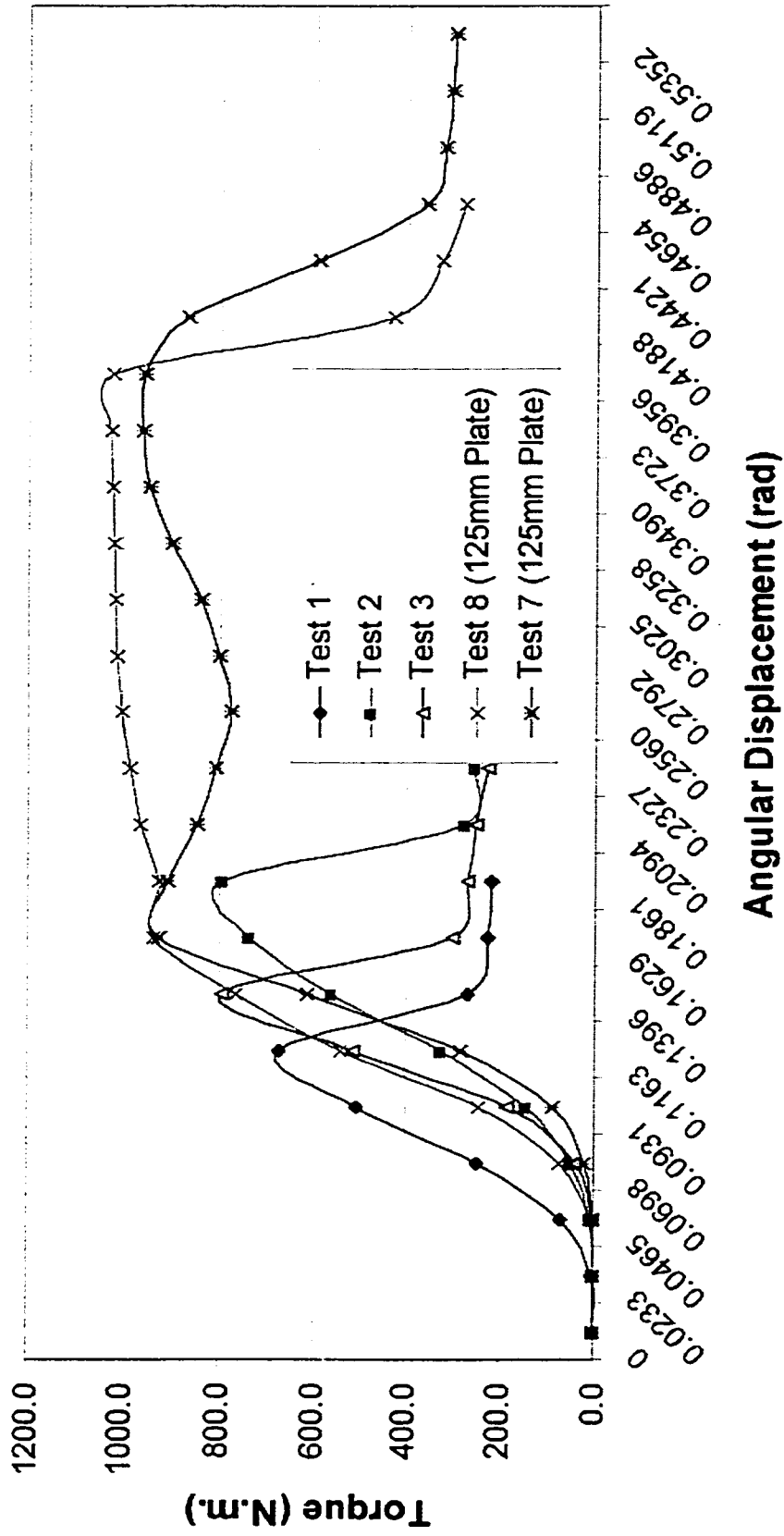
Figure 42: Torque vs. Angular Displacement for InSiSST™ Tests

Table 17: Comparison of Torque Per Unit Twist for 92mm and 125mm Plates

	Torque Per Unit Twist (N*m/rad)	
	92 mm Test Plates	**125 mm Test Plates**
	11100	12155
	11329	11255
	13148	
Average	**11859**	**11705**
STDev	**1122**	**n/a**
COV	**9.5**	**n/a**

A second possible explanation of this behaviour could be the existence of an "aging gradient" throughout the depth of the asphalt pavement. As previously mentioned, asphalt concrete undergoes stiffening with time due to oxidation, rain and sunlight. However, it is unlikely that the stiffening is consistent throughout the layer. It is more likely that the pavement surface is the most stiff, and that decreasing stiffness is observed with increasing depth. Therefore, it is possible that the initial yield point observed with the 125 mm plates represented the failure of the upper "crust", while the large amount of secondary strain was associated with the softer asphalt concrete underneath. This softer layer was likely not penetrated with the 92 mm plates.

Although the TUT values were independent of load plate diameter, the resulting shear modulus values were not. Since virtually the same torque was required to initially yield (or fail) the asphalt surface with both test plate diameters, the shear modulus resulting from the 125 mm plates was much lower than the 92 mm test plates according to Equation 8 as shown in Table 18. The asphalt modulus

was calculated both at the initial yield point and at the ultimate failure. As shown, the average modulus at yield was 8650 kPa according to Equation 8 with a COV of 14.8%, while the modulus at failure was 2588 kPa due to the large strain incurred. The shear modulus at yield represented a 65% reduction compared to the 92 mm test plate at the same temperature, reflecting the fact that the radius of the test plate is raised to the third power in Equation 8.

Table 18: Results of InSiSST Testing with 125 mm Plates

Test No.	Shear Modulus at Yield (kPa)	Shear Strain at Yield (%)	Shear Modulus at Failure (kPa)	Shear Strain at Failure (%)	Pavement Temp. (°C)
I7	9552.40	0.074	2593.08	0.283	32
I8	7748.38	0.092	2582.14	0.302	32
Average	**8650**	**0.08**	**2588**	**0.29**	
STDev	**1276**	**0.01**	**7.7**	**0.01**	
COV	**14.8**	**15.6**	**0.30**	**4.4**	

5.2.6 Discussion of Field Test Results and Analytical Modelling

In theory, the Torque Per Unit Twist (TUT) measure is a load per unit displacement, not a stress per unit strain. Therefore, while it is not strictly a "stiffness" or modulus, it is directly proportional to the modulus. Indeed, for the 92 mm test plates, the ultimate shear modulus (in kPa) was 1.75 times the TUT (in N*m/rad). For the 125mm plates, the ultimate shear modulus (in kPa) was 0.75 times the TUT (in N*m/rad).

As previously mentioned, fundamental engineering properties should be unique to the individual material, not dependent upon boundary conditions, or loading plate diameter in the current case. The discrepancy between modulus values calculated for the 92 and 125 mm test plates using Equation 8 appeared to indicate that further investigation and potential modification to Equation 8 is required prior to its use to provide asphalt modulus. This is beyond the scope of the current investigation, however is under analysis at Carleton University at this time. However, the TUT values appear independent of load plate diameter. Therefore, the TUT measure may be considered a fundamental engineering property of the asphalt mix and will be investigated further during future testing with the InSiSST™.

5.2.7 Comparison of Field and Laboratory Results

A final exercise of the verification stage was to compare the field stiffness calculated from the InSiSST™ results to the laboratory values observed by Zahw (1995). As shown in Table 16, the average shear modulus was 20828 kPa for the HL3 mix. Modulus values from the Zahw database are attached in Appendix C. The laboratory shear modulus values ranged from 930 kPa for a sand-asphalt mix to 3700 kPa for an HL4 mix. The various HL3 mixes yielded shear moduli ranging between 2500 and 3500 kPa. Therefore, the field shear moduli were approximately 6 times greater than those observed in the laboratory during the 1995 investigation. This result was most likely due to aging of the asphalt mix. As previously mentioned, the HL3 tested was constructed in 1992, therefore was 8 years old. The laboratory testing in 1995 was completed on newly compacted asphalt, therefore, it had not been subjected to environmental conditioning and subsequent stiffening of the asphalt binder.

CHAPTER 6: Conclusions and Recommendations

6.1 Review of Project Objectives

The phenomenon of permanent deformation or rutting in asphalt concrete pavements is extremely complex and has been the focus of concentrated research efforts in the past decade. Although the term "rutting" is often used interchangeably with permanent deformation, it is only one of four manifestations observed in North America. In general, *rutting* is characterized by channelized depressions (troughs) that run longitudinally in the wheelpaths. However, rutting is usually the most common form of permanent deformation analyzed. The Strategic Highway Research Program (SHRP) has identified that rutting appears to be more closely related to shear stresses and strains than normal or horizontal ones. Subsequently, it is important to investigate the shear properties of asphalt layers. As explained earlier, shear strength of an asphalt concrete mix is achieved through both aggregate particle contact to form a tight, load-bearing skeleton and the asphalt binder that holds the particles in place. As a result, the main objectives of this thesis were as follows:

1. To review the phenomenon of permanent deformation and identify its main causes,

2. To study the main factors contributing to the rutting phenomenon and determine the relationship between these factors and the shear properties of the asphalt mix, and

3. To design and build an advanced test facility to provide reliable data concerning the shear properties of the mix in the field.

These objectives were achieved and discussed throughout the thesis. This Chapter presents the main conclusions and major findings of the research as related to the above mentioned objectives.

6.2 Review of Permanent Deformation and Previous Investigations

Permanent deformation or rutting of asphalt roads has been found to progress in three stages. The first stage begins with continued densification of the asphalt layer under traffic loading. During this stage, rutting is directly proportional to traffic. The second stage involves a stable shear period during which the rate of rutting decreases with increasing traffic until a third and final stage when a condition of plastic flow occurs and the rate of rutting again increases (rapid unstable shear failure). It is the onset of rapid shear failure that is of particular interest to the objectives of this investigation. In depth review of available information on the subject showed that the rutting phenomenon is very complex. One of the main conclusions of this study was that at present, there is no single independent variable that captures or predicts rutting with a significant degree of confidence. In addition, a single "deficiency" in a given property, such as excessive asphalt content, can nullify the over all quality obtained when other good properties, such as coarse aggregate with 100% fractured faced count, are available. Another important observation was the fact rutting is caused by various combinations of pavement layer instability and heavy truck-tires. Until recently, laboratory and field investigations of the rutting phenomenon did not address the fundamental property of a pavement to resist rutting; *shear strength*. SHRP research has acknowledged the importance of shear properties, and the new Superpave design

method may soon incorporate shear properties as important inputs toward the long-term performance of mixes in the field. However, it should be noted that Superpave shear tests are completed in the laboratory on laboratory prepared specimens or cores retrieved from constructed pavements.

These findings led to the consideration of data and test results reported by two previous studies on the subject completed at Carleton University. The first study was the comprehensive and intensive laboratory-testing program carried out by Zahw to identify the influence of the main factors of an asphalt mix on rutting resistance. In this thesis, the author imported the data and test results reported by Zahw and a more rigorous analysis was performed. This step produced a set of new statistically based equations relating the most important factors affecting the rutting phenomenon to the shear properties of the mix as shown in the following section.

The second study completed by Abdel Naby resulted in the construction of a first generation test device, known as the Carleton In-Situ Shear Strength Test (CiSSST). The results of Abdel Naby provided two important conclusions. First, the CiSSST was able to differentiate between the shear properties of different mixes, as well as the differences within the same mix placed in different geometries (curved sections vs. straight sections). Second, greater variation between replicate specimen results was observed during laboratory testing than in-situ testing.

6.3 Asphalt Mix Properties and Shear Characteristics

Consideration of the extensive data collected by Zahw (1995) showed that a number of mix characteristics contribute to the shear properties of the mix. Two

equations were developed to describe the shear modulus and shear strength. These
equations incorporate traditional mix properties that should be recorded by any agency.
However, many of these variables have been combined in such a way that all aspects of
mix design (binder properties, gradation, aggregate angularity, density, compactive
effort and volumetric properties) are included without the introduction of collinear
variables. Equations 4 and 5 are shown below:

$$G = 560 - 2.7 * PVR + 232 * CU + 344 * C_{bin} - 14135 * ARD + 10670 * VMA$$

(4)

$(R^2 = 0.83)$

$$\tau = -66 - 0.9 * PVR + 50 * CU + 65 * C_{bin} - 2410 * ARD + 2552 * VMA$$

(5)

$(R^2 = 0.88)$

where: G (kPa) = Shear Modulus (Stiffness) at 25°C;

τ (kPa) = Shear Strength at 25°C;

PVR (mm/Pa*s) = Ratio of Penetration (mm) to Viscosity at 25°C (Pa*s);

CU = Coefficient of Uniformity (D60/D10);

C_{bin} = Crushed Coarse Aggregate Present in Mix? (Binary choice of 1 for Yes
or 0 for No);

ARD = Average Rate of Densification (ratio of final mix density to the square
root of the number of blows with Marshall hammer); and

VMA = Voids in the Mineral Aggregate (%)

According to the models developed, the asphalt binder properties (PVR)
represented 22% of the shear modulus and 44% of the shear strength. Aggregate

gradation (CU) accounted for 49% of the shear modulus and 35% of the shear strength, while coarse aggregate angularity (C_{bin}) accounted for 23% of the shear modulus and 17% of the shear strength. Volumetric properties (ARD and VMA) represented 8% and 7% of the shear modulus and 10% and 5% of the shear strength, respectively. These findings are in general agreement as research completed under the US-SHRP (1994).

6.4 Asphalt Shear Characteristics and Rutting

Mix shear strength and modulus were highly correlated to rutting at various stress levels as predicted by laboratory creep testing (Shell Method), although mix stiffness (modulus) appeared to be a slightly better indicator of mix performance. Rutting models based on shear modulus and strength were also developed as shown below.

Creep Test Stress Level (MPa)	Laboratory Rutting Models	
	Shear Modulus @ 25C (kPa)	Shear Strength @ 25C (kPa)
0.1	$Rut = 245*G^{-0.742}$ (R^2=0.80)	$Rut = 18.25*\tau^{-0.515}$ (R^2=0.63)
0.3	$Rut = 4301*G^{-1.037}$ (R^2=0.60)	$Rut = 62.92*\tau^{-0.626}$ (R^2=0.47)
0.6	$Rut = 3E6*G^{-1.820}$ (R^2=0.73)	$Rut = 11791*\tau^{-1.383}$ (R^2=0.67)

6.5 Modelling In-Situ Shear Properties

A review of previous modelling efforts as well the development of new constitutive equations provided the following conclusions:

i) The boundary conditions observed during field testing with the CiSSST device and the InSiSST™ were significantly different than those experienced in the laboratory torsion testing. During the development of the CiSSST device by Abdel Naby, Equation 6 was developed to calculate shear strength of the mix from field torsion testing. While acceptable for that investigation, it has been subsequently determined that Equation 6 does not likely best characterize mix shear strength. Therefore, a new analysis procedure based on the Reissner-Sagoci problem was developed by Bekheet et. al. (2000) and adopted for this investigation. This model (Equation 8) directly provides shear modulus based on applied torque, and was subsequently verified for the linear elastic condition both with finite element modelling and field testing at room temperature.

ii) Additional verification and/or modification to Equation 8 may be completed in future investigations for cases of non-linear behaviour such as those encountered at lower test speeds and higher pavement temperatures.

The conclusions and findings obtained after achieving the first two objectives paved the way to the development of the new InSiSST™ as discussed below.

6.6 Design, Development and Verification of the InSiSST™

The primary objective of this investigation was the development of an advanced in-situ shear stiffness test (InSiSST™) for asphalt concrete pavements. The successful completion of this objective provided the following conclusions:

i) The InSiSST™ device was designed and developed based on a sound theory and thorough analysis of deficiencies observed with the CiSSST device and additional design considerations. The result is a test facility that is portable, stable, and rugged. The test requires only a single operator, no heavy lifting or complex set-up, and can be completed rapidly. The test results are accurate and are available instantly. All of the individual systems operate under the same power requirements as provided by the central generator. To date, the newly built InSiSST has been towed a total of 4800 Km at speeds as high as 120km/h. Clearly, this is a testimony to the reliability and toughness of the new facility.

ii) Field verification of the InSiSST™ has indicated that the device accurately and repeatedly measures shear properties of the asphalt mix. Additional verification testing is required, however, to further explore the effect of test plate diameter on measured shear properties.

6.7 Recommendations for Future Modifications to INSISST™

6.7.1 Environmental Chamber

Asphalt concrete shear strength and stiffness are highly dependent on temperature due to its viscoelastic nature. In its current form, the InSiSST™ can test only at the pavement temperature present in the field. Therefore, the results obtained in the field must be normalized to a standard or reference temperature before comparison with other sections may be completed. A temperature master curve may be used to do this, however, the master curve must first be developed. The addition of an environmental chamber to the InSiSST™ test frame will allow

the development of temperature master curves, as well as reduce the cure time for the epoxy by allowing the introduction of heat prior to the test.

6.7.2 Hydraulics

For this concept exploration project, the use of hydraulics or pneumatics instead of the electromechanical system for applying to torque was prohibitively expensive. However, if the InSiSST™ is to be developed further by a manufacturing company for mainstream use, it is recommended that hydraulics or pneumatics be used for three primary reasons. First, all mechanical systems including the jacking system, positioning system and load application system may be driven from a single pump, thus reducing the number of components (the InSiSST™ uses 4 individual electric motors). Second, hydraulic systems may be very quickly and accurately reversed, thus allowing dynamic loading of the pavement in addition to the current static testing. Finally, hydraulic systems are generally more rugged and resistant to the elements than electromechanical systems. When assembled in larger quantities, hydraulic systems would likely become much more cost effective than for a single prototype.

6.7.3 Shear Vane

Although the InSiSST™ design greatly reduced the time required for testing over the CiSSST, the epoxy cure time remained as the overall governing factor. The use of epoxies with more rapid cure times improved the test time significantly, however, an improved affixation method is recommended to remove the dependency on epoxy altogether. One such method would be the use of a shear vane, similar to those used in soil mechanics to test the shear properties of clays in-situ. For newly constructed pavements, the vane could be placed on the asphalt

surface behind the spreader and compacted into the pavement, thus allowing for both current and future testing. For existing pavements, a saw could be used to cut the pavement surface and the vane could be inserted for testing. Standard formulas exist for vane testing, however, additional analysis would need to be completed to ensure the accuracy of the test. Comparison with laboratory values could assist that effort.

6.8 Recommendations for Further Testing

6.8.1 Additional Verification Testing

The initial verification testing completed during this investigation was sufficient to provide general trends and relationships to ensure that the InSiSST™ device was measuring the desired shear properties accurately and repeatedly. However, significant additional testing will be required to further observe the effects of temperature, directly compare to laboratory torsion tests and explore the phenomenon observed with the 125 mm test plates.

6.8.2 Long Term Performance

One of the primary goals of in-situ shear testing will be to ultimately model and predict rutting in the field. Extensive field testing at numerous test sites will be required to provide the necessary data to develop such models due to the large number of variables that contribute to rutting (as presented in Chapter 2).

At the time of this writing, Carleton University has partnered with the Ontario Ministry of Transportation (MTO) to complete field and laboratory shear testing on approximately 8 of the 16 test sections.

6.8.3 Additional Testing for QC/QA Specification Development

As mentioned previously, there is a great need for a simple performance test for the Superpave asphalt mix design system, largely for use as a quality control and quality assurance (QC/QA) test. In-situ shear testing with the InSiSST™ could potentially provide such testing as the device is well suited for rapid and accurate testing in the field as opposed to in the laboratory.

Clearly, the continuous testing and improvements of this new testing facility should ultimately provide the pavement industry with a reliable tool that is designed: (1) To enhance new construction methods through adequate quality control, and (2) To improve the ability to predict long term performance of asphalt surfaces and pavements.

References

Abd El Halim, A. O., Zahw, M.A., and Bahgat, A.G. 1995. Influences of Types of Asphalt Binders on the Tensile and Shear Strengths of Asphalt Mixes. Proceedings of the Canadian Technical Asphalt Association, 40: 291-304.

Abdel Nabi, R. M. 1995. Influence of Highway Geometry on Distress of Asphalt Concrete Pavements. A Ph.D. thesis. Zagzig University, Cairo.

Alavi, S. H. and Monismith, C. L. 1994. Time and Temperature Dependent Properties of Asphalt Concrete Mixes Tested as Hollow Cylinders and Subjected to Dynamic Axial and Shear Loads. Journal of the Association of Asphalt Paving Technologists, 63: 152-181.

American Association of State Highway and Transportation Officials (AASHTO). 1999. Superpave Implementation Survey III 1998-1999. AASHTO Task Force on SHRP Implementation and FHWA Lead State Program, Washington, DC.

American Association of State Highway and Transportation Officials (AASHTO). 1993. AASHTO Guide for Design of Pavement Structures. Washington, DC.

Anani, B. A., Balghunaim, F. A., and Al-Hazzaa, A. S. 1990. Laboratory and Field Study of Pavement Rutting in Saudi Arabia. Transportation Research Record, 1259: 79-90.

Asphalt Institute. 1998. Construction of Hot Mix Asphalt Pavements, Second Edition. Manual Series No. 22 (MS-22). Lexington Kentucky.

Asphalt Institute. 1997a. Performance Graded Asphalt Binder Specification and Testing. Superpave Series No. 1 (SP-1). Lexington, Kentucky.

Asphalt Institute. 1997b. Superpave Mix Design. Superpave Series No. 2 (SP-2). Lexington, Kentucky.

Asphalt Institute. 1991. Thickness Design – Asphalt Pavements for Highways and Streets. Manual Series No. 1 (MS-1). Lexington, Kentucky.

Aschenbrener, T. 1995. Evaluation of Hamburg Wheel Tracking Device to Predict Moisture Damage in Hot-Mix Asphalt. Transportation Research Record, 1492: 193-201.

Aschenbrener, T. 1994. Comparison of Results Obtained from the LCPC Rutting Tester with Pavements of Known Field Performance. Transportation Research Record, 1454: 66-73.

Aschenbrener, T., Terrel, R., and Zamora, R. 1994. Comparison of Hamburg Wheel Tracking Device and the Environmental Conditioning System to Pavements of Known Stripping Performance. CDOT-DTD-R-94-1. Colorado Department of Transportation, Denver Colorado.

Beer, F.P. and Johnson Jr., E.R. 1988. Vector Mechanics for Engineers – Statics. Second Metric Edition. McGraw-Hill Book Company, Singapore.

Bekheet, W., Hassan, Y. and Abd El Halim, A.O. 2000. Assessing the Effect of Elastic Properties of Asphalt Concrete Pavements on Shear Strength. Proceedings of the Canadian Society for Civil Engineering 3rd Transportation Specialty Conference (CD-ROM), pp. 229-235.

Bonse, R. P. H. and Kuhn, S. H. 1959. Dynamic Forces Exerted by Moving Vehicles on a Road Surface. Bulletin of the Highway Research Board, 233: 9-32.

Brown, E. R., and Bassett, C.E. 1990. Effects of Maximum Aggregate Size on Rutting Potential and Other Properties of Asphalt-Aggregate Mixtures. Transportation Research Record, 1259: 107-119.

Brown, E.R. and Cross, S.A. 1998. A Study of In Place Rutting of Asphalt Pavements. Journal of the Association of Asphalt Paving Technologists, 58: 1-39.

Bruce, B. 1987. Asphalt as a Variable – Big Timber Test Sections. Journal of the Association of Asphalt Paving Technologists, 56: 688-710.

Button, J.W., Perdomo, D., and Lytton, R.L. 1990. Influence of Aggregate on Rutting in Asphalt Concrete Pavements. Transportation Research Record, 1259: 141-152.

Canadian Meteorological Centre. 2000. Data from CMC website at www.cmc.doe.ca

Canadian Strategic Highway Research Program (C-SHRP). 1999. Superpave 2000: Improved Standards for a New Millenium. C-SHRP Technical Brief No. 17. Ottawa.

Canadian Strategic Highway Research Program (C-SHRP). 1998. C-SHRP Phase III Program Proposal 1999-2004. Ottawa.

Canadian Strategic Highway Research Program (C-SHRP). 1997. C-LTPP Database User's Guide: Second Edition. Ottawa.

Carpenter, S. H. 1993. Permanent Deformation: Field Evaluation. Transportation Research Record 1417: 135-143.

Carpenter, S.H. and Enockson, L. 1987. Field Analysis of Rutting in Overlays of Concrete Interstate Pavements in Illinois. Transportation Research Record, 1136: 46-56.

Célard, B. 1977. Esso Road Design Technology. Proceedings of the Fourth International Conference on the Structural Design of Asphalt Pavements, Vol. 2, pp. 76-77.

Coree, B.J. 1999. HMA Volumetrics Revisited – A New Paradigm. Transportation Research Board (TRB) 78th Annual Meeting Preprint CD-ROM, National Research Council, Washington DC.

Energy, Mines and Resources Canada. 1974. The National Atlas of Canada, Fourth Edition. Macmillan Company of Canada Ltd. Toronto.

Cross, S. A. and Brown, E. R. 1992. A National Study of Rutting in Hot Mix Asphalt (HMA) Pavements. Journal of the Association of Asphalt Paving Technologists, 61: 535-582.

Cross, S. A. and Brown, E.R. 1991. A National Study of Rutting in Asphalt Pavements. NCAT Draft Report No. 91-8, National Centre for Asphalt Technology, Auburn University, Alabama.

Farris, R.E. 1992. The Overall Challenge: A New Look." Proceedings of the 1992 Transportation Association of Canada (TAC) Annual Conference, Quebec City. Volume 6. pp. A21-A30.

Federal Highway Administration (FHWA). 1999a. LTPP: 1998 Year in Review. Report FHWA-RD-99-111. United States Department of Transportation, Washington DC.

Federal Highway Administration (FHWA). 1999b. DataPave 2.0 CD-ROM. Long Term Pavement Performance Program. United States Department of Transportation, Washington DC.

Federal Highway Administration (FHWA). 1998a. LTPP: The Next Decade. Report FHWA-RD-98-109. United States Department of Transportation, Washington, DC.

Federal Highway Administration. 1998b. Simulation, Imaging, and Mechanics of Asphalt Pavements (SIMAP). Report FHWA-RD-98-128. United States Department of Transportation, Washington, DC.

Federal Highway Administration. 1998c. Performance of Coarse-Graded Mixes at

Westrack – Premature Rutting Final Report. United States Department of

Transportation, Washington DC.

Federal Highway Administration. 1998d. A Simple Test for Superpave Mix

Performance. Focus. December 1998 Issue. United States Department of

Transportation, Washington DC.

Gerrard, C. M. and Harrison, W. J. 1970. Circular Loads Applied to a Cross-Anistropic

Half Space. Division of Applied Geomechanics Technical Paper No. 8.

Commonweath Scientific and Industrial Research Organization, Australia.

Gervais, F. and Abd El Halim, A. O. 1990. Rutting of Asphalt Overlays: Analytical and

Field Studies. Proceedings of the Canadian Technical Asphalt Association, Vol. 35,

pp. 34-45, Winnipeg, Manitoba.

Goodman, S. and Abd El Halim, A.O. 1997. Design, Development and Verification of

an Advanced In-Situ Shear Strength Test for Asphalt Concrete Pavements.

Proposal submitted to the United States Transportation Research Board (TRB)

Innovations Deserving Exploratory Analysis (IDEA) Program. Carleton University,

Ottawa.

Harvey, J., Ericksen, K., Sousa, J. J. and Monismith, C.L. 1994. Effects of Laboratory

Specimen Preparation on Aggregate-Asphalt Structure, Air Void Content

Measurement, and Repetative Simple Shear Test Results. Transportation Research

Record, 1454: 113-122.

Harvey, J. and Monismith C. L. 1993. Effects of Laboratory Asphalt Concrete Specimen

Preparation Variables on Fatigue and Permanent Deformation Test Results using

Strategic Highway Research Program A-003A Proposed Testing Equipment. Transportation Research Record, 1417: 38-48.

Hicks, Tyler G. 1994. Standard Handbook of Engineering Calculations. Third Edition. McGraw-Hill Publishing Company.

Hofstra, A. and Kolomp. 1972. Permanent Deformation in Flexible Pavements under Simulated Road Traffic Condition. 3rd International Conference on Structural Design of Asphalt Pavement, 1: 613-671.

Huang, Yang H. 1993. Pavement Analysis and Design. Prentice Hall, New Jersey.

Huber, G. 1999. Methods to Achieve Rut-Resistant Durable Pavements. NCHRP Synthesis 274. Transportation Research Board, National Research Council, Washington, DC.

Huber, G. A. and Hieman, G. H. 1987. Effect of Asphalt Concrete Parameters on Rutting Performance: A Field Investigation. Journal of the Association of Asphalt Paving Technologists, 56: 33-61.

Jennings, P. W., Pribanic, J. A., Smith, J. and Mendes, T. M. 1988. Predicting the Performance of Montana Test Sections by Physical and Chemical Testing. Transportation Research Record, 1171: 59-65.

Kandhal, P. S., Cross, S. A., and Brown, E. R. 1993. Heavy Duty Asphalt Pavements in Pennsylvania: An Evaluation for Rutting. NCAT Report 93-2. National Centre for Asphalt Technology, Auburn University, Alabama.

Kaweski, D. and Nickeson, M. 1997. C-SHRP Bayesian Modelling: A User's Guide. Canadian Strategic Highway Research Program (C-SHRP). Ottawa.

Krutz, N.C. and Sebaaly, P.E. 1993. The Effects of Aggregate Gradation on Permanent Deformation of Asphalt Concrete. Journal of the Association of Asphalt Paving Technologists, 62: 450-473.

Krutz, N.C. and Stroup-Gardiner, M. 1990. Relationship Between Permanent Deformation of Asphalt Concrete and Moisture Sensitivity. Transportation Research Record, 1259: 169-177.

Lai, J. S. 1986. Development of a Simplified Test Method to Predict Rutting Characteristics of Asphalt Mix. Georgia DOT Project 8503, Final Report. Georgia Department of Transportation, GA.

Lai, J.S. 1993. Results of Round-Robin Test Program to Evaluate Rutting of Asphalt Mixes Using Loaded Wheel Tester. Transportation Research Record, 1417: 127-134.

Marks, V.J., Monroe, R.W., and Adam, J.F. 1990. Effects of Crushed Particles in Asphalt Mixtures. Transportation Research Record, 1259: 91-106.

Marwick, H. D. and Starks, H. J. H. 1941. Stresses Between Tire and Road. Journal of the Institution of Civil Engineers, 16.

McGee, Ken. 1999. Summary of the Proposed 2002 Pavement Design Guide: NCHRP Project 1-37A. AASHTO Draft Paper. American Association of State Highway and Transportation Officials, Washington, DC.

Miller, I., Freund, J.E., and Johnson, R.A. 1990. Probability and Statistics for Engineers. Fourth Edition. Prentice Hall Publishing. New Jersey.

Ministry of Transportation, Ontario (MTO). 2000. Quick Notes on...Pulling a Trailer Safely. Available in Adobe Portable Document Format (PDF) through the MTO website at www.mto.gov.on.ca. Toronto.

Ministry of Transportation, Ontario. 1998. PGAC Grades Redefine Asphalt Technology. Road Talk Magazine, Vol. 4, Issue 2. Toronto.

National Cooperative Highway Research Program. 1998. Quality Control and Acceptance of Superpave-Designed Hot Mix Asphalt. NCHRP Report 409. Transportation Research Board, National Research Council, Washington DC.

Nievelt, G. and Thamfld, H. 1988. Evaluation of the Resistance to Deformation of Different Road Structures and Asphalt Mixtures Determined in the Pavement Rutting Tester. Journal of the Association of Asphalt Paving Technologists, 57: 320-345.

Parker, F. and Brown, E.R. 1990. A Study of Rutting of Alabama Asphalt Pavements. Final Report Project ST 2019-9, Alabama Highway Department, GA.

Peck and Lowe. 1960. Moderator's Report on the Shear Strength of Undisturbed Cohesive Soils. Proceedings of the 1960 ASCE Research Conference on Shear Strength of Cohesive Soils, Colorado.

Prowell, B.D. and Schreck, R.J. 2000. Virginia's Use of Laboratory Wheel-Tracking as a Mix Performance Predictor. Transportation Research Board (TRB) Annual Meeting Preprint CD-ROM, National Research Council, Washington DC.

Rickards, I. 1998. AMIR – HIPAC Trials in Australia. Pioneer Road Services Pty. Ltd., Melbourne, Australia.

Reissner, E. and Sagoci, H. 1944. Forced Torsional Oscillation of an Elastic Half-Space. Journal of Applied Physics, 15: 652-654.

Roads and Transportation Association of Canada (RTAC). 1986. Canadian Strategic Highway Research Program (C-SHRP). Council on Highway and Transportation Research and Development, Ottawa.

Romero, P., and Stuart, K. 1998. Evaluating Accelerated Rut Testers. Public Roads July/August. Federal Highway Administration, Washington, DC.

Sherline Products Incorporated. 1999. Trailer Loading and Towing Guide. California, USA. Available online at www.sherline.com.

Simpson, A. L., Daleiden, J. F. and Hadley, W. O. 1995. Rutting Analysis from a Different Perspective. Transportation Research Record 1473: 9-16.

Sneddon, N. 1946. Note on a Boundary Value Problem by Reissner and Sagoci. Journal of Applied Physics, 18: 130-132.

Sousa, J.J., Harvey, L., Deacon, A. and Monismith, C.L. 1991. Evaluation of Laboratory Procedures for Compacting Asphalt-Aggregate Mixtures. Technical Memorandum TM-UCB-A-003A-90-5. Institute of Transportation Studies, University of California at Berkeley.

Terrel, R. L. and Epps, J.A. 1988. Using Additives and Modifiers in Hot-Mix Asphalt. Quality Improvement Series 114. National Asphalt Pavement Association (NAPA), Lanham, Maryland.

Transportation Association of Canada (TAC). 1997. Pavement Design and Management Guide. Ottawa.

Transport Canada. 1999. Transportation in Canada: 1999. Transport Canada Report TP 13198E. Ottawa.

Transportation Research Board (TRB). 2000. Innovations Deserving Exploratory Analysis (IDEA): Program Announcement 2000/2001. National Research Council, Washington, DC.

United States Strategic Highway Research Program (US-SHRP). 1994. Permanent

Deformation Response of Asphalt-Aggregate Mixes. SHRP-A-415. National

Research Council, Washington, DC.

United States Strategic Highway Research Program (US-SHRP). 1992. SHRP Product

Catalog. National Research Council, Washington, DC.

Van de Loo, P. J. 1974. Creep Testing: A Simple Tool to Judge Asphalt Mix Stability.

Journal of the Association of Asphalt Paving Technologists, 43: 253-284.

Witczak, M. 2000. Personal conversation with Dr. Matt Witczak during the 1st

International World of Asphalt Pavements Conference in Sydney, Australia held

February 20-24, 2000. Dr. Witczak is the primary investigator for the flexible

(asphalt) sections of the 2002 design guide.

Wu, Y., Parker, F., and Kandhal, K. 1998. Aggregate Toughness/Abrasion Resistance

and Durability/Soundness Tests Related to Asphalt Concrete Performance in

Pavements. NCAT Report 98-4, National Centre for Asphalt Technology, Auburn

University, Alabama.

Zahw, Magdy A. 1995. Development of Testing Framework for Evaluation of Rutting

Resistance of Asphalt Mixes. A Ph.D. thesis. Carleton University, Ottawa.

Appendices

Appendix A: Correlation Matrix for Zahw Database

	Selected Variables				
	Penetration-Viscosity Ratio (mm/Pa*s)	Coefficient of Uniformity (D60/D10)	Crushed Stone?	Avg. Rate of Densification (Density/sqrt(# blows))	VMA
PV Ratio	1.000				
Uniformity	0.040	1.000			
Crushed Stone?	-0.008	0.550	1.000		
ARD	-0.110	0.523	0.531	1.000	
VMA	0.123	0.236	0.201	0.304	1.000
Shear strength/stiffness	-0.665	0.589	0.410	0.314	0.214
Shear Strain	-0.813	0.067	0.215	0.304	-0.069
Shear Modulus	-0.468	0.697	0.477	0.277	0.260
Mean Rut @ 0.1 MPa	0.179	-0.703	-0.668	-0.332	-0.357
Mean Rut @ 0.3 MPa	0.290	-0.573	-0.432	0.194	0.006
Mean Rut @ 0.6 MPa	0.135	-0.583	-0.556	0.285	0.113

Appendix B1: Selected Variables for Mixes 1 through 5

Mix Design Designation	Selected Variables				
	Penetration-Viscosity Ratio at 25C (mm/Pa*s)	Coefficient of Uniformity (D60/D10)	Crushed Coarse Material	Avg. Rate of Densification (Density/sqrt(# blows))	VMA
m1-1	56.250	15.83	1	0.251	0.149
m1-2	56.250	15.83	1	0.252	0.160
m1-3	56.250	15.83	1	0.255	0.170
m1-4	56.250	15.83	1	0.254	0.180
m1-5	56.250	15.83	1	0.251	0.189
m2-1	56.250	19	1	0.262	0.151
m2-2	56.250	19	1	0.263	0.161
m2-3	56.250	19	1	0.265	0.171
m2-4	56.250	19	1	0.266	0.181
m2-5	56.250	19	1	0.264	0.191
m3-1	56.250	15.83	0	0.251	0.148
m3-2	56.250	15.83	0	0.252	0.158
m3-3	56.250	15.83	0	0.255	0.168
m3-4	56.250	15.83	0	0.254	0.178
m3-5	56.250	15.83	0	0.253	0.188
m4-1	10.714	15.83	1	0.251	0.149
m4-2	10.714	15.83	1	0.252	0.160
m4-3	10.714	15.83	1	0.254	0.170
m4-4	10.714	15.83	1	0.256	0.180
m4-5	10.714	15.83	1	0.254	0.189
m5-1	10.714	19	1	0.257	0.151
m5-2	10.714	19	1	0.259	0.161
m5-3	10.714	19	1	0.263	0.171
m5-4	10.714	19	1	0.268	0.181
m5-5	10.714	19	1	0.267	0.191

Appendix B2: Selected Variables for Mixes 6 through 12

Mix Design Designation	Selected Variables				
	Penetration-Viscosity Ratio at 25C (mm/Pa*s)	Coeff. of Uniformity (D60/D10)	Crushed Coarse Material	Avg. Rate of Densification (Density/sqrt(# blows))	VMA
m6-1	10.714	15.83	0	0.252	0.148
m6-2	10.714	15.83	0	0.253	0.158
m6-3	10.714	15.83	0	0.253	0.168
m6-4	10.714	15.83	0	0.249	0.178
m6-5	10.714	15.83	0	0.247	0.188
m7-1	386.364	15.83	1	0.250	0.149
m7-2	386.364	15.83	1	0.251	0.160
m7-3	386.364	15.83	1	0.252	0.170
m7-4	386.364	15.83	1	0.254	0.180
m7-5	386.364	15.83	1	0.253	0.189
m8-1	386.364	19	1	0.262	0.151
m8-2	386.364	19	1	0.262	0.161
m8-3	386.364	19	1	0.265	0.171
m8-4	386.364	19	1	0.266	0.181
m8-5	386.364	19	1	0.265	0.191
m9-1	386.364	15.83	0	0.249	0.148
m9-2	386.364	15.83	0	0.251	0.158
m9-3	386.364	15.83	0	0.253	0.168
m9-4	386.364	15.83	0	0.252	0.178
m9-5	386.364	15.83	0	0.252	0.188
m10-1	10.714	22	1	0.274	0.143
m10-2	10.714	22	1	0.276	0.153
m10-3	10.714	22	1	0.275	0.164
m10-4	10.714	22	1	0.273	0.174
m11-1	10.714	15.83	1	0.302	0.149
m11-2	10.714	15.83	1	0.306	0.160
m11-3	10.714	15.83	1	0.307	0.170
m11-4	10.714	15.83	1	0.307	0.180
m11-5	10.714	15.83	1	0.307	0.189
m12-1	10.714	11	0	0.216	0.124
m12-2	10.714	11	0	0.220	0.134
m12-3	10.714	11	0	0.219	0.144
m12-4	10.714	11	0	0.216	0.154

Appendix C1: Shear and Rutting Properties for Mixes 1 through 5

Mix Design Designation	Shear Properties of Mix			Rutting Properties of Mix		
	Avg. Shear Strength (kPa)	Avg. Shear Strain at Peak	Avg. Shear Modulus (kPa)	Mean Rut Depth (0.1 MPa) (mm)	Mean Rut Depth (0.3 MPa) (mm)	Mean Rut Depth (0.6 MPa) (mm)
m1-1	581	0.204	2846	0.652	1.57	1.479
m1-2	612	0.213	2876	0.646	1.238	1.386
m1-3	641	0.341	2763	0.624	0.974	1.907
m1-4	541	0.2	2705	0.699	1.527	2.19
m1-5	521	0.194	2695	0.709	1.752	2.107
m2-1	691	0.21	3386	0.64	0.917	1.493
m2-2	706	0.204	3505	0.609	0.908	1.372
m2-3	719	0.203	3595	0.574	0.855	1.18
m2-4	712	0.201	3556	0.574	0.934	1.281
m2-5	711	0.206	3463	0.578	1.01	1.558
m3-1	444	0.197	2312	1.153	2.696	2.287
m3-2	463	0.186	2493	0.887	2.518	2.361
m3-3	482	0.187	2597	0.841	1.817	1.883
m3-4	510	0.192	2651	0.764	1.823	2.62
m3-5	471	0.184	2554	0.844	2.052	2.853
m4-1	599	0.21	2852	0.583	0.995	1.395
m4-2	628	0.211	2991	0.577	0.952	1.231
m4-3	656	0.21	3116	0.57	0.954	1.094
m4-4	709	0.217	3323	0.561	0.819	1.034
m4-5	644	0.232	2764	0.585	0.886	1.298
m5-1	801	0.236	3471	0.566	0.777	1.133
m5-2	824	0.225	3691	0.56	0.749	1.088
m5-3	855	0.226	3792	0.557	0.728	0.982
m5-4	845	0.226	3755	0.554	0.743	1.01
m5-5	821	0.227	3612	0.564	0.762	1.102

Appendix C2: Shear and Rutting Properties for Mixes 6 through 12

Mix Design Designation	Shear Properties of Mix			Rutting Properties of Mix		
	Avg. Shear Strength (kPa)	Avg. Shear Strain at Peak	Avg. Shear Modulus (kPa)	Mean Rut Depth (0.1 MPa) (mm)	Mean Rut Depth (0.3 MPa) (mm)	Mean Rut Depth (0.6 MPa) (mm)
m6-1	503	0.212	2438	0.864	1.175	2.151
m6-2	575	0.21	2472	0.763	1.171	2.342
m6-3	542	0.216	2563	0.727	1.134	2.573
m6-4	539	0.215	2494	0.717	1.108	2.263
m6-5	818	0.211	2484	0.815	1.133	1.91
m7-1	241	0.156	1548	0.781	1.702	not available
m7-2	254	0.15	1690	0.761	1.387	
m7-3	269	0.15	1823	0.724	1.648	
m7-4	238	0.144	1643	0.756	1.673	
m7-5	227	0.153	1475	0.794	1.831	
m8-1	322	0.148	2169	0.759	1.072	not available
m8-2	340	0.153	2228	0.741	1.087	
m8-3	351	0.155	2264	0.72	1.062	
m8-4	372	0.156	2389	0.692	1.258	
m8-5	367	0.157	2340	0.708	1.711	
m9-1	215	0.158	1380	1.275	2.075	not available
m9-2	231	0.16	1500	1.226	1.909	
m9-3	240	0.143	1681	1.034	2.114	
m9-4	256	0.143	1783	1.199	1.975	
m9-5	217	0.159	1398	1.389	1.988	
m10-1	725	0.233	3122	0.572	0.885	1.328
m10-2	737	0.232	3191	0.562	0.864	1.14
m10-3	719	0.229	3136	0.572	0.933	1.355
m10-4	709	0.236	3054	0.661	0.951	1.431
m11-1	418	0.229	1837	1.21	2.421	2.448
m11-2	452	0.24	1882	0.985	2.214	2.441
m11-3	468	0.246	1918	0.926	2.074	2.681
m11-4	486	0.25	1947	0.915	1.995	2.684
m11-5	469	0.244	1934	0.952	2.242	2.661
m12-1	197	0.209	946	1.526	not available	not available
m12-2	238	0.221	1101	1.396		
m12-3	223	0.211	1058	1.399		
m12-4	181	0.197	931	1.575		

Appendix D: CiSSST Test Results

Test No.	Test Temperature (deg. C)	Maximum Torque		Plate Diameter (m)	Failure Depth (m)	Upper Failure Diameter (m)	Lower Failure Diameter (m)
		(lbf*in)	N*m				
C2	29	3315	374.54	0.092	0.015	0.1	0.06
C3	29	3600	406.74	0.092	0.01	0.103	0.08
C4	29	4500	508.43	0.092	0.012	0.105	0.07
C5	29	4600	519.73	0.092	0.01	0.11	0.07
C6	29	4600	519.73	0.092	0.01	0.105	0.07

Appendix E: InSiSST™ Test Results

InSiSST Software
TEST I1

Test Speed (rpm)	1800	Pavement Temp (deg. C)	35
Recording (s)	1	Test Plate Diameter (mm)	92
Calibration	23928	Date:	Aug-04
First Reading	-85	Time	18:10

RAW TEST DATA

Torque Cell Output	Angle (radians)	Torque (lb.ft)	Torque (lb.in)	Torque (N.m.)	Shear Modulus (kPa)
-42	0.0000	1.1	12.7	1.4	
27	0.0233	2.8	33.2	3.8	310.61
1981	0.0465	51.0	612.5	69.2	2864.80
7258	0.0698	181.4	2177.1	246.0	6788.08
14968	0.0931	371.9	4463.1	504.3	10436.56
20045	0.1163	497.4	5968.3	674.3	11165.24
7832	0.1396	195.6	2347.3	265.2	3659.35
6617	0.1629	165.6	1987.1	224.5	2655.22
6447	0.1861	161.4	1936.7	218.8	2264.39

Raw Graph - Torque

Processed Graph - Torque

$$y = 11100x - 528.85$$
$$R^2 = 1$$
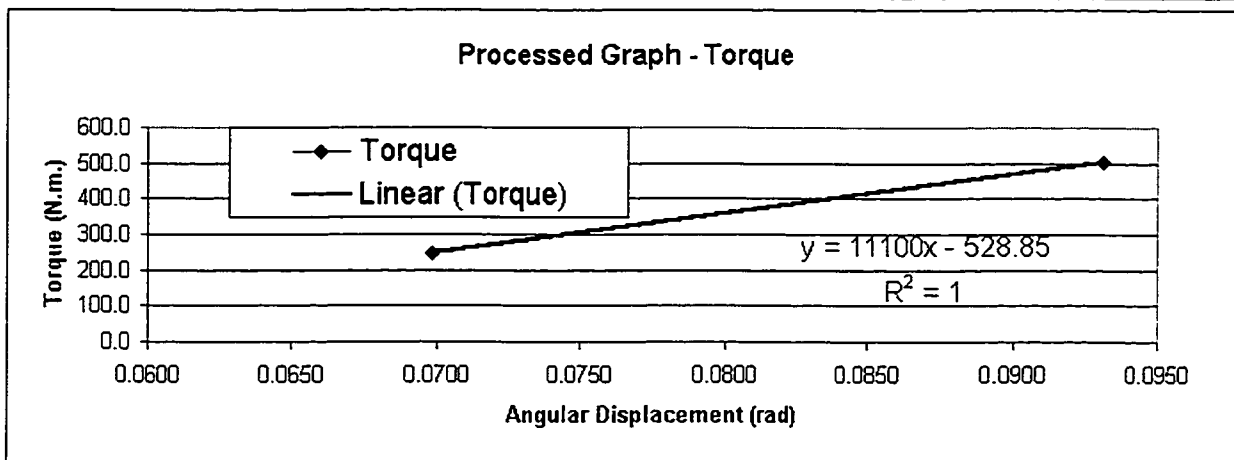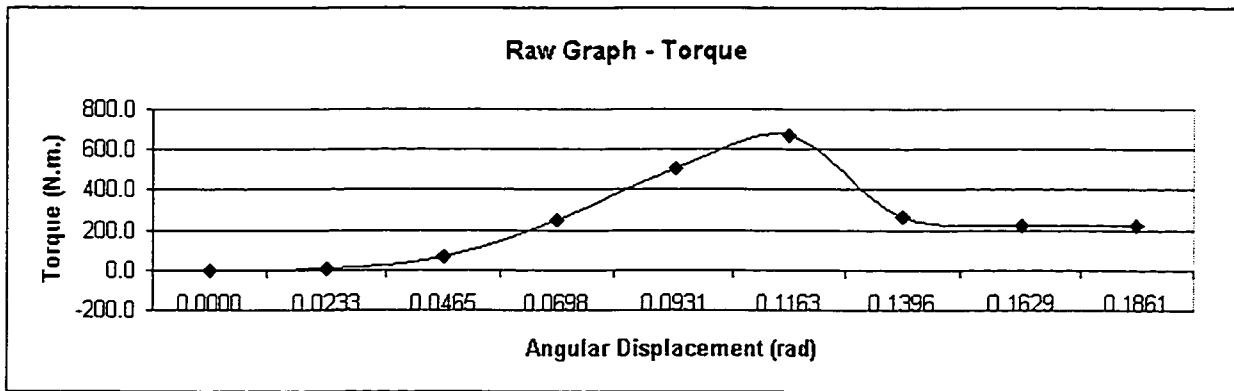
InSiSST Software

TEST I2

Test Speed (rpm)	1800	Pavement Temp (deg. C)	35
Recording (s)	0.75	Test Plate Diameter (mm)	92
Calibration	23971	Date:	Aug-04
First Reading	-33	Time	18:10

RAW TEST DATA

Torque Cell Output	Angle (radians)	Torque (lb.ft)	Torque (lb.in)	Torque (N.m.)	Shear Modulus (kPa)
-27	0	0.1	1.8	0.2	
0	0.0175	0.8	9.8	1.1	122.07
167	0.0349	4.9	59.3	6.7	369.91
1471	0.0524	37.2	446.1	50.4	1854.48
4230	0.0698	105.4	1264.4	142.9	3942.32
9646	0.0873	239.2	2870.8	324.4	7160.72
16755	0.1047	414.9	4979.3	562.6	10350.08
21929	0.1222	542.8	6513.9	736.0	11605.66
23612	0.1396	584.4	7013.1	792.4	10933.15
8123	0.1571	201.6	2419.1	273.3	3352.21
7471	0.1745	185.5	2225.7	251.5	2775.80

$y = 11329x - 647.96$

$R^2 = 1$
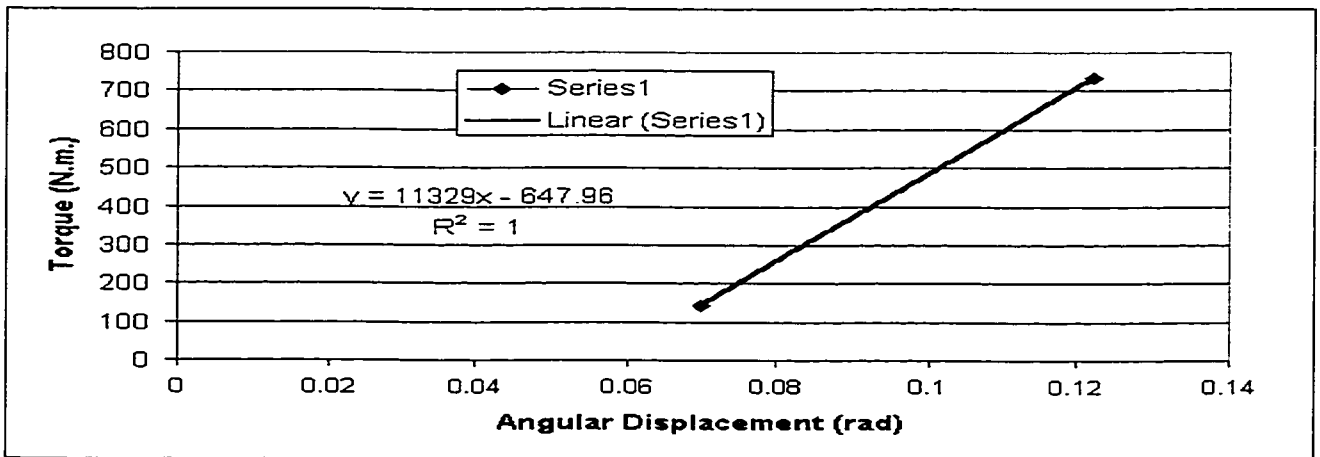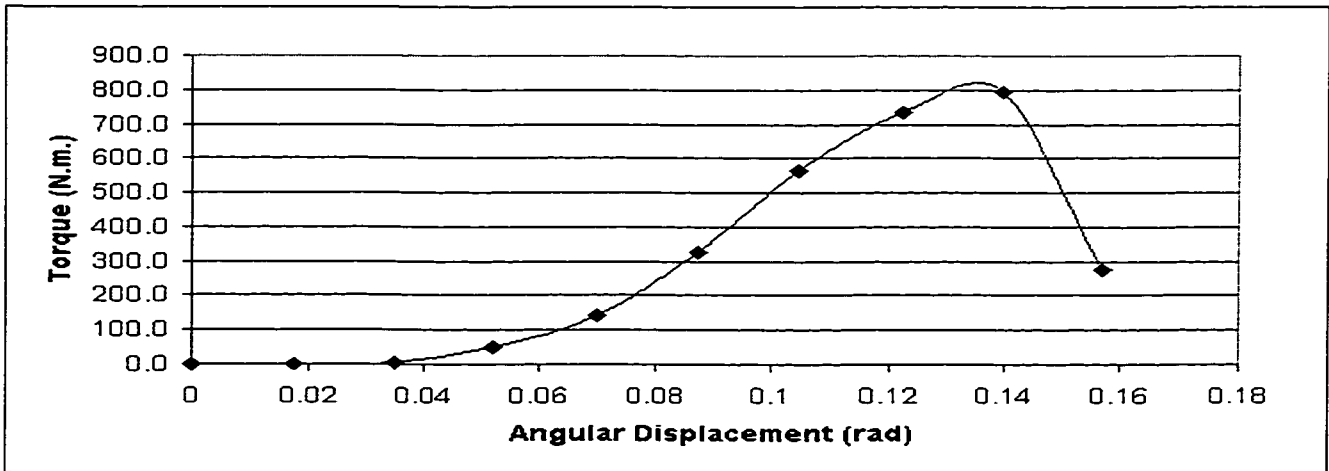
InSiSST Software

TEST I3

Test Speed	1800	Pavement Temp (deg. C)		32
Recording	1	Test Plate Diameter (mm)		92
Calibration	23977	Date:		Aug-04
First Reading	-32	Time		18:20

RAW TEST DATA

Torque Cell Output	Angle (radians)	Torque (lb.ft)	Torque (lb.in)	Torque (N.m.)	Shear Modulus (kPa)
-28	0	0.1	1.2	0.1	
0	0.0233	0.8	9.5	1.1	88.76
99	0.0465	3.2	38.8	4.4	181.68
1095	0.0698	27.8	334.2	37.8	1042.00
5374	0.0931	133.6	1603.1	181.1	3748.72
15256	0.1163	377.8	4533.5	512.2	8481.01
23636	0.1396	584.9	7018.5	793.0	10941.51
8835	0.1629	219.1	2629.4	297.1	3513.54
7924	0.1861	196.6	2359.3	266.6	2758.49
7364	0.2094	182.8	2193.2	247.8	2279.40
6641	0.2327	164.9	1978.8	223.6	1850.92

$$y = 13148x - 1042.6$$
$$R^2 = 1$$
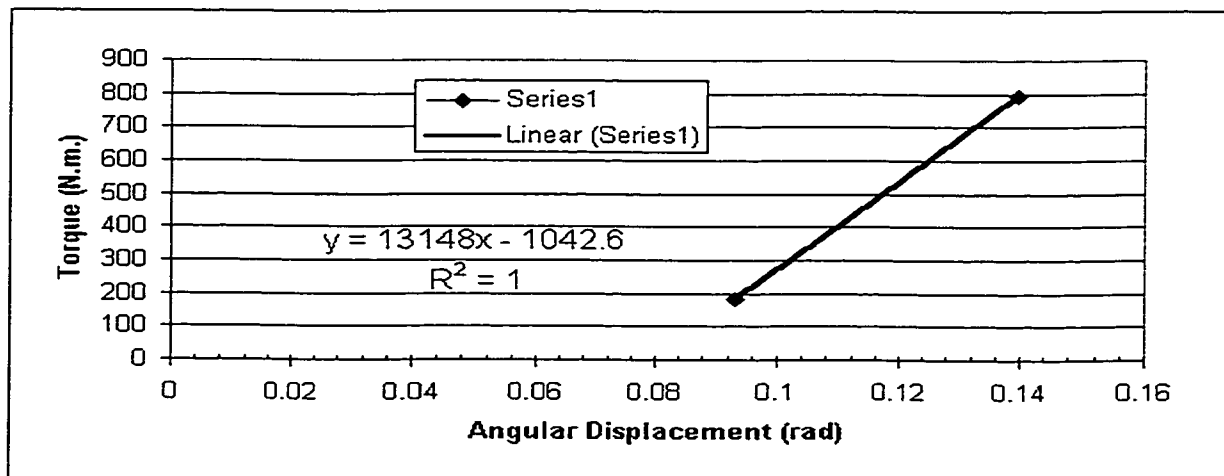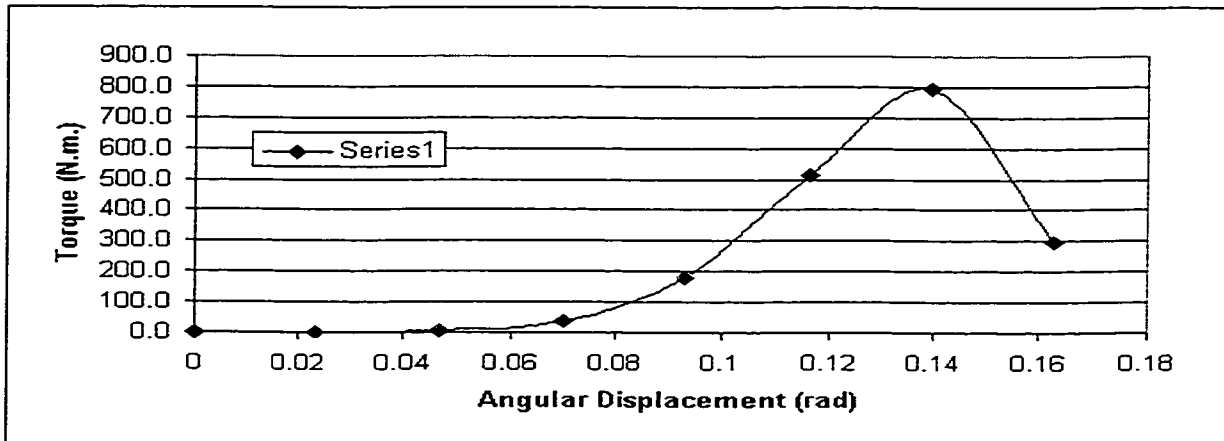
InSISST Software
TEST I7

Test Speed	1800	rpm		Pavement Temp	30 C
Recording	1	seconds		Test Plate Diameter	125 mm
Calibration	23964			Date:	Aug-04
First Reading	-52			Time	18:53
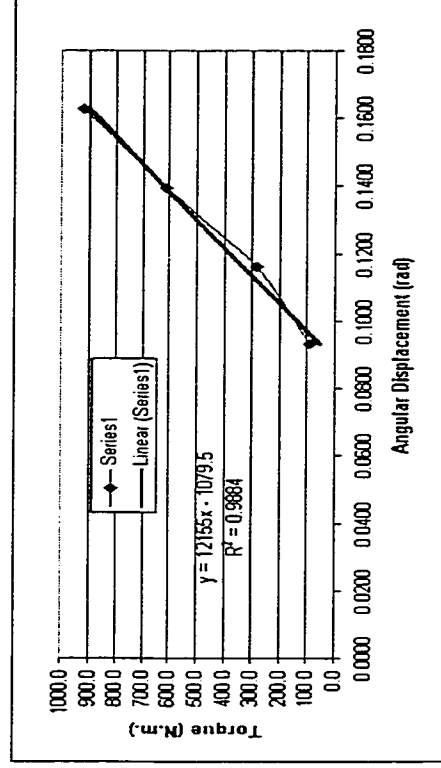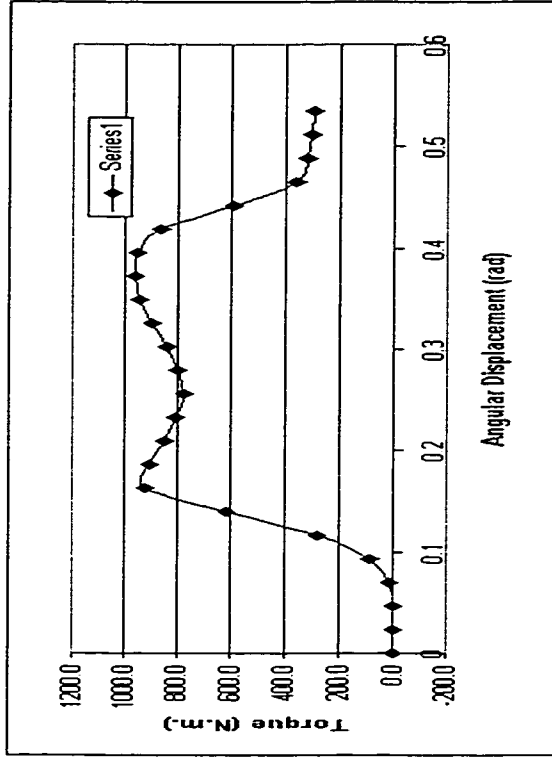
Torque Cell Output	Angle (radians)	Torque (lb.ft)	Torque (lb.in)	Torque (N.m.)	Shear Modulus (kPa)
-53	0	0.0	-0.3	0.0	
0	0.0233	1.3	15.4	1.7	57.49
0	0.0465	1.3	15.4	1.7	28.74
527	0.0698	14.3	171.6	19.4	213.37
2605	0.0931	65.6	787.7	89.0	734.35
8348	0.1163	207.5	2490.2	281.4	1857.30
18249	0.1396	452.1	5425.4	613.0	3372.08
27452	0.1629	679.5	8153.6	921.2	4343.82
26926	0.1861	666.5	7997.7	903.6	3728.15
25171	0.2094	623.1	7477.4	844.8	3098.33
24029	0.2327	594.9	7138.9	806.6	2662.25
23102	0.2560	572.0	6864.1	775.5	2327.06
23818	0.2792	589.7	7076.3	799.5	2199.10
25020	0.3025	619.4	7432.7	839.8	2132.16
26790	0.3258	663.1	7957.4	899.1	2119.63
28137	0.3490	696.4	8356.7	944.2	2077.60
28524	0.3723	706.0	8471.4	957.1	1974.49
28430	0.3956	703.6	8443.6	954.0	1852.23
25802	0.4188	638.7	7664.5	866.0	1587.92
17617	0.4421	436.5	5238.0	591.8	1028.09
10647	0.4654	264.3	3171.7	358.4	591.41
9484	0.4886	235.6	2827.0	319.4	502.02
9113	0.5119	226.4	2717.0	307.0	460.56

In second chart: y = 12155x - 1079.5, R² = 0.9884

Test Speed	1800	Pavement Temp	29
Recording	1	Test Plate Diameter	125
Calibration	23990	Date:	Aug-04
First Reading	-24	Time	18:53

RAW TEST DATA

Torque Cel Output	Angle (radians)	Torque (lb.ft)	Torque (lb.in)	Torque (N.m.)	Shear Modulus (kPa)
-23	0	0.0	0.3	0.0	
0	0.0233	0.6	7.1	0.8	26.54
145	0.0465	4.2	50.1	5.7	93.43
2190	0.0698	54.7	656.4	74.2	815.95
7224	0.0931	179.1	2148.9	242.8	2003.40
16131	0.1163	399.1	4789.6	541.2	3572.29
22860	0.1396	565.4	6784.6	766.6	4216.87
27823	0.1629	688.0	8256.0	932.8	4398.35
27565	0.1861	681.6	8179.5	924.2	3812.90
28661	0.2094	708.7	8504.4	960.9	3523.89
29344	0.2327	725.6	8706.9	983.8	3247.01
29854	0.2560	738.2	8858.1	1000.8	3003.09
30130	0.2792	745.0	8940.0	1010.1	2778.26
30275	0.3025	748.6	8983.0	1014.9	2576.88
30380	0.3258	751.2	9014.1	1018.5	2401.11
30462	0.3490	753.2	9038.4	1021.2	2247.08
30571	0.3723	755.9	9070.7	1024.9	2114.17
30416	0.3956	752.1	9024.8	1019.7	1979.73
12798	0.4188	316.8	3801.4	429.5	787.58
9666	0.4421	239.4	2872.9	324.6	563.87

y = 11255x - 792.58
$R^2 = 0.9936$
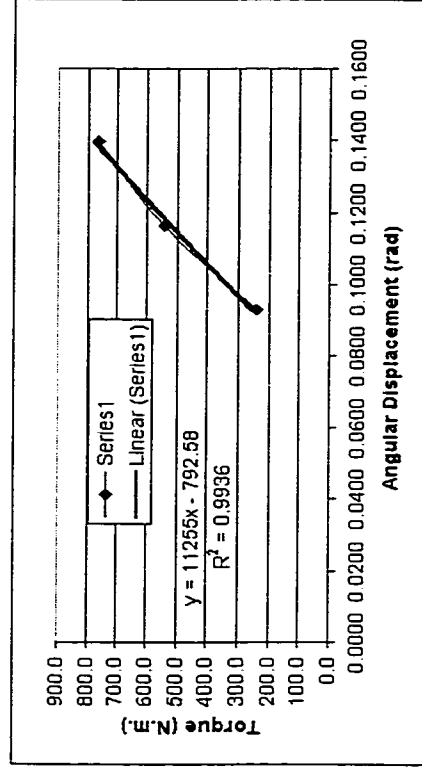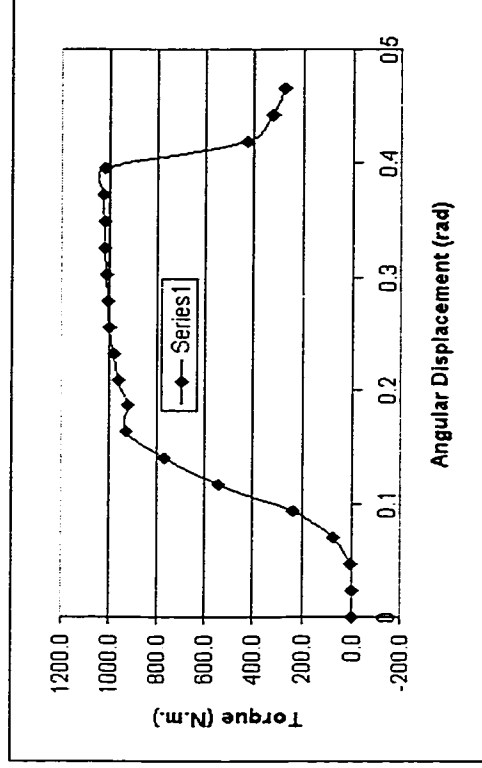
InSiSST Software

TEST: BF1 - BOND FAILURE

Test Speed (rpm)	1800	Pavement Temp (deg. C)	28
Recording (s)	1	Test Plate Diameter (mm)	92
Calibration	23954	Date:	Jul-31
First Reading	-71	Time	

RAW TEST DATA

Torque Cell Output	Angle (radians)	Torque (lb.ft)	Torque (lb.in)	Torque (N.m.)	Shear Modulus (kPa)
-45	0.0000	0.6	7.7	0.9	
919	0.0233	24.4	293.4	33.1	2744.18
5490	0.0465	137.3	1648.0	186.2	7707.27
12676	0.0698	314.8	3777.5	426.8	11777.80
19696	0.0931	488.1	5857.8	661.8	13698.04
24990	0.1163	618.9	7426.6	839.1	13893.32
26303	0.1396	651.3	7815.7	883.1	12184.35
26753	0.1629	662.4	7949.1	898.1	10621.92
27075	0.1861	670.4	8044.5	908.9	9405.75
27356	0.2094	677.3	8127.8	918.3	8447.21
27566	0.2327	682.5	8190.0	925.3	7660.70
27756	0.2560	687.2	8246.3	931.7	7012.15
-77	0.2792	-0.1	-1.8	-0.2	-1.39

Raw Graph - Torque

Processed Graph - Torque

$y = 10221x - 289.45$

$R^2 = 1$
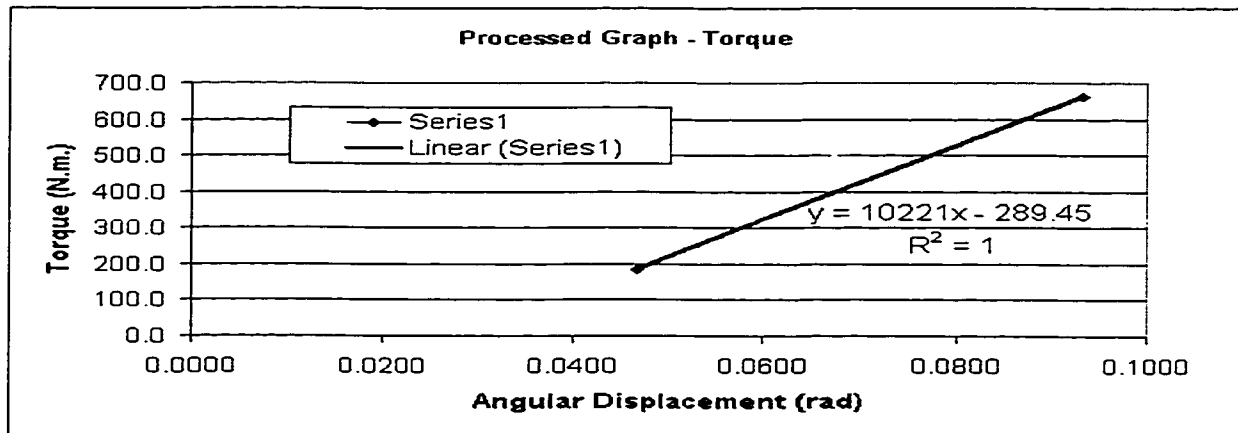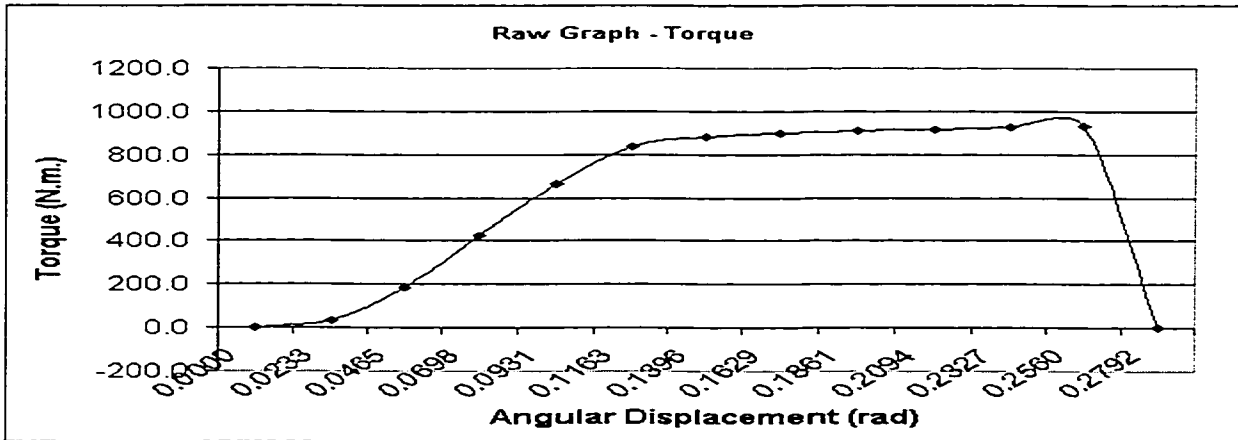
InSiSST Software
TEST: BF2 - BOND FAILURE

Test Speed (rpm)	1800	Pavement Temp (deg. C)	28
Recording (s)	1	Test Plate Diameter (mm)	92
Calibration	23930	Date:	Jul-31
First Reading	-75	Time	

RAW TEST DATA

Torque Cell Output	Angle (radians)	Torque (lb.ft)	Torque (lb.in)	Torque (N.m.)	Shear Modulus (kPa)
-58	0.0000	0.4	5.0	0.6	
24	0.0233	2.4	29.4	3.3	274.65
5471	0.0465	137.1	1644.9	185.8	7692.88
14626	0.0698	363.3	4360.1	492.6	13594.55
22086	0.0931	547.7	6572.7	742.6	15369.81
25029	0.1163	620.5	7445.6	841.2	13928.75
24918	0.1396	617.7	7412.6	837.5	11555.97
448	0.1629	12.9	155.1	17.5	207.27

Raw Graph - Torque

Processed Graph - Torque

$y = 11964x - 370.92$

$R^2 = 1$
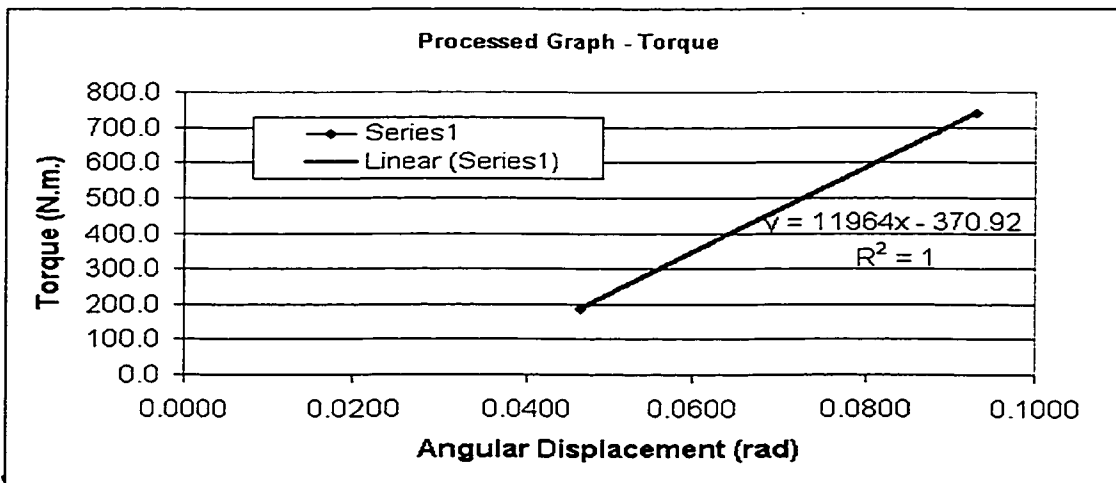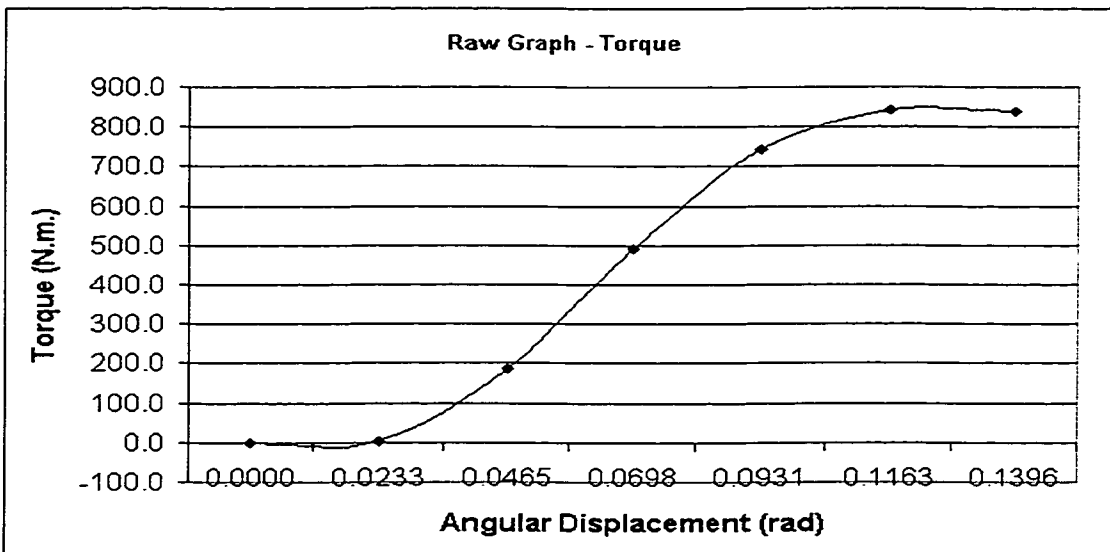
In|

TEST: BF3 - BOND FAILURE

Test Speed (rpm)	1800	Pavement Temp (deg. C)	28
Recording (s)	1	Test Plate Diameter (mm)	92
Calibration	23953	Date:	Jul-31
First Reading	-67	Time	

RAW TEST DATA

Torque Cell Output	Angle (radians)	Torque (lb.ft)	Torque (lb.in)	Torque (N.m.)	Shear Modulus (kPa)
-57	0.0000	0.2	3.0	0.3	
383	0.0233	11.1	133.4	15.1	1247.61
2822	0.0465	71.4	856.3	96.7	4004.84
10862	0.0698	269.9	3239.4	366.0	10100.13
34	0.0931	2.5	29.9	3.4	70.01

Raw Graph - Torque

Processed Graph - Torque

$$y = 11572x - 441.75$$
$$R^2 = 1$$
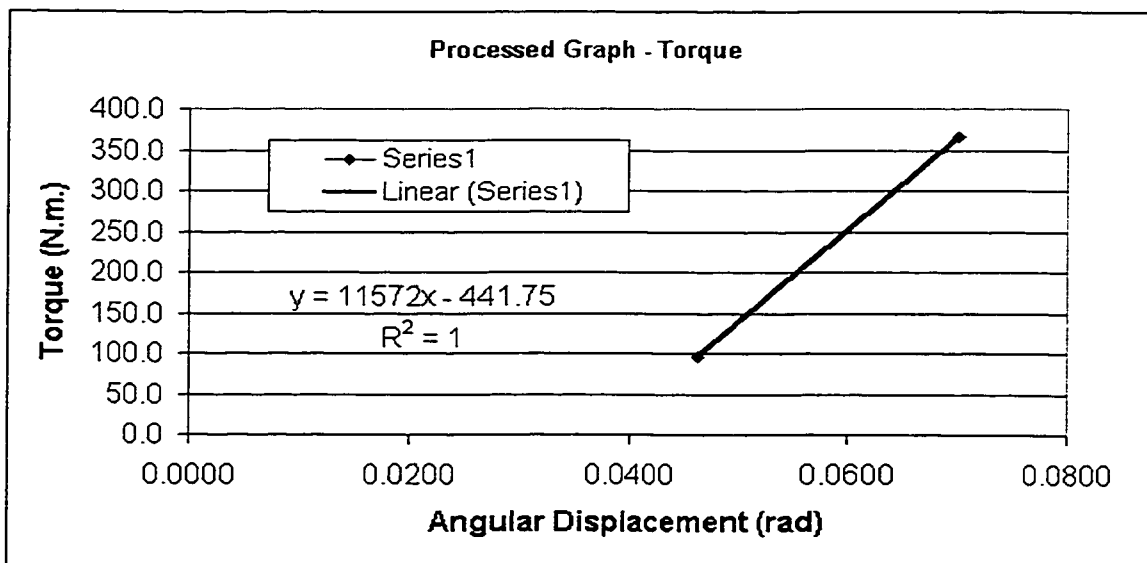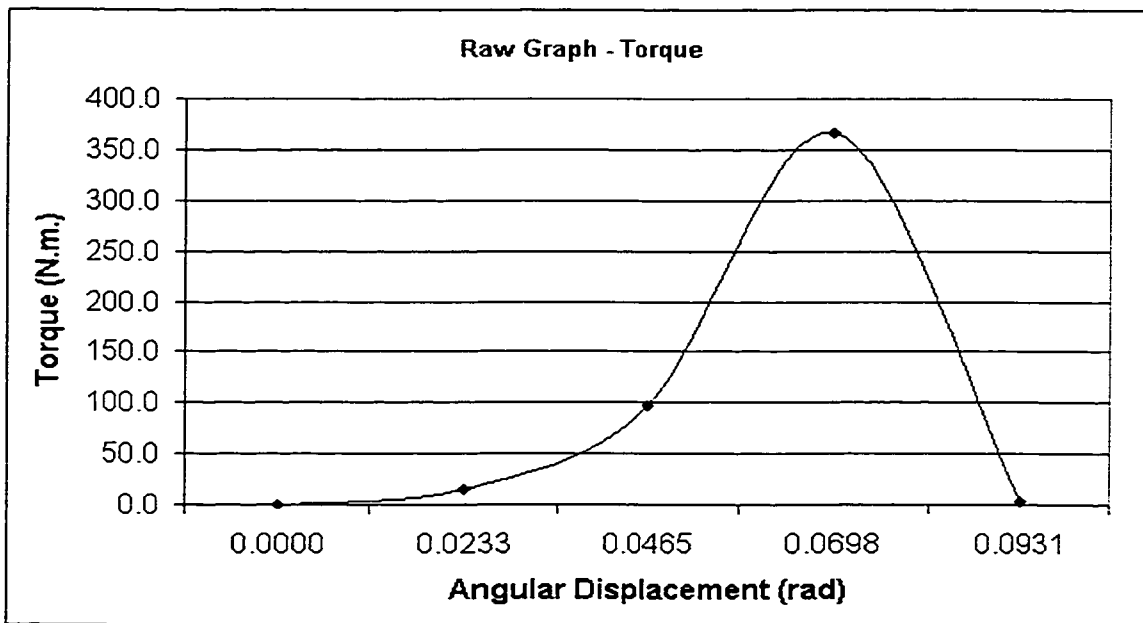
InSiSST Software

TEST: BF4 - BOND FAILURE

Test Speed (rpm)	1800	Pavement Temp (deg. C)	28
Recording (s)	1	Test Plate Diameter (mm)	92
Calibration	23953	Date:	Jul-31
First Reading	-50	Time	

RAW TEST DATA

Torque Cell Output	Angle (radians)	Torque (lb.ft)	Torque (lb.in)	Torque (N.m.)	Shear Modulus (kPa)
-54	0.0000	-0.1	-1.2	-0.1	
59	0.0233	2.7	32.3	3.7	302.41
642	0.0465	17.1	205.3	23.2	959.96
4373	0.0698	109.3	1311.9	148.2	4090.45
13615	0.0931	337.8	4053.2	458.0	9478.18
-53	0.1163	-0.1	-0.9	-0.1	-1.66

Raw Graph - Torque

Processed Graph - Torque

$y = 13311x - 780.95$

$R^2 = 1$
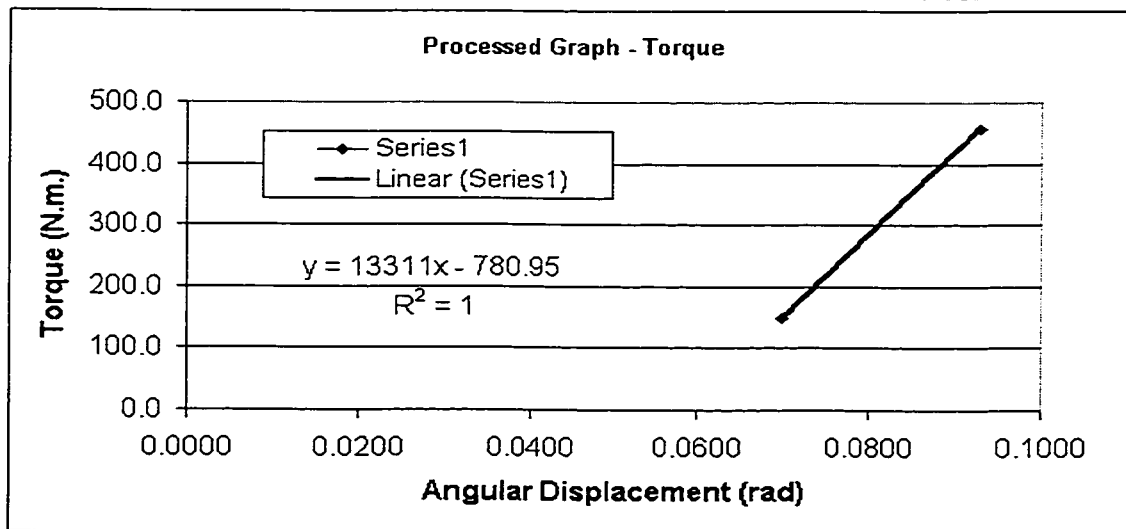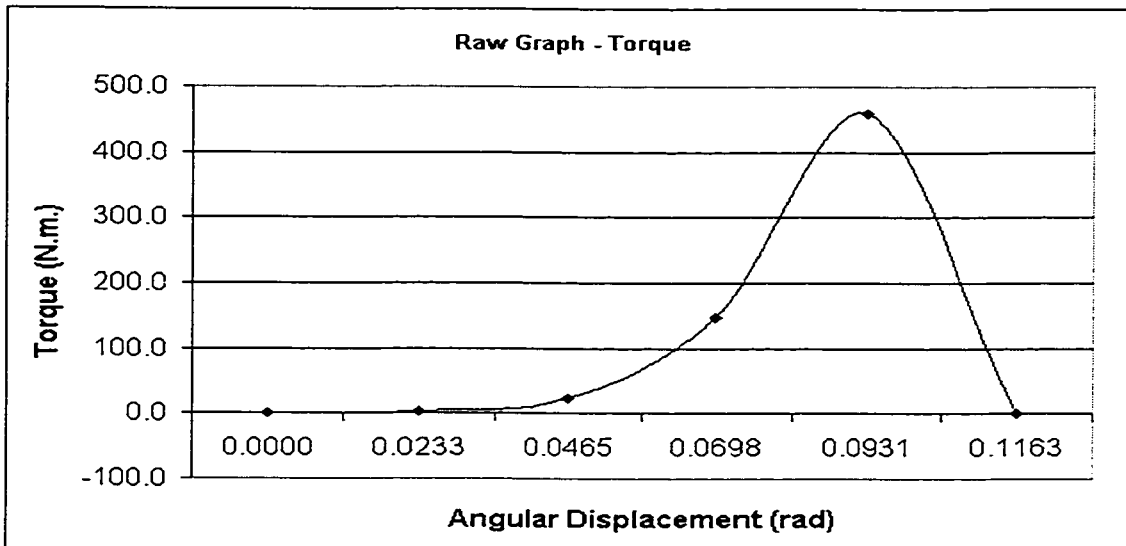
InSiSST Software

TEST: BF5 - BOND FAILURE

Test Speed (rpm)	1800	Pavement Temp (deg. C)	28
Recording (s)	1	Test Plate Diameter (mm)	92
Calibration	23956	Date:	Jul-31
First Reading	-60	Time	

RAW TEST DATA

Torque Cell Output	Angle (radians)	Torque (lb.ft)	Torque (lb.in)	Torque (N.m.)	Shear Modulus (kPa)
-52	0.0000	0.2	2.4	0.3	
0	0.0233	1.5	17.8	2.0	166.38
848	0.0465	22.4	269.2	30.4	1258.91
5646	0.0698	141.0	1691.6	191.1	5274.13
13889	0.0931	344.6	4135.2	467.2	9669.93
-52	0.1163	0.2	2.4	0.3	4.44

Raw Graph - Torque

Processed Graph - Torque

$$y = 11866x - 637.17$$
$$R^2 = 1$$
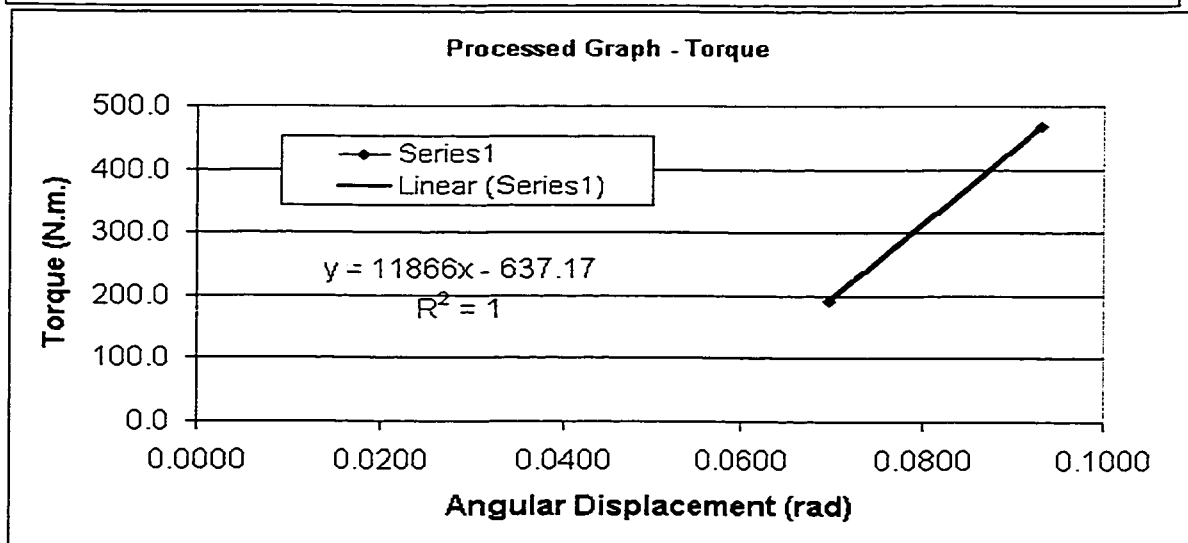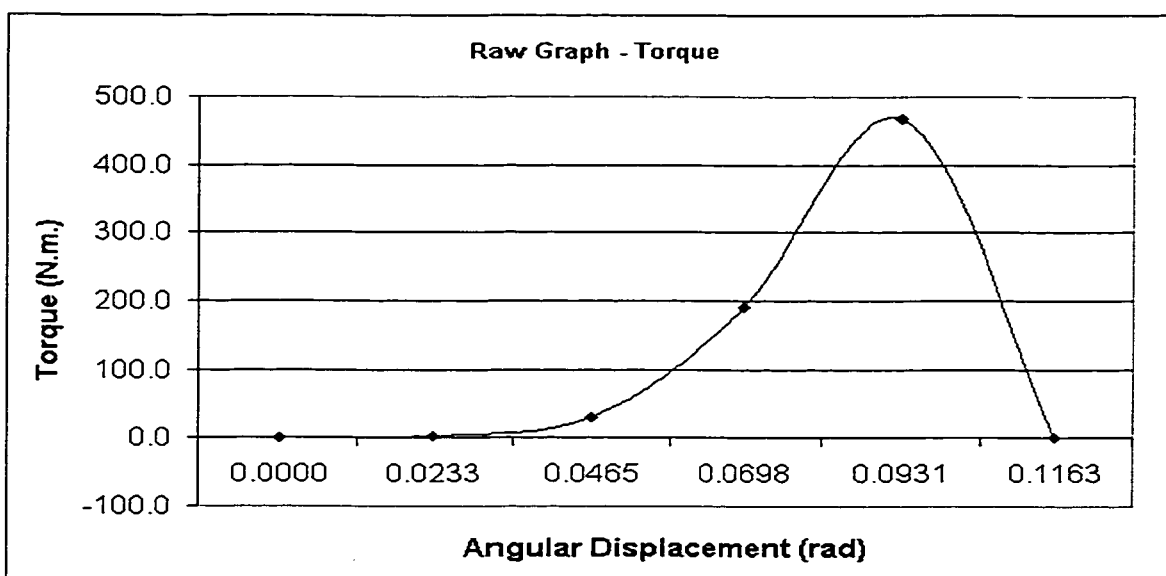
InSiSST Software
TEST: BF6 - BOND FAILURE

Test Speed (rpm)	1800	Pavement Temp (deg. C)	28
Recording (s)	1	Test Plate Diameter (mm)	92
Calibration	23931	Date:	Jul-31
First Reading	-69	Time	

RAW TEST DATA

Torque Cell Output	Angle (radians)	Torque (lb.ft)	Torque (lb.in)	Torque (N.m.)	Shear Modulus (kPa)
-58	0.0000	0.3	3.3	0.4	
574	0.0233	15.9	190.7	21.6	1784.19
5210	0.0465	130.5	1566.0	176.9	7324.05
13164	0.0698	327.1	3925.6	443.5	12239.59
21850	0.0931	541.9	6502.3	734.7	15205.14
26928	0.1163	667.4	8008.7	904.9	14982.19
27003	0.1396	669.2	8030.9	907.4	12519.84
27491	0.1629	681.3	8175.7	923.7	10924.73
-72	0.1861	-0.1	-0.9	-0.1	-1.04

Raw Graph - Torque

Processed Graph - Torque

$$y = 12512x - 429.85$$
$$R^2 = 1$$
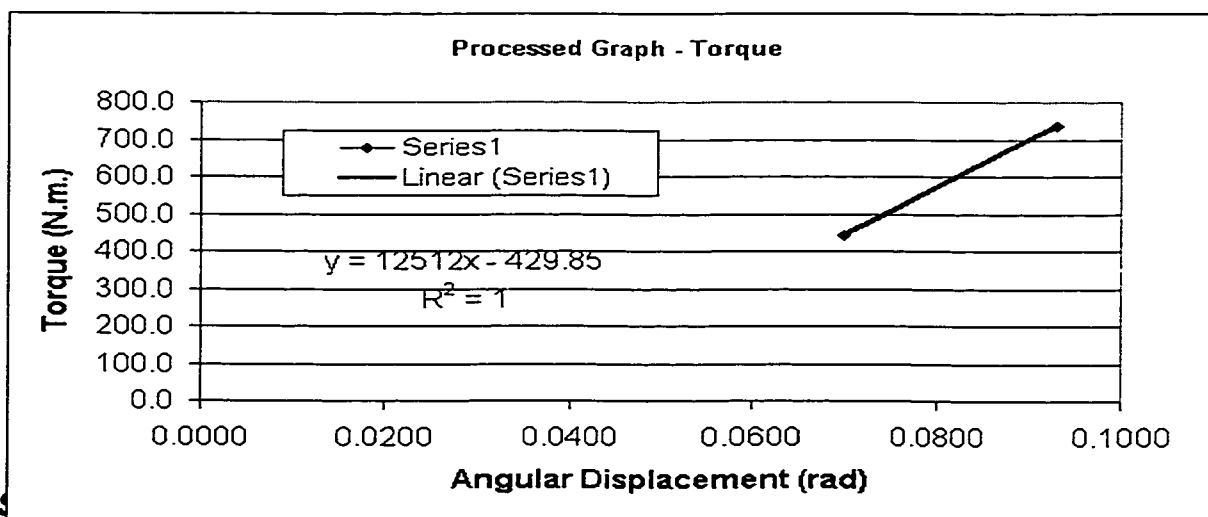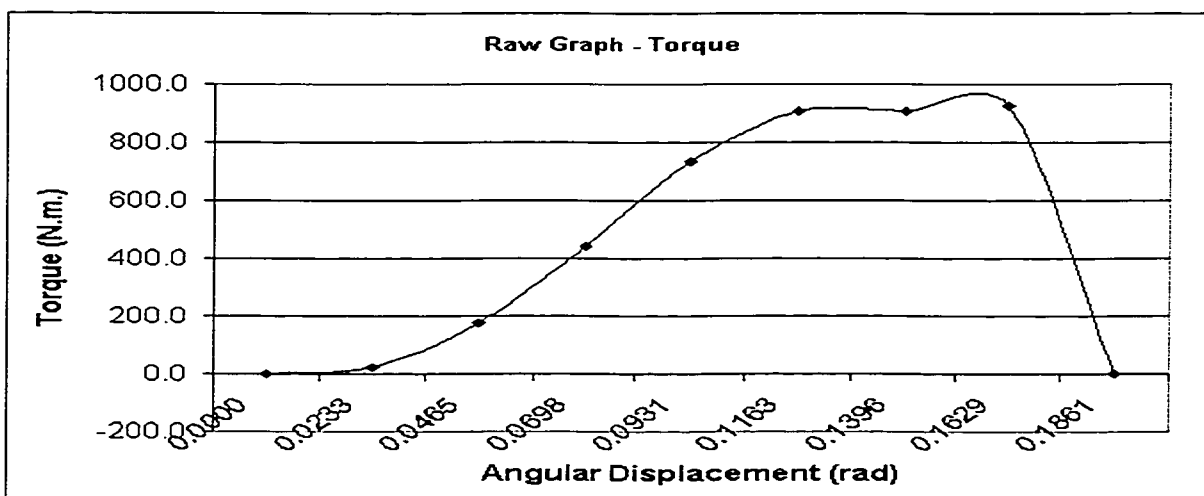
InS

TEST: BF7 - BOND FAILURE

Test Speed (rpm)	1800	Pavement Temp (deg. C)	28
Recording (s)	1	Test Plate Diameter (mm)	92
Calibration	23924	Date:	Jul-31
First Reading	-82	Time	

RAW TEST DATA

Torque Cell Output	Angle (radians)	Torque (lb.ft)	Torque (lb.in)	Torque (N.m.)	Shear Modulus (kPa)
-67	0.0000	0.4	4.4	0.5	
58	0.0233	3.5	41.5	4.7	388.37
1608	0.0465	41.8	501.2	56.6	2344.11
9654	0.0698	240.6	2887.5	326.2	9002.86
18773	0.0931	466.0	5591.9	631.8	13076.38
25221	0.1163	625.4	7504.3	847.9	14038.58
27641	0.1396	685.2	8222.0	929.0	12817.70
28236	0.1629	699.9	8398.4	948.9	11222.40
28465	0.1861	705.5	8466.4	956.6	9899.01
0	0.2094	2.0	24.3	2.7	25.28

Raw Graph - Torque

Processed Graph - Torque

$y = 13132x - 590.45$

$R^2 = 1$
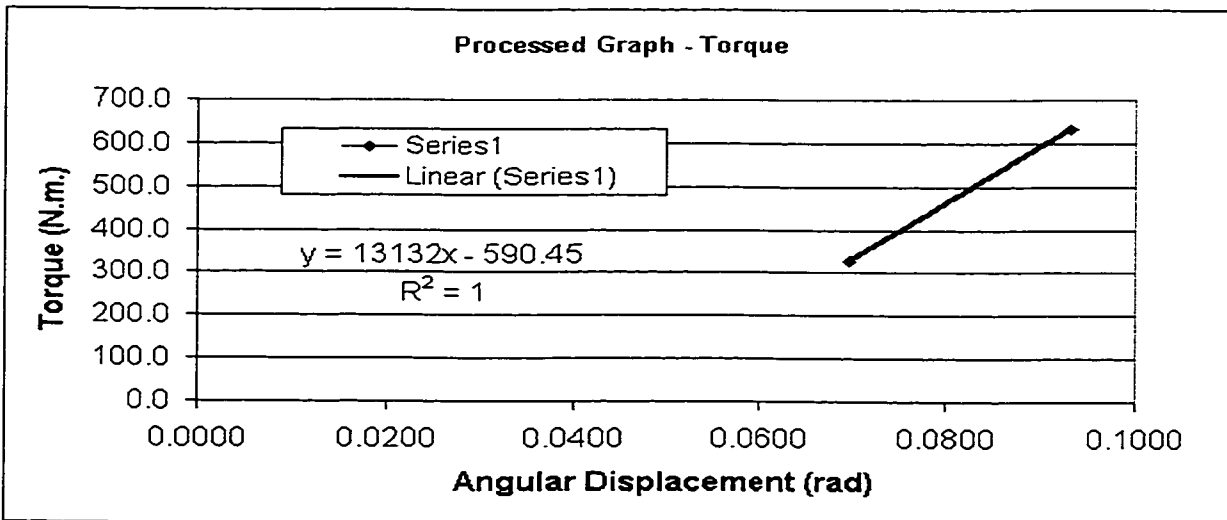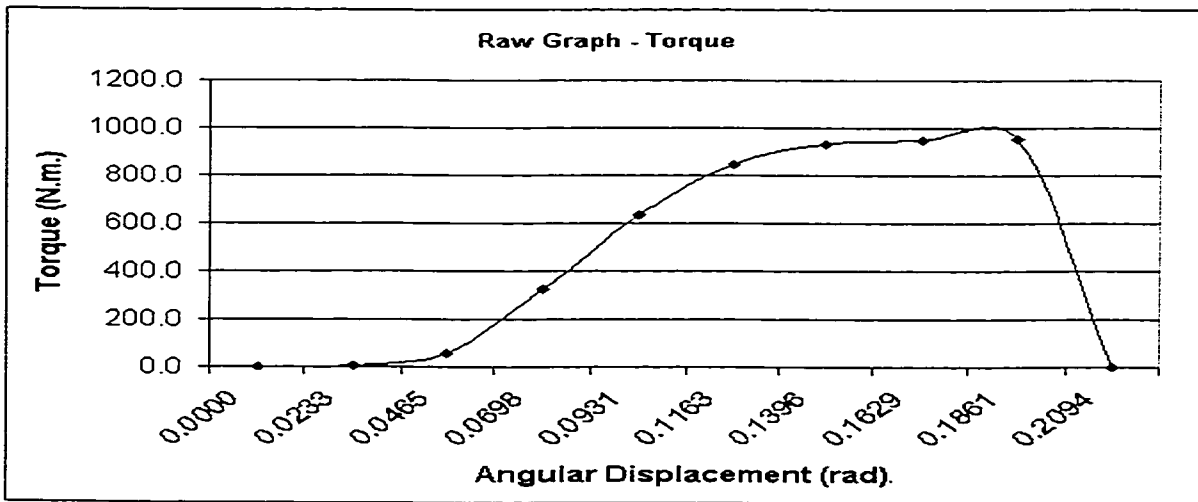
InSiSST Software

TEST: BF8 - BOND FAILURE

Test Speed (rpm)	1800	Pavement Temp (deg. C)	28
Recording (s)	1	Test Plate Diameter (mm)	92
Calibration	23952	Date:	Jul-31
First Reading	-52	Time	

RAW TEST DATA

Torque Cell Output	Angle (radians)	Torque (lb.ft)	Torque (lb.in)	Torque (N.m.)	Shear Modulus (kPa)
-35	0.0000	0.4	5.0	0.6	
0	0.0233	1.3	15.4	1.7	144.26
3486	0.0465	87.4	1049.4	118.6	4907.78
11893	0.0698	295.2	3542.9	400.3	11046.44
22687	0.0931	562.0	6744.4	762.0	15771.34
27383	0.1163	678.1	8137.2	919.4	15222.72
28260	0.1396	699.8	8397.4	948.8	13091.11
-69	0.1629	-0.4	-5.0	-0.6	-6.74

Raw Graph - Torque

Processed Graph - Torque

$y = 13827x - 524.89$

$R^2 = 1$